Cardiac Mitochondrial Respiration in Two Rodent Models of Obesity

By Wing Yin Anna Chan

Submitted for the Degree of Master of Science in Medicine

Faculty of Health Sciences

University of Cape Town

2006

Supervisor: Dr. M. Faadiel Essop

Hatter Heart Research Institute

世上無難事，只怕有心人

Nothing is impossible to a willing "heart"

Table of Contents

II: ANALYSIS

VI: REFERENCES

VII: APPENDIX

Declaration

I, Wing Yin Anna Chan, hereby declare that the work on which this dissertation is based is my original work (except where acknowledgments indicate otherwise) and that neither the whole work nor any part of it has been, is being, or is to be submitted for another degree in this or any other university.

I empower the University of Cape Town to reproduce for the purpose of research either the whole or any portion of the contents in any manner whatsoever.

Signed by candidate

Signature

29-05-2006

Date

Acknowledgements

I would like to thank my supervisor, Dr. M. Faadiel Essop for his enthusiastic supervision, scientific guidance and intellectual input. Also, I am grateful for his unlimited patience while reviewing this thesis.

Prof. Lionel Opie, for his advice, scientific guidance and inputs especially regarding the clinical aspects of diabetes.

Joy McCarthy, Lydia Lacerda and Dr. Sandrine Lecour for their advice and skillful technical assistance. Your patience and advice are highly appreciated especially on those stressful days on the oxygraph.

Sylvia Dennis, Pat van de Walt and Beauty Kom, thank you for all your hard work behind the scenes. You always tried to keep everything in place and your assistance is highly appreciated.

Thanks to all the bachelors (Makhosi, Sarin and Deon), "first lady" (Tazz) and Naushaad for making the lab very enjoyable. All your support and care are highly appreciated. Thank you all for your friendship and those treasured memories.

A very special thanks to Victor Claasen for always making the atmosphere in the lab so pleasant, always available to provide skillful technical support and locating the requested references.

I would like to thank everyone in the Animal Unit especially Noel Markgraaff, Jaap Visser and Hiram Arendse. I appreciate your support, expertise and skillful assistance.

Danie Rademeyer and Mohamed Jaffer for helping with the electron microscopy analysis. Morea Petersen and Dr. Christopher Maske for your patience and skillful technical assistance regarding the histological analysis.

Thanks to our collaborators at the Univesity of Tromso, Norway (Dr. Ellen Aasum) and the University of Stellenbosch (Dr. Eugene du Toit).

I also wish to thank NRF for a Labour Scarce Skills Scholarship for my MSc.

Finally, to my parents, my brother, Arthur, Hollis and Nonie, thank you for all your support, understanding and coping with my frustration during the study and while writing my thesis.

ABSTRACT

Obesity is a major contributor to the global burden of disease and is closely associated with the development of type II diabetes. Recent studies have demonstrated that increased circulating free fatty acid (FFA) levels may have detrimental effects on the diabetic heart. In this study, we hypothesized that with obesity and obesity-induced insulin resistance/ type II diabetes, increased FFA supply decreases cardiac mitochondrial bioenergetic capacity. Furthermore, we also hypothesized that females possess innate cardioprotective programs that will result in enhanced bioenergetic capacity compared to males. We examined our hypothesis employing two rodent models i.e. a) a rat model of diet-induced obesity and b) a transgenic (leptin receptor deficient) mouse model of obesity-induced type II diabetes. For the diabetic mouse model, we determined cardiac mitochondrial respiratory function in an age-dependent (10-12, 18-20 and 55-56 weeks) and gender-dependent (male versus female) manner.

We found impaired mitochondrial respiratory capacity in obese rats at baseline and when isolated mitochondria were stressed by anoxia-reoxygenation. We speculate that this may be due to reduced expression of mitochondrial respiratory chain complexes in the insulin resistant rat heart. For the mouse model of type II diabetes we found increased respiratory capacity at 10-12 weeks, thought to represent the stage of metabolic syndrome, with no evidence of oxygen wastage or reduction of respiratory capacity. However, 18-20 week-old obese mice were unable to increase respiratory capacity. We also found increased mitochondrial ultrastructural damage and intracellular lipid accumulation in 18-20 week-old diabetic mouse hearts. We propose that this occurs as a result of a mismatch between increased FA uptake and

decreased FA oxidative capacity.

We found interesting gender-dependent changes in younger female mice which showed enhanced protection when mitochondria were stressed by anoxia-reoxygenation. These data were paralleled by increased intracellular ATP levels, suggesting that young female mice possess increased mitochondrial bioenergetic capacity at baseline. Moreover, our electron microscope data suggest that the ultrastructure of male mitochondria is more disorganized when compared to female controls. However, the protective phenotype in females is abolished with obesity. Our data therefore suggest that female mice possess an innate cardioprotective program that enhances mitochondrial biogenetic capacity to protect the female heart against anoxic/ ischemic stress. However, with the onset of obesity-induced type II diabetes this cardioprotective program is perturbed.

Mitochondrial respiratory function and bioenergetic capacity is reduced in both male and female mice at 55-56 weeks. We suggest this is an age-dependent phenomenon and speculate that it may due to increased ROS production. In summary, this study highlights the significance of sustained biogenetic capacity to ensure an organism's survival. However, with obesity and obesity-induced type II diabetes this energetic homeostasis is perturbed and therefore I postulate that it may negatively impact on cardiac contractility.

Abbreviations

Acetyl-CoA	Acetyl coenzyme A
Acyl-CoA	Acyl coenzyme A
ADP	Adenosine diphosphate
ATP	Adenosine triphosphate
Akt/ PKB	Akt (also known as protein kinase B)
BAT	Brown adipose tissue
BMI	Body Mass Index
BSA	Bovine serum albumin fraction V
CAD	Coronary artery disease
CDC	Centers for Disease Control and Prevention
CE	Cardiac efficiency
CoQ	Coenzyme Q
CP	Carnitine-L-palmitoyl
CPT	Carnitine palmitoyltransferase
CPT 1	Carnitine palmitoyltransferase-1
CVD	Cardiovascular disease
Cyt C	Cytochrome C
DAG	Diacylglycerol
db/+ mouse	Leptin receptor deficient mouse (heterozygous control)
db/db mouse	Leptin receptor deficient mouse (homozygous mutant)
$\Delta\mu H^+$	electrochemical proton gradient
EM	Electron microscopy
FA	Fatty acid
FABP	Fatty acid binding protein

FAD	Flavin adenine dinucleotide (oxidized form)
$FADH_2$	Flavin adenine dinucleotide (reduced form)
FAT	Fatty acid transporter
FFA	Free fatty acid
Formaldehyde	Also known as formalin
g	Force of gravity
GK	Goto-Kakizaki rats
GLUT	Glucose transporter
GLUT4	Glucose transporter-4
GP_x	Glutathione peroxidase
H^+	proton
H_2O	water
H_2O_2	Hydrogen peroxide
H&E	Hematoxylin and eosin
HbA1c test	Glycosylated hemoglobin A1c test
HDL	High-density lipoprotein
HK	Hexokinase
IDDM	Insulin dependent diabetes mellitus
IDF	International Diabetes Federation
IGT	Impaired glucose tolerance
IL-6	Interleukin 6
IRS-1	Insulin receptor substrate-1
JAK/ STAT	Janus kinase/ signal transducers and activator of transcription
KE	Potassium-EDTA
LDL	Lipoprotein

Lepr	Leptin receptor gene
LV	Left ventricular
Malonyl-CoA	Malonyl coenzyme A
MAP kinase	Mitogen activated protein kinase
MCP	Malate and carnitine-L-palmitoyl
Mito	Mitochondria
Mitochondrial complex I	NADH-Ubiquinol Oxidoreductase
Mitochondrial complex II	Succinate-Ubiquinol Oxidoreductase
Mitochondrial complex III	Ubiquinol-Cytochrome c Oxidoreductase
Mitochondrial complex I	Cytochrome c Oxidase
Mn-SOD	Manganese-superoxide dismutase
MVO_2	Myocardial oxygen consumption
NAD^+	Nicotine-amide-dinucleotide (oxidized form)
NADH	Nicotine-amide-dinucleotide (reduced form)
NAFLD	Non-alcoholic fatty liver disease
NASH	Non-alcoholic steatohepatitis
NCEP:ATPIII	US National Cholesterol Education Program's Adult Treatment Panel III.
NEFA	Non-esterified fatty acid
$NF\text{-}_KB$	Nuclear factor kappa B
NHLBI	US National Heart, Lung and Blood Institute
NIDDM	Non-insulin dependent diabetes mellitus
NIH	UN National Institutes of Health
$O_2^{\cdot -}$	Superoxide
O_2	Oxygen
ob/ob mouse	Leptin deficient mouse

O_SO_4	Osmium tetroxide
PAI1	Plasminogen activator inhibitor 1
PDH	Pyruvate dehydrogenase
PFK	Phosphofructokinase
Pi	Inorganic orthophosphate
PI3 kinase	Phosphatidylinostitol-3 kinase
PKB	Protein kinase B (also known as Akt)
PKC	Protein kinase C
PPARα	Peroxisome proliferator-activated receptor- alpha
ROS	Reactive oxygen species
SEM	Scanning electron microscopy
Ser	Serine
STZ	Streptozotocin
TEM	Transmission electron microscopy
TG	Triglyceride
TNFα	Tumour necrosis factor alpha
Tyr	Tyrosine
UCP	Uncoupling protein
UCP2	Uncoupling protein-2
UCP3	Uncoupling protein-3
VLDL	Very low-density lipoprotein
WHO	World Health Organization
ZDF	Zucker fatty rat
ZT	Zeitgeber time

Units of measurements and others

%	percentage
°C	degree celsius
ANOVA	Analysis of variance
cm	centimeters
g	gram
et al.	and others
kg	kilograms
L	liter
m^2	square meters
µg	microgram
µIU	micro-international unit
µl	microliter
µm	micrometer
µM	micromolar
M	molar
mg	milligram
min	minute
ml	milliliter
mM	millimolar
mmol	millimole
N.D	not determined
ng	nanogram
nm	nanometer
nmol	nanomole
S.E.M.	standard error of the mean

vs. versus

List of Tables

List of Figures

I: INTRODUCTION

1. Epidemiology of Obesity

Obesity is a chronic condition characterized by excessive body fat accumulation. Its underlying causes are multifactorial, resulting from interactions between genetics and environment [1] and include human factors e.g. metabolic, psychological, hormonal, social status, cultural habitats and modern lifestyle trends. The latter includes for e.g. increased consumption of energy-dense foods (high in saturated fat and sugars) and reduced energy expenditure (lack of physical activity). [2]

The incidence of obesity has reached global epidemic proportions, with estimates of more than a billion overweight adults and ~ 300,000 of these thought to be clinically obese. [3] Recently, the World Health Organization (WHO) ranked obesity in the top 10 risks to human health worldwide including developed and developing nations. [3] A recent study reported that more than 56% of South African women are overweight/ obese, thereby a major contributor to the local burden of disease. [4] Moreover, the prevalence of obesity is continuously rising and the incidence of childhood obesity has reached alarming proportions. [5]

Obesity is commonly assessed by using body mass index (BMI) as well as the abdominal girth/ waist circumference and waist-to-hip ratio. [6,7] BMI is an assessment in relation to an individual's weight and height and is calculated as weight in kilograms (kg) divided by the square of height in meters (m^2). BMI generally increases with age and is usually higher amongst middle-aged people. [7] The representation of overweight and obesity determined by different measurements is given in Table 1.

Both waist circumferences and waist-to-hip ratio provide an independent prediction for weight-related health risk. For example, an individual with a high waist circumference is associated with an increased risk for high blood pressure, high cholesterol, type II diabetes and heart disease. [8] Furthermore, due to differences in ethnicity, waist circumference and/ or waist-to-hip ratio is considered an improved measurement to predict the relative disease risk compared to BMI. [9] For example, the BMI mean for the average African and Asian adult is 22-23 kg/ m^2 compared to 25-27 kg/ m^2 for Europeans and North Africans. Although these criteria are generally used to assess obesity, the degree of risk varies depending on ethnicity and BMI levels. [7]

Table 1. Representation of the most widely used criteria to assess obesity

Common obesity criteria	Assessment
Body Mass Index (BMI):	
Below 18.5	Underweight
18.5 - 24.9	Healthy weight
25.0 - 29.9	Overweight
≥ 30	Obese
Waist circumference:	
Male	
Waist > 37 inches (~ 94 cm)	Slight health risk
Waist > 40 inches (~ 102 cm)	High risk
Female	
Waist > 31 inches (~ 80 cm)	Slight health risk
Waist > 35 inches (~ 88 cm)	High risk
Waist-to-hip ratio:	
Male	
> 0.95	High risk
Female	
> 0.8	High risk

BMI of 30 - 34.9 and 35 - 39.9 kg/m^2 are classified as obesity classes I and II, respectively. Extreme obesity is classified as obesity class III, where the BMI ≥ 40 kg/ m^2.

Data modified from Centers for Disease Control and Prevention (CDC) and US National Heart, Lung, and Blood Institute (NHLBI). [6, 7]

1.1. Lifestyle changes

Modern-day individuals are continually striving for increased convenience in terms of lifestyle. For example, societies are moving away from traditional foods and the intensive preparation of meals. In contrast, mass-produced processed foods (higher in fat, lower in fiber and micronutrients) are becoming cheaper thereby resulting in increased demand. Moreover, the evolution of modern technologies has created a

new era of sedentary living. For example, modern society has growing access to conveniences such as microwaves, internet, cars, remote-controlled television, computer games, etc. [10] Increased fat consumption and reduced physical activity are considered major factors contributing to increased rates of global obesity and the subsequent development of type II diabetes (Table 2). [11]

Table 2. Lifestyle factors promoting obesity

Modern technologies:	**Lifestyle changes:**
• Processed food, internet shopping	• Less time in supermarket or kitchen
• Automated transportation	• Less movement (by foot) to reach destinations
• Television, computer games	• Children play less outside, prefer watching television or playing computer games [10]

2. Metabolic Syndrome

High incidences of obesity have contributed to the increased global prevalence of metabolic syndrome and its associated complications. [12, 13] Several definitions and criteria for metabolic syndrome have been proposed to identify individuals who are at high risk of developing type II diabetes and cardiovascular disease (CVD). However, at this stage consensus has not been reached. Currently, the most widely used definitions are a) the newly modified version from the International Diabetes Federation (IDF) that takes into account differences in ethnicity, b) US National Cholesterol Education Program's Adult Treatment Panel III (NCEP: ATPIII) and c) WHO (Tables 3 and 4). [13, 14]

Metabolic syndrome is a complex condition with a cluster of metabolic abnormalities, including insulin resistance, impaired glucose tolerance (IGT) and lipid metabolism, abdominal obesity, dyslipidemia, hyperglycemia and hypertension. Moreover, it is regarded as a precursor to type II diabetes and associated with increased risk of CVD. [15]

Table 3. Comparison of metabolic syndrome definitions from the International Diabetes Federation (IDF), US National Cholesterol Education Program's Adult Treatment Panel III (NCEP: ATPIII) and World Health Organization (WHO)

IDF, 2004	BMI >30 kg/m^2 or waist circumference >85-94 cm (male); >80-90cm (female) (range with different ethnic specific cutoffs – Table 4) *Plus 2 or more of the following:* 1. Dyslipidemia: triglycerides >1.7 mmol/L. 2. HDL <1.03 mmol/L (male); <1.29 mmol/L (female) or specific treatment for these lipid abnormalities. 3. Hypertension: blood pressure >130/85 mm Hg or treatment of previously diagnosed hypertension. 4. Fasting plasma glucose ≥5.6 mmol/L (subsequent oral glucose tolerance test is strongly recommended) or previously diagnosed type II diabetes.
NCEP:ATPIII, 2001	*Three or more of the following:* 1. Central obesity: waist circumference >102 cm (male); >88 cm (female). 2. Dyslipidemia: triglycerides ≥1.7 mmol/L. 3. HDL <1.0 mmol/L (male); <1.3 mmol/L (female). 4. Hypertension: blood pressure ≥130/85 mm Hg or medication. 5. Fasting plasma glucose ≥6.1 mmol/L.
WHO, 1999	Diabetes/ impaired fasting glycemia/ impaired glucose tolerance/ insulin resistance (hyperinsulinemia, euglycaemic clamp-glucose uptake in lowest 25%) *Plus 2 or more of the following:* 1. Obesity: BMI >30 kg/m^2 or waist-to-hip ratio >0.9 (male); >0.85 (female). 2. Dyslipidemia: triglycerides ≥1.7 mmol/L. 3. HDL <0.9 mmol/L (male); <1.0 mmol/L (female). 4. Hypertension: blood pressure >140/90 mm Hg. 5. Microalbuminuria: albumin excretion >20 μg/min.

Table adopted and modified from Eckel et al. (2005) [13] *and Alberti et al. (2005).* [14]

Table 4. Waist circumference with different ethnic-specific cutoffs used for identification of metabolic syndrome

Ethnic group	Waist circumference (cm)	
	Male	Female
Europeans, Sub-Saharan Africans	≥ 94	≥ 80
South Asians, South and Central Americans	≥ 90	≥ 80
Chinese	≥ 90	≥ 80
Japanese	≥ 85	≥ 90

Table adopted and modified from Alberti et al. (2005). [14]

3. Type II Diabetes

The incidence of type II diabetes mellitus is a growing global phenomenon and represents a major threat to public health. [3] Epidemiological data published during 2000 reported more than 1.7 million of diagnosed diabetics worldwide. The number of diagnosed diabetic patients in South Africa is currently estimated at ~ 800,000. [3,4] Moreover, the WHO has projected that by 2030 ~ 1.3 million South Africans will be affected by this life-threatening disease (Table 5).

Table 5. The global prevalence of diabetes

Country	2000	2030
Africa	7,020,000	18,234,000
- South Africa	***(814,000)***	***(1,286,000)***
Eastern Mediterranean	15,188,000	35,941,000
America	33,016,000	66,812,000
Europe	33,332,000	47,973,000
South East Asia	46,903,000	119,541,000
Western Pacific	35,771,000	71,050,100
Total	**171,230,000**	**359,551,100**

Data obtained and modified from WHO. [16]

Available at: URL: Available at http://www.who.int/diabetes/facts/world_figures/en/index1.html

There are two types of diabetes i.e. Type I and Type II diabetes mellitus. Type I diabetes mellitus is also known as insulin-dependent diabetes mellitus (IDDM) i.e. in this condition the pancreas fails to secrete insulin. [12] Type II diabetes mellitus, the main focus of this project, is the most common form of diabetes and accounts for ~ 90% of all cases of diabetes diagnosed worldwide. Type II diabetes is also known as

non-insulin dependent diabetes (NIDDM). [17] It is a multifactorial disease that occurs primarily in adults aged 35 – 64 years, and results from impaired insulin sensitivity with progression of IGT. With the increasing incidence of childhood obesity, type II diabetes can occur in obese children even before puberty. [2, 18]

3.1. Type II diabetes and cardiovascular disease

The risk of diabetic patients developing ischemic heart disease and acute myocardial infarction are greater compared to non-diabetic individuals. [19] Evidence suggests that metabolic syndrome and type II diabetes cluster with cardiovascular complications like atherosclerosis, coronary heart disease (CAD) and cardiomyopathy. [13, 20, 21] For example, CAD is currently the single leading cause of death for US patients with type II diabetes, resulting in ~ 500,000 deaths in 2002. [17, 22] The incidence of total events from CAD increases steeply with age. Interestingly, the risk of males developing CAD is much higher and on average presents 10-15 years earlier compared to females (Table 6). [23, 24] This suggests that gender differences may protect especially young women against CAD.

Table 6. Prevalence of CAD increases with age

Age	Prevalence of CAD	
	Males	Female
45-54	6.7%	5.5%
55-64	13.1%	8.4%
65-74	17.7%	11.1%
≥ 75	18.6%	16.1%

Data obtained from Fordor et al. (2004). [24]

Since type II diabetes is the result of altered metabolism, I will now briefly review metabolism of the normal heart before discussing altered metabolic pathways associated with the diabetic phenotype.

3.2. Cardiac fuel substrate utilization

The normal human heart requires an abundant supply of energy ≈ 3.5 - 5 kg of adenosine triphosphate (ATP) to sustain its contractile function. [25] Glucose and fatty acids (FA) are the main fuels for the normal, postnatal mammalian heart. After uptake, fuel substrates are catabolized by intermediate metabolic pathways for energy production in mitochondria, the "power-houses" of the cell. However, substrate utilization by the heart is dynamic i.e. it has the capacity to select the most appropriate fuel substrate depending on the particular physiologic/ pathophysiologic context. For example, during conditions of oxygen lack (exercise, ischemia), cardiac glucose utilization is enhanced [25, 26] Here, cardiac metabolic remodeling occurs since glucose is a more fuel-efficient substrate when oxygen supply is limited. [25, 27]

3.2.1. Glucose metabolism

Glucose uptake from the bloodstream into cardiomyocytes is facilitated by glucose transporters (GLUTs). In the heart, two isoforms predominate i.e. GLUT 1, the fetal isoforms, and GLUT 4 the insulin-responsive adult transporter. [25, 28] After uptake, glucose is rapidly phosphorylated to glucose-6-phosphate by hexokinase (HK). Subsequently, it is converted to fructose-6-phosphate which in turn is converted to fructose-1, 6-bisphosphate by phosphofructokinase (PFK), the rate-limiting enzyme of glycolysis (Fig. 1). [29] Excess glucose can be stored as glycogen and can be reconverted to glucose-6-phosphate if required. [30] Fructose-1, 6-bisphosphate is metabolized to pyruvate via several steps. [29] Pyruvate is transported into the mitochondrion where it is catabolized to acetyl coenzyme A (acetyl-CoA) by pyruvate dehydrogenase (PDH), the rate-limiting enzyme of glucose oxidation. However, under anaerobic conditions lactate is formed from pyruvate. Acetyl-CoA produced from the oxidative decarboxylation of pyruvate represents the link between glycolysis and the citrate acid cycle. Reducing equivalents (NADH and $FADH_2$) from the citrate acid cycle subsequently enter the mitochondrial respiratory chain leading to mitochondrial ATP production, essential for normal cardiac contractile function. [25, 31]

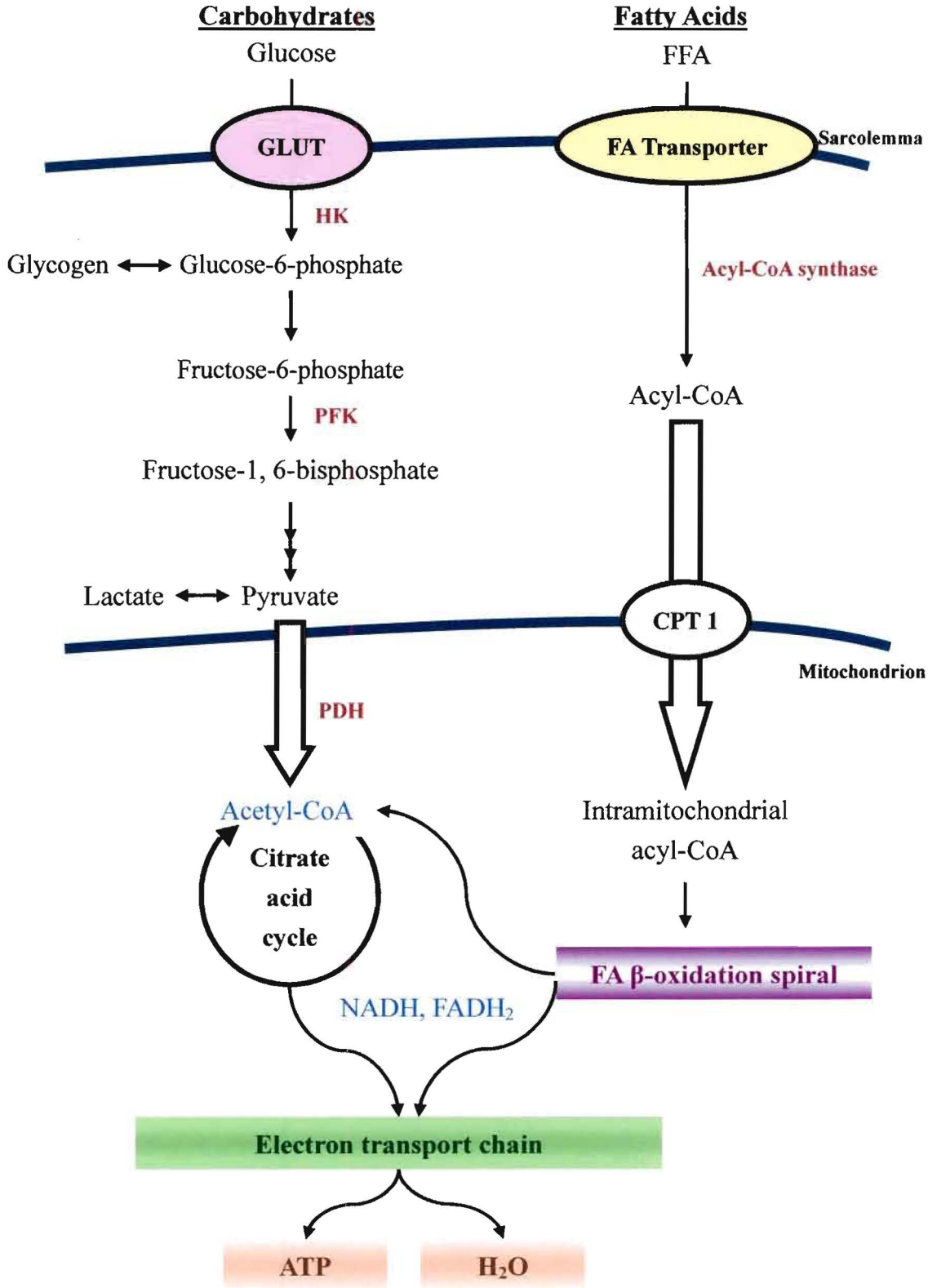

Figure 1. Fuel substrate utilization by the normal heart. *Glucose transporter (GLUT), hexokinase (HK), phosphofructokinase (PFK), pyruvate dehydrogenase (PDH), acetyl coenzyme A (acetyl-CoA), carnitine palmitoyltransferase-1 (CPT1) and acyl coenzyme A (acyl-CoA).*

3.2.2. Fatty acid metabolism

FAs have multiple functions, including its role as a primary energy source for the adult mammalian heart. [25] Moreover, FAs can also act as mediators of signal transduction. For example, pervious studies have shown that FAs may activate protein kinase C (PKC), leading to the initiation of the apoptotic cascade. [32] Furthermore, increased dietary FA intake not only augments the availability of FAs as a fuel substrate, but can also activate FA metabolic genes by acting as ligands for nuclear transcription factors such as peroxisome proliferator-activated receptor alpha (PPARα). [33]

FAs are stored as triglycerides (TG) in adipose tissue and released into circulation by lipolysis. [29] Free FAs (FFA) are taken up from the bloodstream via several sarcolemmal FA transporters, including fatty acid binding protein (FABP) and fatty acid transporter (FAT). [15] Upon uptake into cardiomyocytes, FFAs are activated by acyl coenzyme A (acyl-CoA) synthase to form FA acyl-CoAs that are imported into the mitochondrion via the carnitine palmitoyltransferase (CPT) shuttle (Fig. 1). [34] Here, carnitine palmitoyltransferase-1 (CPT1), located on the outer mitochondrial membrane, is the rate-limiting step of mitochondrial FA uptake. After uptake into the mitochondria, FA acyl-CoAs subsequently undergo β-oxidation generating reducing equivalents (NADH, $FADH_2$).

NADH and $FADH_2$, common products arising from glucose and fatty acid metabolic pathways, will subsequently enter the mitochondrial respiratory chain, the final common pathway in mitochondrial oxidative phosphorylation. Here, oxidation of reducing equivalents generates an electrochemical proton gradient ($\Delta\mu H^+$) across the inner mitochondrial membrane (Fig. 2). As protons re-enter the mitochondrial matrix

via ATP synthase, this potential energy is used to generate ATP. It is estimated that more that 90% of mitochondrial ATP is generated at this step. [29, 35]

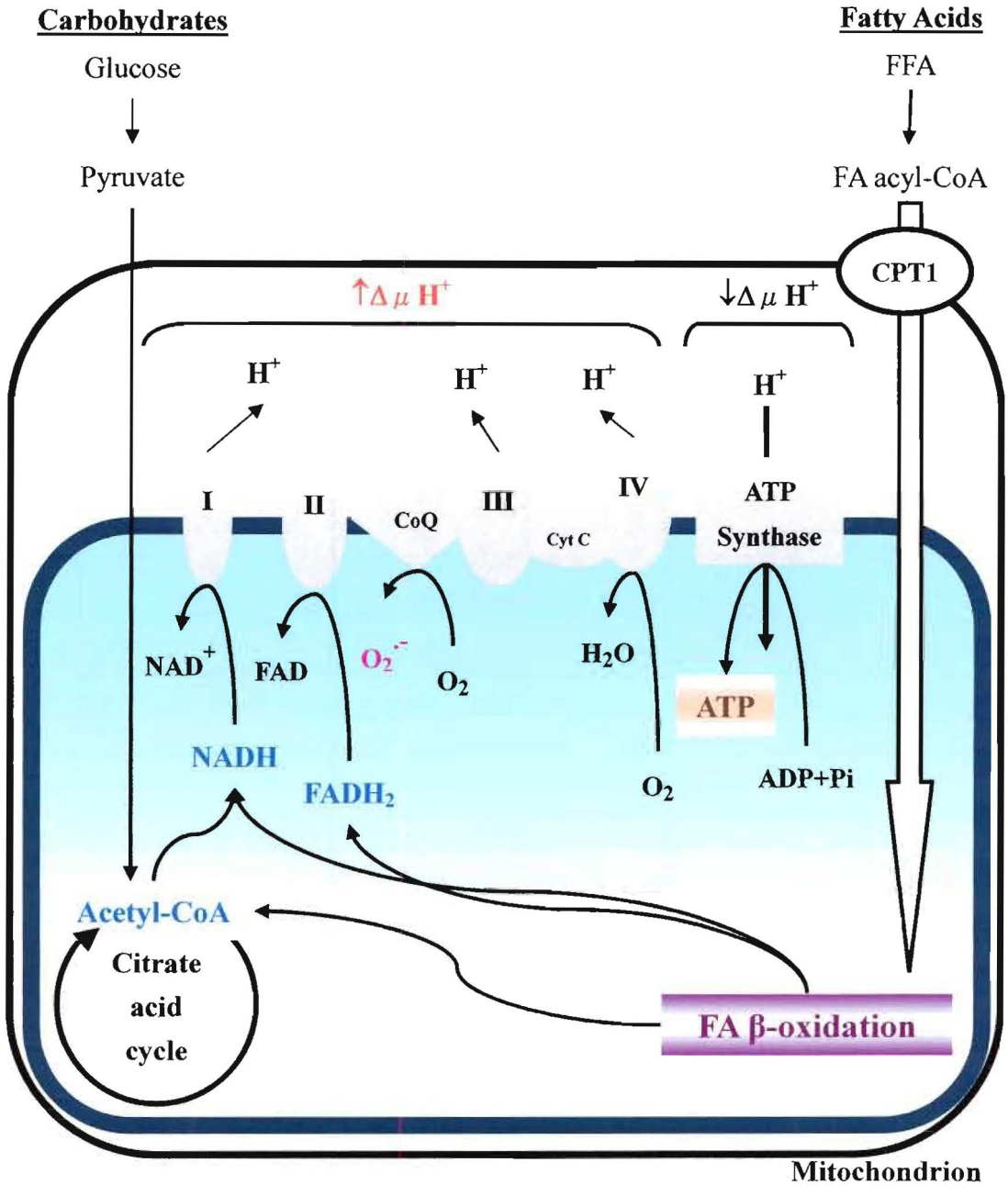

Figure 2. Mitochondrial oxidative phosphorylation. *Diagram of a mitochondrion represents the outer (thin line) and inner (thick line) mitochondrial membranes. Superoxide is produced by coenzyme Q (CoQ) embedded within the inner mitochondrial membrane. Electron donors from the citrate acid cycle (NADH and $FADH_2$) generate an electrochemical proton gradient ($\Delta\mu H^+$) across the inner mitochondrial membrane. $\Delta\mu H^+$ decreases as protons re-enter the matrix, generating ATP via ATP synthase. Mitochondrial complex I – NADH-Ubiquinol Oxidoreductase (I), complex II – Succinate-Ubiquinol Oxidoreductase (II), complex III – Ubiquinol-Cytochrome c Oxidoreductase (III), complex IV – Cytochrome c Oxidase (IV).*

3.2.3. Insulin and leptin: pivotal regulators of fuel substrate utilization

Intracellular glucose and FA levels are tightly regulated by circulating insulin. [25] The main function of insulin is to lower elevated postprandial blood glucose levels. [25, 30, 36] Two major mechanisms for insulin-mediated glucose uptake have thus far been identified (Fig. 3):

1) Insulin promotes glucose uptake and increases both the expression and translocation of glucose transporters (e.g. GLUT 4) to the sarcolemma, thereby promoting glucose metabolism. [37] Insulin is thought to promote these effects by binding to its receptors and initiating a tyrosine kinase cascade via activated protein kinases. Increased tyrosine phosphorylation activates insulin receptor substrate-1 (IRS-1), subsequently leading to an activation of phosphatidylinostitol-3 kinase (PI3 Kinase) and protein kinase B (PKB, also known as Akt). Akt/ PKB activation results in translocation of insulin and GLUT 4 from intracellular vesicles to the sarcolemma, thereby increasing capacity for glucose uptake. Activation of Akt/ PKB also stimulates pro-survival pathways which inhibit apoptosis, the programmed cell-death pathway. [25]

2) Insulin suppresses the secretion of FFAs from adipose tissue, thereby reducing FFA supply, metabolism and its inhibitory effects on glycolysis. Here it is proposed that elevated FFA supply and subsequent FA oxidation result in increased acetyl-CoA/ CoA and NADH/ NAD^+ production. These by-products of FA oxidation are thought to activate PDH kinase, an inhibitor of PDH. This in turn will result in reduced glucose oxidation. [38] Thus, inhibition of FA oxidation should reduce the inhibitory effects on pyruvate oxidation, thereby stimulating glucose utilization. [25, 38]

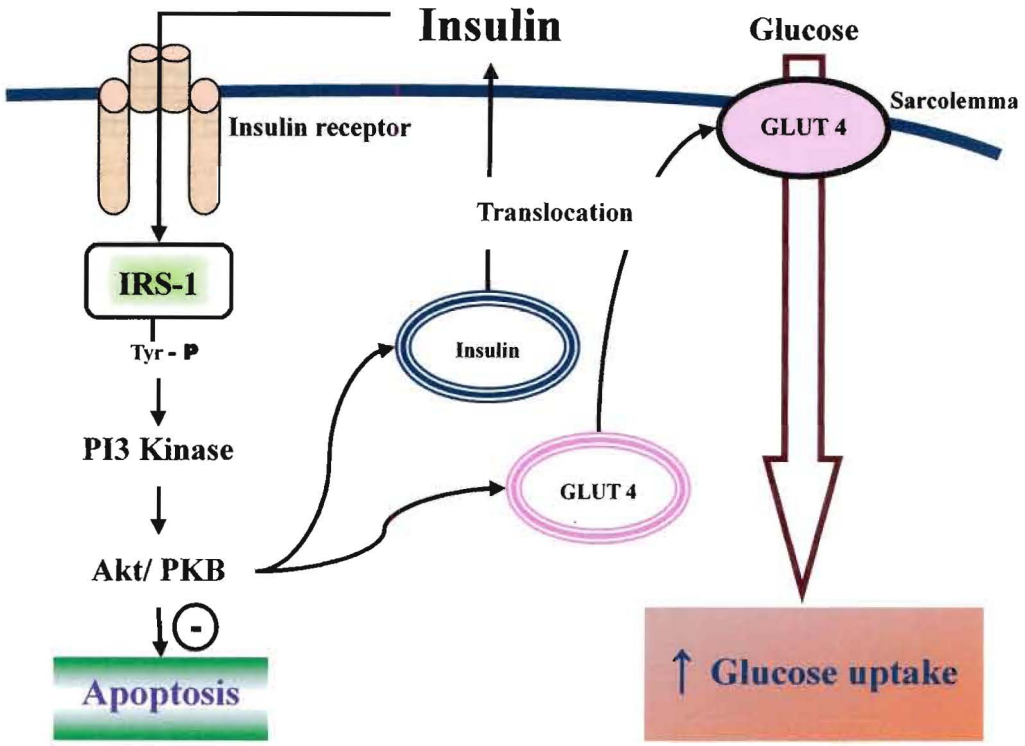

Figure 3. Action of insulin. *Insulin, via its receptor, stimulates glucose uptake by increasing the translocation of insulin and glucose transporter-4 (GLUT 4) to the sarcolemma. It also stimulates pro-survival pathways (inhibit apoptosis and promote growth) regulated by PI3 Kinase and Akt/ PKB. Insulin receptor substrate -1 (IRS-1), tyrosine phosphorylation (Tyr-P), phosphatidylinostitol-3 kinase (PI3 Kinase), protein kinase B (PKB, also known as Akt), glucose transporter-4 (GLUT 4).*

Leptin, another important liporegulatory hormone, is thought to act in concert with insulin. [39, 40] It is secreted by adipose tissue and acts via Janus kinase/ signal transducers and activator of transcription (JAK/ STAT) pathways. Leptin is known to regulate energy balance by decreasing food intake, increasing energy expenditure and stimulating adipose proliferation via the hypothalamus. [41-43] It regulates many well-known insulin downstream targets such as IRS-1, PI3 kinase, Akt/ PKB and mitogen-activated protein (MAP) kinase.

Since its discovery in 1994, [44] many studies have shown that leptin stimulates cardiac FA metabolism by a number of mechanisms i.e. a) upregulating the release of FFAs

from adipose tissue, b) increasing FA oxidation capacity in peripheral tissues and c) reducing lipogenic capability. [43, 45] If such liporegulatory effects are impaired for e.g. due to leptin deficiency or leptin resistance, this will result in hyperphagia. [43] In agreement with this, studies have also found that hyperleptinemia is often associated with diet-induced obesity and subjects display reduced responsiveness to leptin treatment. [46, 47] Leptin deficiency (low leptin levels) or resistance results in hyperplasia and obesity which has been suggested to play a role in the development of metabolic syndrome i.e. it lowers insulin secretion and is associated with hyperinsulinemia. [48]

3.3. Type II diabetes: altered metabolic signatures

The causes of metabolic syndrome and type II diabetes are attributed to central obesity as a consequence of excess nutrient intake, sedentary lifestyle and genetics. [13, 49] However, these causes share a common factor i.e. the inability of insulin to adequately respond to increases in systemic glucose and FFA levels. Resulting lipid/ lipoprotein abnormalities and impaired glucose metabolism, ultimately leads to major metabolic consequences such as hyperglycemia and dyslipidemia. [13, 38]

Insulin resistance is the basis of the pathophysiology of metabolic syndrome and type II diabetes. [13, 38] Himsworth [50] was the first to suggest that patients with diabetes should be divided into "insulin sensitive" and "insulin insensitive" categories and argued that "all causes of human diabetes could be explained by deficiency of insulin". Hence "the more insulin sensitive an individual, the better off he or she is".[17]

3.3.1. FFAs and reduced insulin sensitivity

Reduction of insulin sensitivity has been attributed to the abundant supply of circulating FFAs. [13] FFAs are released mainly from TGs stored in adipose tissue. Here, lipoprotein lipase releases FFAs into circulation through lipolysis. [51] Insulin has profound modulatory effects on systemic FFA levels i.e. it inhibits lipolysis thereby reducing FFA release. [52]

In healthy individuals, increased insulin infusion resulted in reduced systemic FFA while glucose levels remained constant. [53] However, in patients with metabolic syndrome and diabetes, insulin appears to be less efficient/ sensitive in suppressing systemic FFA releasing from adipose tissue and regulating its metabolism. [15] In contrast to the normal physiologic context, insulin increases rather than inhibits lipolysis in this instance. [54] As a result, circulating FFA levels are further increased. Although FFAs have the ability to stimulate insulin secretion, prolonged exposure to excessively high FFA levels is thought to reduce insulin secretion through increased β-cell apoptosis. [13, 55, 56]

Excessive circulating FFA levels have been suggested to not only contribute to insulin resistance, but have also been implicated in reduced glucose uptake in peripheral tissues like skeletal muscle and heart. [13, 38, 57]

3.3.2. FFAs and impaired glucose transport/ oxidation

Patients with elevated FFA supply display impaired insulin action on glucose metabolism. [58, 59] This includes increased hepatic gluconeogenesis and attenuated insulin-mediated glucose transport and oxidation. [27, 36, 60] Potential FFA-mediated inhibitory mechanisms of glucose metabolism are explained below.

FFAs reduce insulin sensitivity and inhibit insulin-mediated glucose uptake in skeletal muscle. [59] This is the consequence of FFA-induced inhibitory effects on insulin-mediated glucose transport. [58, 61] Here, the concept proposed is that increased FA uptake exceeds oxidation capacity leading to the accumulation of intracellular FA metabolites such as acyl-CoAs, diacylglycerol (DAG) and ceramides. It has been suggested that these metabolites activate PKC and a downstream serine/ threonine kinase cascade. [32, 59, 62] This in turn leads to increased serine phosphorylation of IRS-1, thereby blocking IRS-1 tyrosine phosphorylation and inhibiting the activity of PI3 kinase and Akt/ PKB, major stimulators of GLUT 4 translocation. This inhibition results in impaired insulin-mediated glucose transport. Moreover, inhibition of the Akt/ PKB mediated pro-survival pathway will be expected to promote apoptosis (Fig. 4).

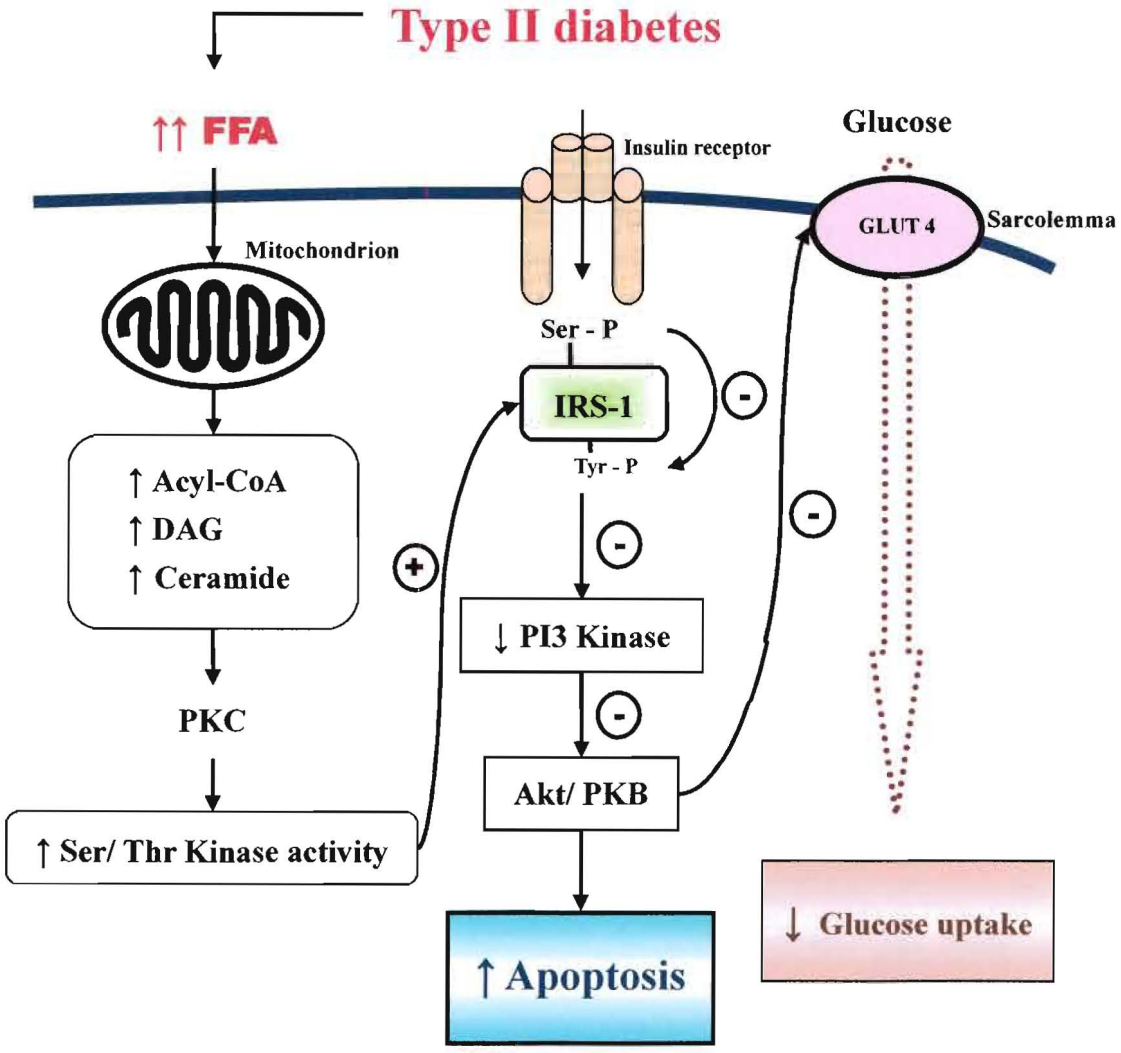

Figure 4. Potential mechanisms of FA-induced impairment of insulin-mediated glucose transport. *With type II diabetes, prolonged exposure to excessive FFA levels increase intracellular FA acyl-CoA, DAG and ceramide content which may lead to an impairment of insulin signaling and inhibition of insulin-mediated glucose transport. Excess intracellular FA acyl-CoA may also promote apoptosis via inhibition of Akt/PKB and ceramide-induced lipoapoptosis. Acyl coenzyme A (acyl-CoA), diacylglycerol (DAG), insulin receptor substrate -1 (IRS-1), serine phosphorylation (Ser-P), tyrosine phosphorylation (Tyr-P), phosphatidylinostitol-3 kinase (PI3 Kinase), protein kinase B (PKB, also known as Akt), glucose transporter (GLUT 4).*

Based on Randle's theory, [38] increased FA oxidation will result in the inhibition of glucose oxidation. Elevated FA oxidation increases the production of acetyl-CoA/ CoA and NADH/ NAD^+ which activates PDH kinase, an inhibitor of PDH. Reduced glucose oxidation rates are thought to lead to an accumulation of upstream

metabolites e.g. fructose-6-phosphate and pyruvate. [34] Previous studies reported that the rate of glycolysis was reduced in isolated perfused diabetic hearts and in normal hearts perfused with fatty acids and ketones. [38, 49, 63] The authors suggested that elevated systemic FFA levels leads to an increase in glycogen content, which may contribute to the reduced rates of glycolysis observed with diabetes. [38, 49, 63] Thus, glycolysis and glucose oxidation are downregulated in the diabetic heart (Fig. 5). [13, 36, 64] Moreover, it has been shown that dichloroacetate, a PDH kinase inhibitor, increases pyruvate oxidation and myocardial contractility in diabetic and to a lesser extent in healthy subjects. [57] These results provide additional support for the concept that attenuated PDH activity plays an important role in impaired contractile function observed in diabetic patients.

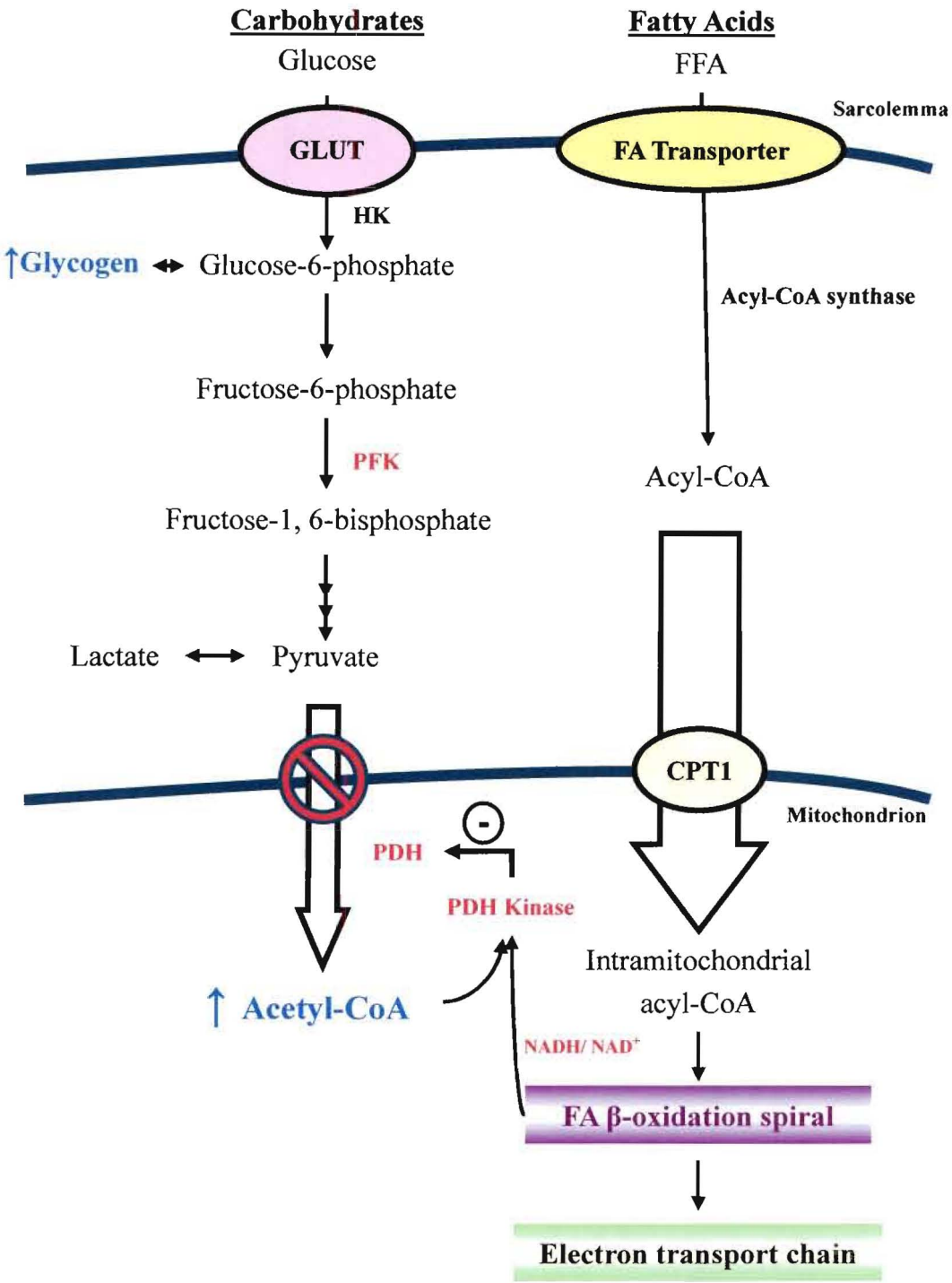

Figure 5. Inhibition of pyruvate oxidation during diabetes. *Increased FFA supply and uptake leads to elevated rates of FA oxidation. As a result, increased acetyl-CoA/ CoA and NADH/ NAD^+ stimulate the acitivity of pyruvate dehydrogenase (PDH) kinase which in turn inactivates PDH, causing the inhibition of glucose oxidation. Increased citrate levels will also downregulate PFK, the rate-limiting enzyme of glycolysis. Carnitine palmitoyltransferase 1 (CPT1) and glucose transporter (GLUT).*

3.3.3. FFAs and hyperinsulinemia/ hyperglycemia

A previous study has reported that not only insulin resistant diabetic patients but also ~ 25% of non-obese insulin resistant patients developed impaired glucose tolerance. [65] Hollenbeck *et al.* (1987) [66] and Golay *et al.* (1986) [65] have suggested that it is normal for patients with insulin resistance to develop glucose tolerance as a compensatory effect. They argued that when these patients produce sufficient insulin to compensate for the insulin resistance to maintain euglycemic state, it reflects the ability of β-cells to regulate insulin secretion. However, if β-cells cannot sustain the hyperinsulinemic state, it will lead to a gross decompensation of glucose homeostasis. [66, 17] Together with the FFA-induced hepatic gluconeogenesis and the impairment of insulin-stimulated glucose transport and oxidation, severe hyperglycemia will develop (Fig. 6). [27, 36, 60]

Moreover, increased circulating insulin stimulates a) release of pro-inflammatory cytokines such as interleukin 6 (IL-6), tumour necrosis factor α (TNFα) and C-reactive protein, and b) inhibits the release of anti-inflammatory cytokines for e.g. adiponectin. [13, 61]

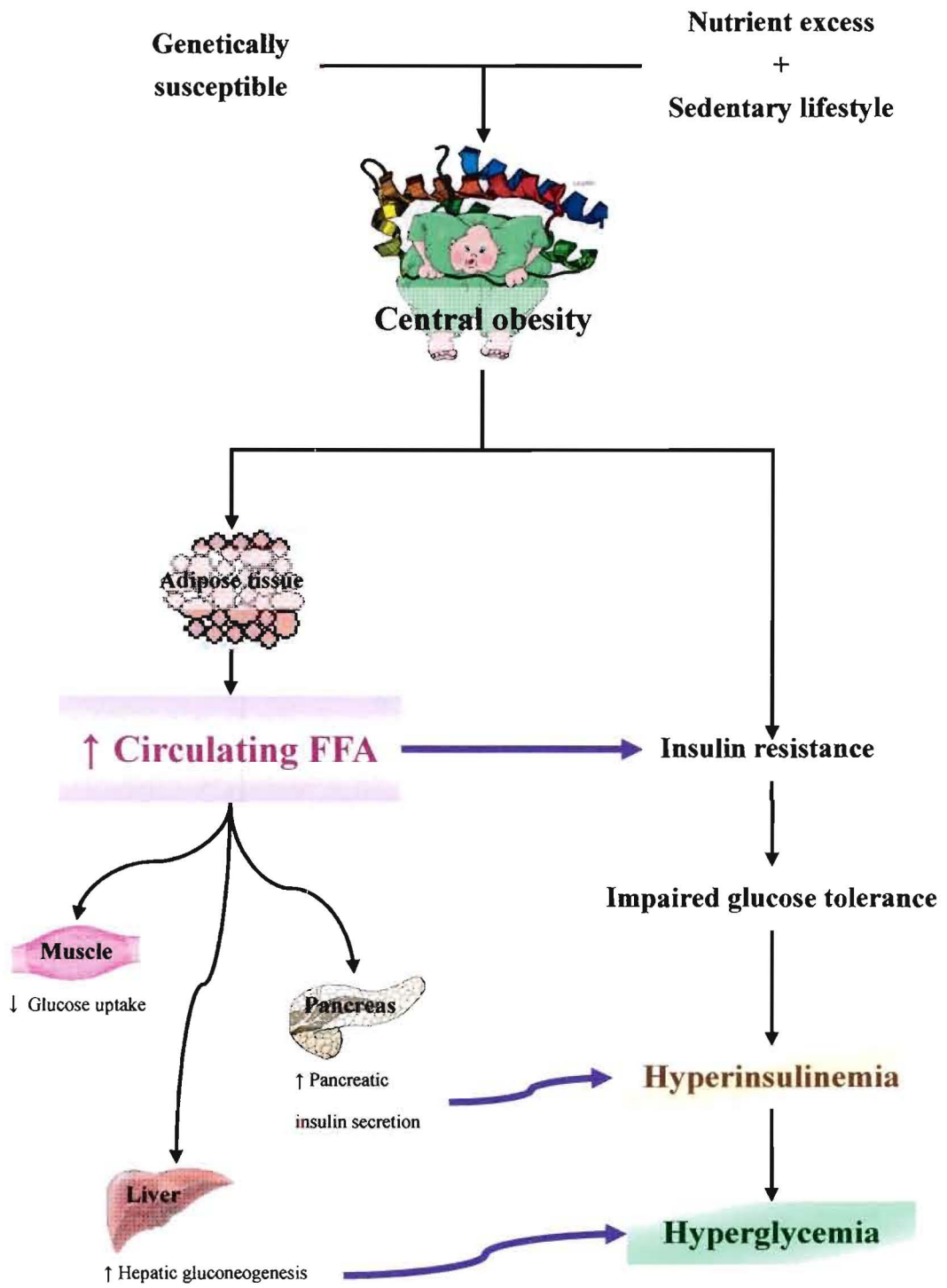

Figure 6. Development of hyperinsulinemia and hyperglycemia due to excess FFA.

3.3.4. FFAs and dyslipidemia

With diabetes, due to the inability of insulin to respond to the increase in systemic circulating FFA levels, lipoprotein abnormities occur. Here, increased FFA flux to the liver stimulate an overproduction of hepatic TG and TG-rich very low density lipoproteins (VLDL) into the circulation. [67] It also suppresses the production of the beneficial high-density lipoproteins (HDL) and lipoprotein lipase leading to inhibitory effects on lipoprotein degradation. [13]

Diabetic hearts with insulin resistance are continuously exposed to a hyperlipidemic and hyperglycemic environment. [26] It initially adapts to this condition by increasing the gene expression of various proteins involved in FA oxidation and utilization e.g. PPARα and its target genes like CPT1 and uncoupling protein 3 (UCP3). [68, 69] However, as soon as sarcolemmal FA uptake exceeds its oxidative capacity, FAs begin to accumulate in organs like liver, pancreatic islet, skeletal muscle, cardiac muscle, etc. This phenomenon of lipid deposition is often referred to as "lipotoxicity" (Fig. 7).

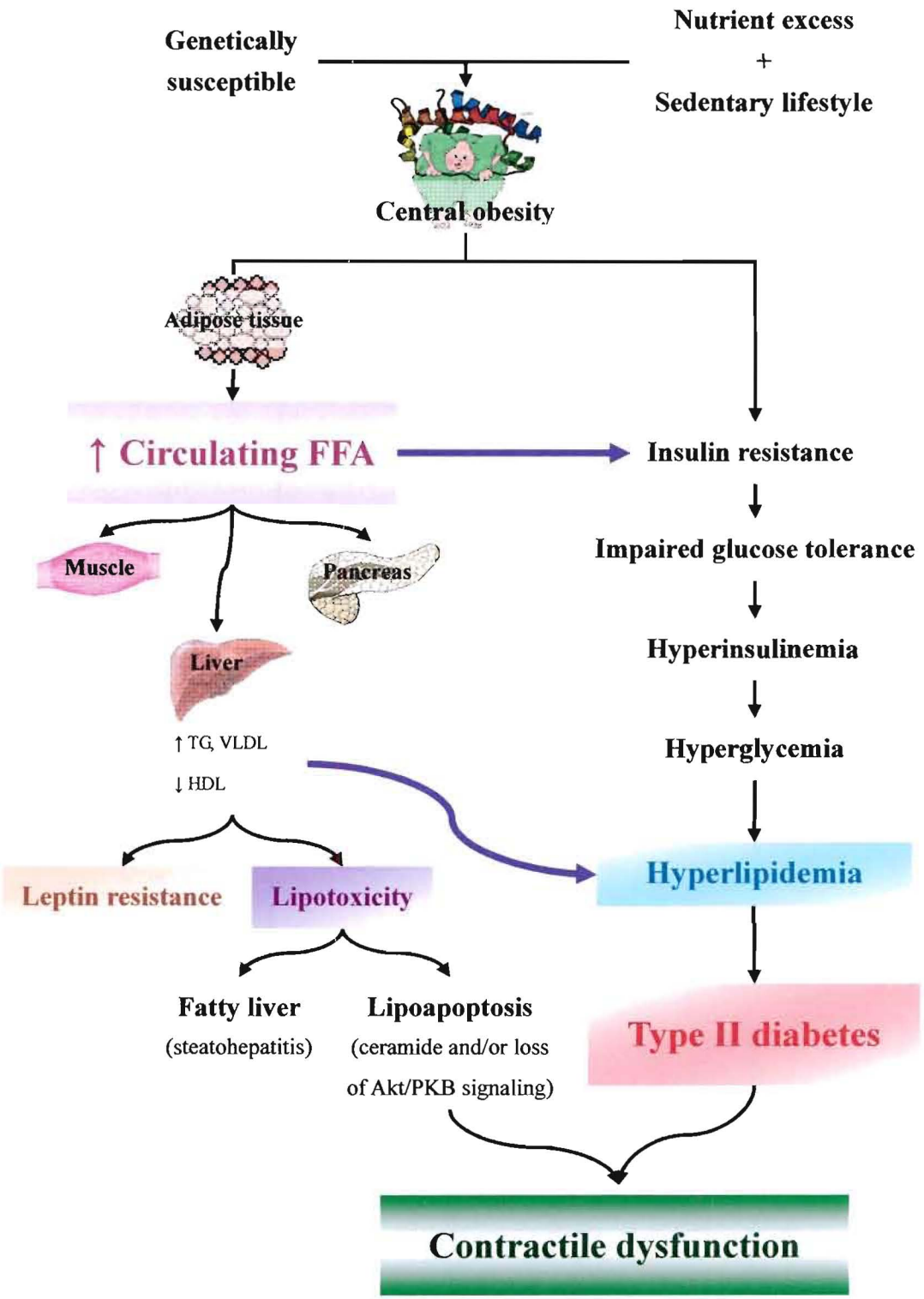

Figure 7. Lipotoxicity. *Lipotoxicity is a consequence of lipid overload which results in intracellular FA accumulation in organs like liver and cardiac muscle. Subsequently, central and peripheral leptin resistance and lipid-induced programmed cell death "lipoapoptosis" through de novo ceramide lipotoxicity may occur. Prolonged exposure to this harmful environment will eventually lead to contractile dysfunction of the heart. Triglyceride (TG), very low-density lipoprotein (VLDL) and high-density lipoprotein (HDL).*

Lipid accumulation (lipotoxicity) in the liver i.e. non-alcoholic steatohepatitis (NASH) has been described clinically. [70, 71] Lipotoxicity includes lipid-induced programmed cell death i.e. "lipoapoptosis". Here, *de novo* ceramide formation and excessive ROS production have been implicated as prime mediators of this condition. [72-74] Prolonged exposure of the heart to this metabolic environment may contribute to the reduction of cardiac contractile function. [26, 27, 75, 76] For example, in the clinical setting this pathological abnormality may result in lipotoxic cardiomyopathy. [49, 63]

3.3.5. Perturbation of mitochondrial energy production

Recently, it has been reported that increased FA oxidation flux associated with the diabetic phenotype results in downregulation of nuclear-encoded genes necessary for mitochondrial oxidative phosphorylation. [69] Also, pivotal transcriptional modulators regulating mitochondrial biogenesis were reported to be downregulated with diabetes. [77] Moreover, increased FA oxidation flux induces mitochondrial superoxide production from co-enzyme Q (CoQ) of the electron transport chain. [35] FA-induced superoxide is associated with increased mitochondrial uncoupling in obese hearts. [35, 78] Such metabolic perturbations are thought to mediate mitochondrial dysfunction, thereby contributing to the development of contractile dysfunction of the diabetic heart. [79]

Elevated systemic FFA levels have been associated with increased expression of uncoupling proteins (UCPs), located within the inner mitochondrial membrane. [69, 80-82] Two isoforms i.e. uncoupling protein 2 (UCP2) and uncoupling protein 3 (UCP3) are expressed in the heart. UCP2 is ubiquitously expressed whereas UCP3 is enriched mainly in skeletal muscle and heart. [79-81] The precise functional roles of UCPs in the heart are still unclear. However, some have proposed that cardiac UCPs

uncouple mitochondrial oxidative phosphorylation by translocation of protons from the inter-mitochondrial membrane space into the matrix. [83] Conversely, other functional roles for cardiac-enriched UCPs include the regulation of lipid oxidation, efficiency in energy production of the heart, and acting as an antioxidant defense system to prevent lipid-induced oxidative damage in the heart. [80, 81, 84, 85] For example, a starvation and refeeding study demonstrated a positive correlation between FFA concentration and UCP3 gene expression, suggesting that UCP3 may be involved in the regulation of FA oxidation. [79, 86] On the other hand, UCP2 is thought to form part of the antioxidant defense mechanism in the heart, acting to prevent damaging ROS production. [84, 85, 87, 88] Additional studies are required to fully delineate the precise roles of UCPs in the heart.

Elevated FA utilization is a hallmark of the obese and diabetic heart. [27, 82, 89] Recently, a study done by Carley *et al.* (2005) [27] has shown reduced cardiac efficiency (work/ myocardial oxygen consumption) in the working rat heart when perfused with high FA levels and myocardial oxygen consumption (MVO_2) was unchanged. However, Boudina *et al.* (2005) [82] reported increased MVO_2 and reduced cardiac efficiency in ob/ob mice, a transgenic mouse model of obesity-induced type II diabetes. Moreover, they found attenuated mitochondrial respiratory function in these mice. Differences in MVO_2 may be due to variation in animal models and/or experimental protocols employed. However, the latter study suggests that cardiac mitochondrial oxidation capacity is reduced in diabetic mice. This suggested "wastage" of oxygen and possibly due to uncoupling of mitochondrial ATP production and oxygen consumption. The precise mechanisms for this reduction are not fully understood, although it has been suggested that elevated circulating FFAs may increase mitochondrial uncoupling and ROS production,

thereby reducing contractile function (Fig. 8).

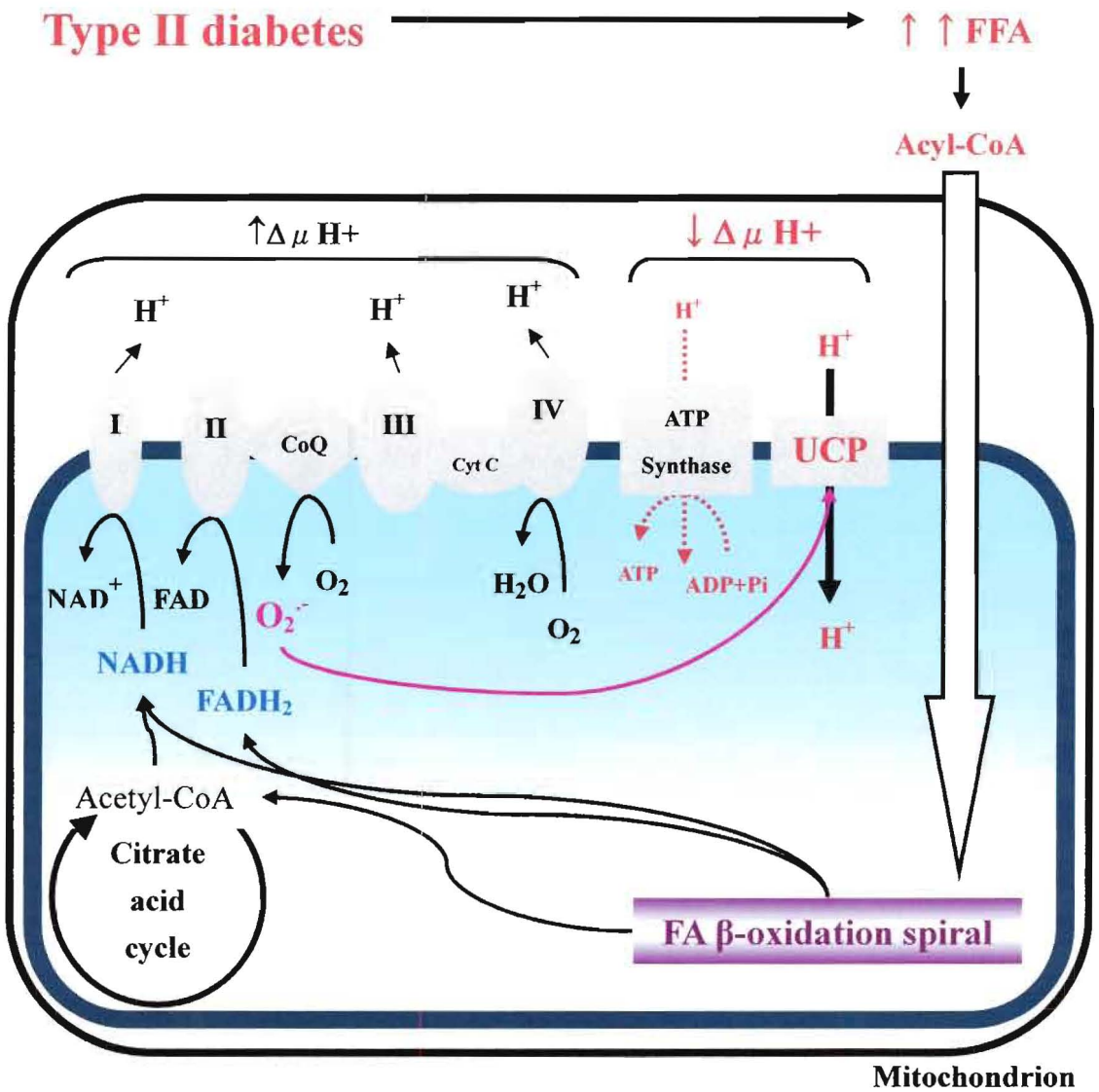

Figure 8. Mitochondrial dysfunction may result from FA-induced mitochondrial uncoupling and increased ROS production. *Diagram of a mitochondrion represents the outer (thin line) and inner (thick line) mitochondrial membranes. UCPs may increase proton leak across the mitochondrial inner membrane and decrease the electrochemical potential, thereby reducing the production of ATP. Superoxide generated by coenzyme Q (CoQ), is suggested to promote additional proton leak and thereby further reducing mitochondrial ATP production. Mitochondrial complex I – NADH-Ubiquinol Oxidoreductase (I), complex II – Succinate-Ubiquinol Oxidoreductase (II), complex III – Ubiquinol-Cytochrome c Oxidoreductase (III), complex IV – Cytochrome c Oxidase (IV).*

Interestingly, a recent study has shown that males produce approximately twice the amount of mitochondrial hydrogen peroxide (H_2O_2) compared to females. [90] Here, higher HDL cholesterol levels and antioxidant gene expression for e.g. glutathione and manganese-superoxide dismutase (Mn-SOD) have been suggested to contribute to diminished oxidative damage in females. [90, 91, 92, 93] An interesting question therefore arises i.e. what activates/ causes such gender-protective mechanisms? It is possible that such differences may be attributed (in part) to hormonal profiles. In agreement, a recent study showed that estrogen exerts an antioxidant effect by upregulating antioxidant gene expression via MAP kinase signaling and nuclear factor kappa B (NF-$_K$B) transcriptional effects. [93]

4. Hypothesis

With obesity-induced insulin resistance/ type II diabetes, excessive FFA supply decreases mitochondrial bioenergetic capacity. Moreover, we propose that females possess innate cardioprotective programs that will result in enhanced bioenergetic capacity compared to males (Fig. 9).

To investigate our hypothesis, we measured cardiac mitochondrial respiratory function and histological parameters in two rodent models of obesity i.e. a) a diet induced-obesity rat model and b) an obesity-induced type II leptin receptor deficient diabetic mouse model (db/db):

1. Mitochondrial respiratory functional analysis in cafeteria diet-induced obese Wistar rats.
2. Age-dependent mitochondrial respiratory function in male db/+ and db/db mice aged 10-12 weeks and 18-20 weeks, respectively.
3. Gender-dependent mitochondrial respiratory function by comparing male and female db/+ and db/db mice at age 18-20 weeks.
4. Pilot study of mitochondrial respiratory function by comparing male and female db/+ and db/db mice at age 55-56 weeks.

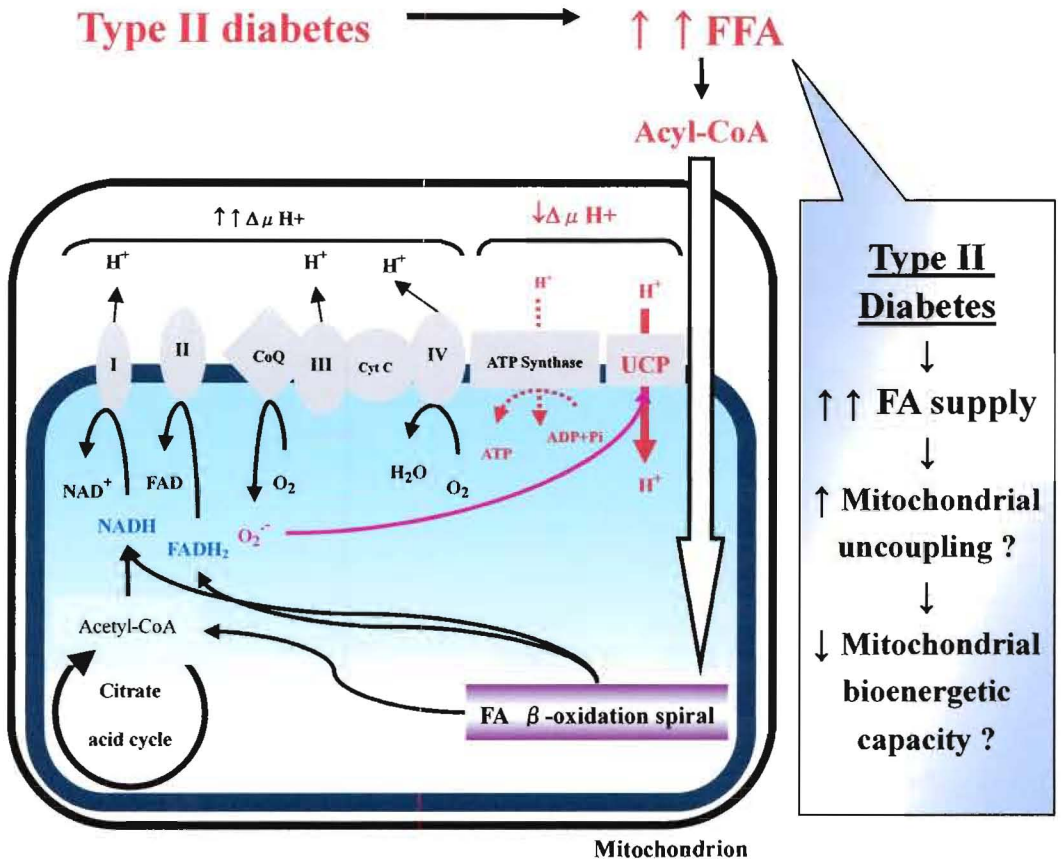

Figure 9. Schematic of proposed hypothesis. *Elevated FFA supply to the insulin resistant/diabetic heart increases mitochondrial uncoupling via cardiac-enriched uncoupling proteins, thereby reducing mitochondrial energy production. Mitochondrial complex I – NADH-Ubiquinol Oxidoreductase (I); complex II – Succinate-Ubiquinol Oxidoreductase (II); complex III – Ubiquinol-Cytochrome c Oxidoreductase (III); complex IV – Cytochrome c Oxidase (IV); coenzyme Q (CoQ); cytochrome c (Cyt c); uncoupling proteins (UCP).*

II: ANALYSIS

5. Material and Methods

5.1. Choice of rodent models of obesity and type II diabetes for this study

Most studies investigating mitochondrial respiration in diabetes were performed using streptozotocin (STZ)-induced type I diabetic animal models. Since obesity-related type II diabetes is a "growing epidemic" in the 21st century, genetically modified rodent models have been developed to more closely simulate the phenotype of type II diabetes e.g. db/db, ob/ob and Zucker fatty rats (ZDF) models. [27] These animal models exhibit the phenotype of obesity, insulin resistance, hyperglycemia and dyslipidemia (Table 7).

Table 7. Phenotypic characterization of rodent models with type II diabetes

Model	Obesity	Plasma glucose	Plasma FA	Plasma TG
Mutations in leptin receptor:				
• **db/db mouse**	↑↑	↑↑	↑	↑
• **ZDF rat**	↑	↑↑	↑	↑↑
Mutations in leptin:				
• **ob/ob mouse**	↑↑	↑	↑	no change

Data obtained and modified from Carley et al. (2005) [27]

The db/db mouse is an inbred strain with a point mutation in the leptin receptor gene, (Lepr). [27] Plasma insulin levels increase as early as day 10 in db/db mice, with β-cell hypertrophy. [76] As body weight increases (3-4 weeks), insulin resistance begins to set in and hyperglycemia develops. By 6 weeks, db/db mice are beginning to become

metabolic syndrome i.e. plasma glucose, insulin, plasma TG and FA levels are elevated associated with a reduction in cardiac power and output. [76, 94, 95] By 8-12 weeks, the pancreatic β-cells hypertrophies and plasma insulin content reaches the peak which will then drop back to normal levels. [94, 96] However, heterozygous mice (db/+) are phenotypically normal.

Notably, the metabolic profile of type II diabetes in db/db mice is similar to the human condition. Thus it makes the db/db strain an ideal rodent model for obesity, metabolic syndrome and type II diabetes research.

For the purpose of the present study, we employed two rodent models of obesity to investigate our hypothesis i.e. a) a diet-induced obese rat model and b) genetically modified mouse model (db/db) to imitate the progression from obesity-induced insulin resistant state (diet-induced obese rat model) to a type II diabetes state (db/db mouse model).

5.2. Diet-induced obese rat model (cafeteria diet feeding)

This section of the study forms part of a collaborative project with Dr. Eugene du Toit of the Department of Medical Physiology at the University of Stellenbosch. Six-week-old male Wistar rats (200 g) were housed under conditions of constant temperature and humidity and exposed to a 12 hour light-12 hour dark cycle with access to food and water *ad libitum*. Rats were randomly assigned in two groups: control and obese. Rats from the control group were fed with normal chow comprised of 60% carbohydrate, 30% protein and 10% fat. Rats within the obese group were fed a cafeteria diet for 16 weeks. Cafeteria diet composed of 65%

carbohydrate, 19% protein and 16% fat (refer Appendix). Animals were anesthetized using a combination of sodium pentobarbital (100 mg/kg intra-peritoneally) and heparin (50 International Units, Centaur Labs). Fasting plasma insulin, HbA1c test (glycosylated hemoglobin A1c test), non-esterified fatty acid (NEFA), TG and HDL cholesterol levels were measured by members of Dr. du Toit's laboratory. Unlike daily blood glucose testing, no fasting is required for the HbA1c test. It is regarded as a more precise measurement of hyperglycemia. The test measures the level of glycosylated hemoglobin. It provides a clearer profile of glucose levels of over the course of several months.

5.2.1. Mitochondrial isolation

Mitochondria were isolated using the method of Sordahl *et al.* (1971) [97] with modifications. Ventricular tissues (the whole heart) were minced and rinsed thoroughly to prevent blood contamination which affects the quality of isolated mitochondria and consequently reduces the rate of mitochondrial respiration. Thereafter, the tissue was gently homogenized in 3 ml ice-cold potassium-EDTA (KE) isolation buffer (Appendix) using a glass homogenizer (Tenbroek, Netherlands) and the homogenate was centrifuged at 755g (Beckman J2-21M, USA) for 5 minutes at 4 °C to eliminate the cellular debris. The supernatant was subsequently centrifuged at 1,480g for 5 minutes and the mitochondrial pellet resuspended gently in 100 µl of incubation buffer (Appendix) and kept on ice at all times. Mitochondrial protein concentrations were determined using the method of Lowry *et al.* (1951). [98]

5.2.2. Protein quantitation

Five µl of mitochondrial protein was added into 1 ml of distilled water (performed in duplicate). One ml of solution A (Appendix) was added to the sample and incubated

for 10 minutes at room temperature followed by the addition of 0.5 ml solution B (Appendix) for 30 minutes to allow for the development of full color. Due to the short half-life of the latter reagent, the mixture was vortexed immediately upon addition of solution B. A standard curve was constructed using 2 μg/μl of bovine serum albumin fraction V (BSA) (Sigma, Germany) and was prepared as detailed in Table 8. The sample is read in a spectrophotometer (Varian 130 dual beam) at 750 nm wavelength and the concentration of the sample protein was expressed as microgram of mitochondrial protein per 5 μl.

Table 8. Construction of standard curve for protein quantitation

BSA quantity	Distilled water added	Amount of 2μg/μl BSA added
0	1000 μl	0
5 μg	997.5 μl	2.5 μl
10 μg	995 μl	5 μl
20 μg	990 μl	10 μl
50 μg	975 μl	25 μl
100 μg	950 μl	50 μl
150 μg	925 μl	75 μl
200 μg	900 μl	100 μl

5.2.3. Standard mitochondrial oxygen consumption parameters

Mitochondrial respiratory function was polarographically measured at 25°C using a thermostatically controlled Clark-type electrode and a rapid stirring device (Hansatech Instruments, London, UK). Incubation buffer (Appendix) was used to calibrate the respirometer and a baseline reading was recorded (for 1 minute) to verify the calibration. Experiments were performed using glycolytic (glutamate) and fatty acid (malate and carnitine-L-palmitoyl [MCP]) substrates, respectively.

Respiratory parameters were determined as described previously. [88]

To initiate experiments, 50 µl of heart mitochondria was added (after 1 minute equilibration) to the electrode chamber containing 340 µl incubation buffer. Mitochondrial respiration was initiated by the addition of substrate for e.g. 12.5 mM glutamate. State 3 respiration was stimulated by the addition of ADP to a final concentration of 714 µM. Mitochondrial respiration was also measured using fatty acid substrates (3.3 mM of malate and 54 µM of CP).Total volume of the reaction was 819 µl.

Standard respiratory parameters measured include:

State 1 respiration - mitochondrial endogenous oxygen consumption before the addition of substrates.

State 2 respiration - mitochondrial endogenous oxygen consumption before the addition of ADP.

State 3 respiration - mitochondrial oxygen consumption stimulated by ADP, where oxygen is used to phosphorylate ADP to ATP.

State 4 respiration - mitochondrial oxygen consumption after completion of ADP phosphorylation. It is a marker for endogenous uncoupling.

ADP/O ratio - ratio between nmol of ADP phosphorylated and oxygen consumed (in atoms) during state 3 respiration. It is an indicator for the ability of mitochondria to link oxygen used for the phosphorylation of ADP. [Babsky; 2001]

Rate of phosphorylation - nmol of ADP phosphorylated per minute during state 3 respiration. [Estabrook; 1967]

5.2.4. Percentage recovery of state 3 respiration after anoxia

The ability of mitochondria to recover respiratory capacity after an anoxic stress was also determined. Here, anoxia was achieved by addition of ADP to a final concentration of 7.14 mM after state 4 respiration was reached (Fig. 10). The underlying principle being that a 10 times more concentrated ADP concentration added to the closed chamber will result in all remaining oxygen in the chamber being used to convert ADP to ATP until an anaerobic condition has been reached. The chamber was sealed for 20 minutes after ADP addition. The chamber was thereafter opened for 1 minute of reoxygenation (open chamber and bubble through using disposable plastic pipette). Thereafter, the oxygraph chamber was closed again and state 3 respiration determined for the remaining substrate. The rate of recovery of state 3 respiration after 15 minutes of anoxia was determined by measuring the oxygen uptake for 5 minutes and the percentage of recovery after 20 minutes of anoxia was calculated as per the following equation:

% Recovery of state 3 respiration = (State 3a / State 3) x 100.

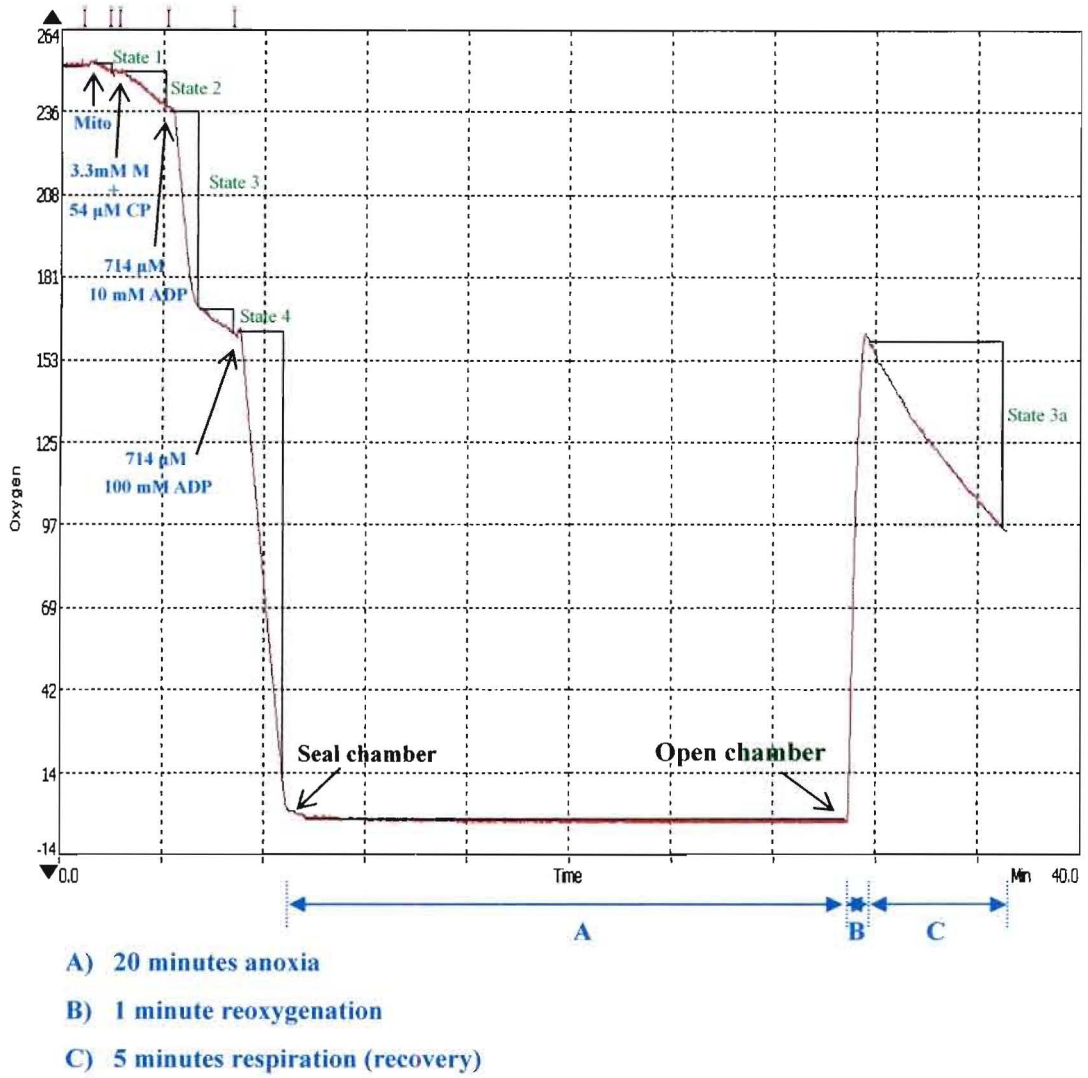

Figure 10. Experimental protocol of mitochondrial respiration in response to an anoxic stress. *A typical polarographic trace of oxygen consumption during anoxia-reoxygenation. State 2 respiration was stimulated by 3.3 mM malate and 54 µM carnitine-L-palmitoyl. State 3 respiration was stimulated by the addition of 714 µM ADP. Anoxia was achieved by addition of 714 µM of 100 mM ADP after state 4 respiration was reached. Mitochondria (Mito), malate (M) and carnitine-L-palmitoyl (CP).*

5.3. Transgenic mouse model of type II diabetes

Leptin receptor deficient db/db mice (aged 10-12, 18-20 and 55-56 weeks) were housed under conditions of constant temperature and humidity and exposed to a 12 hour light-12 hour dark cycle. Free access to standard mouse chow and water were allowed for the duration of experiments. Two genotypes were included in this study

i.e. the age-matched heterozygous control db/+ and homozygous mutant db/db mice. Based on previous studies from our collaborators in Norway, age-dependent changes in cardiac metabolism were detected i.e. at ages 10-12 weeks and 16-18 weeks. [75] For this study we employed two time points i.e. 10-12 and 18-20 weeks. We also did a pilot study at a later time point i.e. 55-56 weeks. Animals were anesthetized using sodium pentobarbital (50mg/kg intra-peritoneally, Centaur Labs) and heparinized to prevent blood clotting (50 International Units, UNIPRINT-L). Subsequently, mouse hearts were dissected out for mitochondrial isolation. All animals used in this study were the BKS.Cg-m+/+Lepr^{db}/J strain, obtained from the Animal Unit of University of Cape Town's Faculty of Health Sciences and The Jackson Laboratories (Bar Harbor, Maine). Experiments were approved by University of Cape Town's Animal Research Ethics Committee and the investigation conforms to the Guide for the Care and Use of Laboratory Animals published by the US National Institutes of Health (NIH Publication No. 85-23, revised 1996).

Stavinoha *et al.* (2004) [99] demonstrated a diurnal variation in cardiac fatty acid metabolism, with greatest responsiveness being displayed during the dark cycle. In light of this, we employed a reverse dark cycle to ensure that our experimental work was performed during the middle of the dark cycle. Three weeks before mice were to be sacrificed they were housed in a separate animal room. The strict 12 hour light-12 hour dark cycle regime was enforced (lights switched on at 4:00 pm and switched off at 4:00 am and termed zeitgeber time [ZT] 0 and 24, respectively). Two weeks before mice were sacrificed, fasting blood glucose levels were measured using a glucose-meter (ACCU-CHEK® Active Meter, Roche) after a 6 hours fast. For the 55-56 week time point, levels of ketone bodies were measured using a urine test strip

(UriCHECK 9, South Africa). After 3 weeks of acclimatization, mice were euthanized at ZT 17 - 19.

Note: Heparin is known to stimulate the activity of lipoprotein lipase. It acts upon TG associated with blood lipoproteins, resulting in release of FFAs. Hence, heparin is not suitable for blood collection and determination of plasma FFA levels. [100]

5.3.1. Mitochondrial isolation

Mitochondria were isolated using the method of Sordahl *et al.* (1971) [97] as described in section 5.2.1. with modifications. After homogenization, the homogenate was centrifuged at 660g (Sigma 202MK, Germany) for 5 minutes at 4 °C to eliminate the cellular debris. The supernatant was subsequently centrifuged at 960g for 5 minutes and the mitochondrial pellet resuspended gently in 50 µl of incubation buffer (Appendix) and kept on ice at all times. Mitochondrial protein concentrations were determined using the method of Lowry *et al.* (1951) as described in section 5.2.2. [98]

5.3.2. Standard mitochondrial oxygen consumption parameters

Mitochondrial respiratory function was polarographically measured at 25 °C using a thermostatically controlled Oxytherm equipped with Clark-type electrode and a rapid stirring device (Hansatech Instruments, London, UK). Incubation buffer (Appendix) was incubated in the Oxytherm for approximately one minute before the start of each experiment, during which time a baseline reading was recorded and used to verify the calibration. Experiments were performed using fatty acid (MCP) as substrate. After one minute of equilibration period, 25 µl of heart mitochondria was added to the electrode chamber containing incubation buffer to a final volume of 420 µl. Mitochondrial respiration was initiated by the addition of substrates for e.g. 7 mM

malate and 25 μM CP. State 3 respiration was stimulated by the addition of 300 μM of ADP.

5.3.3. Percentage recovery of state 3 respiration after anoxia

Similar to diet-fed rats, anoxia was achieved by the addition of an additional 300 μM of ADP after state 4 respiration was reached. A 10 times more concentrated ADP solution was added to the closed chamber to facilitate maximal mitochondrial respiration. As a result, oxygen in the closed chamber was all used to convert ADP to ATP and an anaerobic condition was reached. The chamber was sealed for 20 minutes followed by 1 minute of reoxygenation (open chamber and bubble throughout using a disposable plastic pipette). Thereafter, the oxygraph chamber was closed again and the remaining substrates were used for mitochondrial respiration. The rate of recovery after 20 minutes anoxia was estimated by measuring 5 minutes of the oxygen uptake. The percentage of recovery after anoxia was calculated the same way as for the diet fed rats:

% Recovery of state 3 respiration = (State 3a / State 3) x 100.

5.3.4. Determination of plasma glucose levels

Blood was collected by cardiac puncture at both experimental time points to determine the plasma glucose levels. Body weights were measured after the animals were anesthetized using a combination of ketamine and xylosine (50mg/kg intra-peritoneally). Blood was collected and left at room temperature for one hour before centrifugation (Sigma 202 MK) at 660g for 5 minutes to obtain maximum plasma yield and prevent blood clotting. A 10 μl aliquot of plasma was sent to the

Department of Chemical Pathology (Groote Schuur Hospital, South Africa) to determine plasma glucose levels. It was measured using a spectrophotometric glucose oxidase method. [101]

5.3.5. Measurement of mitochondrial ATP

Mitochondrial ATP concentration was assayed using a luciferin-luciferase luminometry luminescence method modified from Fryer *et al.* (2000) [102]. Freshly isolated mitochondria were placed into boiling water (3 x sample volume) for 10 minutes and thereafter on ice for 10 minutes to disrupt mitochondrial membranes. The mixture was subsequently centrifuged at 960g for 5 minutes (Sigma 202MK, Germany) at 4 °C. A 10 µl of supernatant was added into 175 µl of distilled water and 25 µl firefly (Bioluminescent Somatic Cell Assay Kit (FL-AA), Sigma Germany). The principle being that firefly contains luciferin and luciferase, commonly used in medical research laboratories worldwide, two rare chemicals which are not able to be produced synthetically. The reaction of luciferin-luciferase mixture, energy donor (ATP) and oxygen results in the emission of light. The intensity of the bioluminescence detected from the luminometer was used to be determined the concentration of mitochondrial ATP within the mitochondria. Mitochondrial protein concentration was determined using the Lowry assay [98], and the standard curve was constructed using 1 x 10^{-5} M to 1 x 10^{-9} M of ATP. The concentration of mitochondrial ATP was expressed as micromolar of cellular ATP per milligram of mitochondrial protein.

5.3.6. Histology and electron microscopy

After the mouse hearts were weighed to determine the heart to body weight ratio, the remaining heart tissues were collected for histological analysis. A total of six cross sections of heart tissues were collected for histology and three small portions of the left ventricle were collected for electron microscopy (EM). Small portions of heart tissues generated from cardiac puncture were stored in 10% formaldehyde (formalin) for hematoxylin and eosin (H&E) staining and glutaraldehyde for osmium tetroxide (O_SO_4) staining or EM. All tissue specimens were stored in fixative and sent to the Department of Anatomical Pathology, University of Cape Town for further preparation (Appendix). Electron microscopic analysis was performed at the Electron Microscopy Unit, University of Cape Town. Five representative blocks on the grid were selected and the whole area was examined under high magnification 25 000X. Pictures were taken of representative mitochondria.

Tissue specimens are generally prepared via the following steps: [103]

Fixation - *To stabilize and preserve fresh tissue morphology and molecular composition.* Routine fixation such as formaldehyde (formalin) and glutaraldehyde are used to stabilize molecular structure to minimize shrinkage and swelling. The advantage of formaldehyde is the higher rate of tissue penetration compared to glutaraldehyde or O_SO_4. Thus, this procedure allows for large blocks of tissue to be fixed. However, formaldehyde is not the ideal fixative for EM, yielding poorer image quality compared to O_SO_4.

Embedding - *To provide support to sectioning.* A thin tissue section can be sliced by embedding tissue specimens into a solid material such as plastic paraffin wax or resin.

Sectioning/ slicing *- To provide very thin specimen for microscopy.* A typical thickness for light microscopy is 4-6 μm and 50-100 nm for EM.

Staining *- To provide a visual contrast in the transparent tissue sections and help distinguish intracellular compartmentation and different ultrastructural components.* For light microscopy studies, colored stains (termed chromophores) such as H&E staining are widely used. However, for EM studies, electron-dense heavy metal salts such as lead citrate and uranyl acetate are employed. Most of the colored stains bind selectively to particular components due to their chemical behavior. The basic stain with an affinity for negatively charged nuclei and ribosomes are termed basophilic. The acid stain with an affinity for positively charged cytoplasm and mitochondria are termed acidophilic.

i) Hematoxylin and eosin staining

The combination of hematoxylin and eosin is the most widely used general purpose stains i.e. useful in visualizing the various tissue components and differentiating one cell component from another. Hematoxylin is a basic stain with an affinity for basophilic cell components like nuclei and ribosomes-stains deep purple or blue color. The acidic eosin stains cytoplasm, mitochondria, muscle and connective tissues in pink (Appendix). [104]

ii) Osmium tetroxide staining

O_SO_4 has a strong affinity for lipid. It is not only used as a fixative but as a stain for lipids as well. It is one of the oldest stains for visualizing unsaturated fatty acids (it reacts primarily with the double carbon bonds of unsaturated fatty acids such as oleic acid) although it is primarily employed as a post-fixative in electron microscopy. The

well documented advantages of O_SO_4 are the preservation of the ultrastructural features, strong affinity for lipids and osmium blackening. The reduction of unsaturated fatty acids and the alcohol dehydration result in osmium blackening (staining) which is responsible for improved visualization and ultrastructural preservation (Appendix).

iii) Electron microscopy

Electron microscopy functions the same way as normal light microscopy except that it uses a highly energetic electron beam to provide higher magnification of specimens. The two types of electron microscopy include a) two dimensional transmission electron microscopy (TEM), and b) three dimensional scanning electron microscopy (SEM). In this study we employed TEM to investigate ultrastructural abnormalities of mitochondria isolated from diabetic mice. TEM uses the transmission of an electron beam that is focused on a metal aperture and magnified by a series of condenser lenses. The beam transmits to the specimen and is then focused by the objective lens. The objective aperture is used to enhance the contrast and the intermediate and the projector lenses magnify the image. These interactions are detected and the enlarged image of the specimen is then projected onto the monitor or computer system. [105]

5.4. Statistical analysis

The data is presented as mean ± standard error of the mean (S.E.M.). Statistical significance between the groups was performed using the unpaired Student's t-test using GraphPad InStat version 3.06 (GraphPad Software, USA). Values were considered significant when $p<0.05$.

III: RESULTS

6. Rat Model of Diet-Induced Obesity

This part of the study forms part of a collaborative project with Dr. Eugene du'Toit (Dept. Medical Physiology, University of Stellenbosch Medical School).

6.1. Baseline metabolic characterization

After three months of cafeteria diet feeding, body weight was significantly higher in the fed group compared to controls (504.7±12.1 vs. 456.8±16.2 gram [$p<0.05$]) (Table 9).

Table 9. Metabolic parameters in rats fed cafeteria diet for 3 months

	Control	Obese
Body weight (g)	456.8±16.2	504.7±12.1 *
Heart: body weight ratios (x 1000)	2.6±0.02	2.9±0.02 *
Fasting plasma glucose (mmol/L)	4.8±0.2	5.25±0.2
Fasting plasma insulin (µIU/ml)	27.8±3.5	43.4±4.2 *
HbA1c (% Glycosylation)	3.5±0.1	4.0±0.1 §
FFA (mM)	0.8±0.1	1.7±0.3 *
Total cholesterol (mmol/L)	1.4±0.1	1.3±0.1
TG (mmol/L)	0.7±0.1	2.0±0.2 §
HDL (mmol/L)	0.9±0.02	0.6±0.04 §

Values are expressed as mean ± S.E.M. for 6-13 animals.

** $p<0.05$ compared with age-matched control rats.*

§ $p<0.001$ compared with age-matched control rats.

Also, obese rats displayed significantly increased heart: body weight ratios. Moreover, fasting plasma insulin, HbA1c test, NEFA and TG levels were significantly elevated and HDL cholesterol level was significantly reduced in the fed group versus controls. These parameters (Table 9) were measured by members of Dr. du Toit's laboratory.

6.2. Mitochondrial respiration

Mitochondria were isolated and respiratory function assessed using standard protocols. We also employed different oxidative substrates to gain some insight regarding fuel substrate utilization i.e. glycolytic (glutamate) and fatty acid (MCP). Endogenous mitochondrial respiration (state 2) was decreased from 22.2±1.0 to 19.2±0.6 nmol/min/mg protein ($p<0.05$) in mitochondria isolated from obese rats when incubated with MCP (Table 10). However, no differences were detected when glutamate was employed as substrate. State 3 respiration and ADP/O ratio were similar for obese and control mitochondria. ADP phosphorylation rate was decreased from 278.1±8.3 to 245.6±11.3 nmol/min/mg protein ($p<0.05$) in mitochondria isolated from obese rats when incubated with MCP (Fig. 11) Furthermore, state 4 respiration did not differ when MCP was employed as oxidative substrate. However, when glutamate was used as substrate, state 4 respiration was reduced from control values of 10.5±1.4 to 5.9±1.0 nmol/min/mg protein ($p<0.05$) for mitochondria isolated from obese mice.

Table 10. Standard respiratory parameters for cardiac mitochondria isolated from diet-induced obese rats and its control littermates

	Glutamate		Malate and carnitine-L-palmitoyl	
	Control	**Obese**	**Control**	**Obese**
State 2 respiration (nmol/min/mg protein)	11.2±1.1	10.8±1.2	22.2±1.0	19.2±0.6 *
State 3 respiration (nmol/min/mg protein)	123.4±15.9	121.5±8.6	126.2±4.6	117.1±5.0
State 4 respiration (nmol/min/mg protein)	10.5±1.4	5.9±1.0 *	11.8±1.7	14.1±1.8
ADP/O ratio	2.4±0.1	2.3±0.03	2.2±0.06	2.1±0.04
Phosphorylation rate (nmol/min/mg protein)	298.7±44.6	248.0±22.4	278.1±8.3	245.6±11.3 *

Cardiac mitochondria were isolated as described in the Material and Methods section of this thesis. Respiration parameters were determined at 25°C using glycolytic (glutamate) or fatty acid (malate and carnitine-L-palmitoyl [MCP]) substrates, respectively. Values are expressed as mean ± S.E.M. for 5-6 animals.

**$p<0.05$ compared with age-matched control rats.*

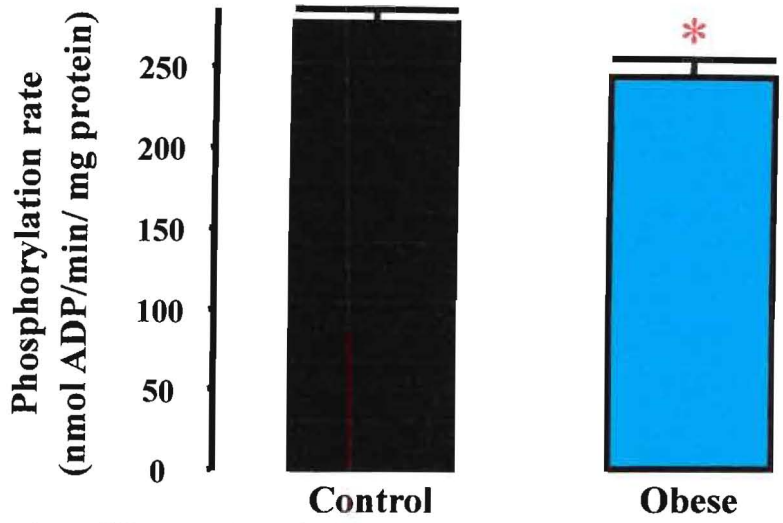

Figure 11. ADP phosphorylation rate in control vs. obese heart mitochondria. *MCP was used as substrate. Values are expressed as mean ± S.E.M. (n=5-6).*

**p<0.05 compared with age-matched control rats.*

To further assess the effects of diet-induced obesity on mitochondrial respiratory function, we exposed mitochondria to a 15 minute anoxic insult followed by 5 minutes of reoxygenation. We subsequently determined state 3 respiration (using MCP as substrate) as an index of mitochondrial function in response to the anoxic stress. Here, the percentage of state 3 recovery was significantly lower in mitochondria isolated from obese rats compared to controls (51.7±8.2 vs. 28.7±5.4 nmol/min/mg protein) (Fig. 12). These data suggest that mitochondria isolated from obese rats have altered respiratory capacity in response to acute oxygen depletion.

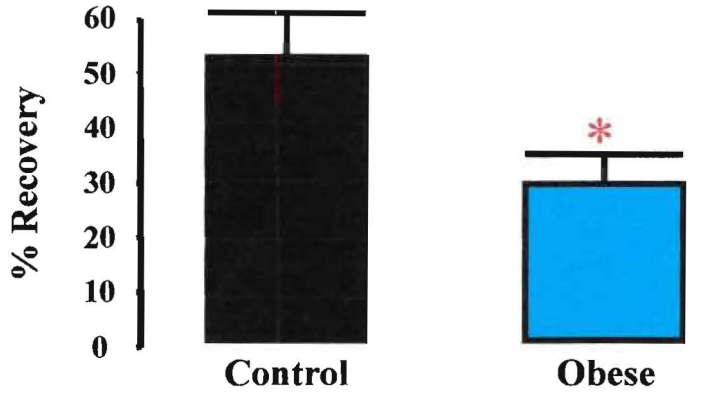

Figure 12. State 3 respiration recovery in isolated control vs. obese heart mitochondria when incubated with MCP. *MCP was used as substrate. Values are expressed as mean ± S.E.M. (n=5-6). *p<0.05 compared with age-matched control rats.*

7. Mouse Model of Obesity-induced Type II Diabetes

7.1. Temporal analysis of mitochondrial respiratory function

7.1.1. Baseline metabolic characterization (10-12 weeks)

For the second part of this study, we investigated mitochondrial respiratory function in a leptin receptor-deficient mouse model (db/db) of type II diabetes. This study formed part of a collaborative study with Dr. Ellen Aasum (Department of Medical Physiology, University of Tromso, Norway).

We began our investigations by analyzing metabolic changes in a temporal manner i.e. in db/db mice at the age of 10-12 weeks and 18-20 weeks, respectively. Earlier studies by our collaborators documented metabolic and functional changes in db/db mice aged 10-12 weeks versus control heterozygous littermates db/+. [95, 106] Here, they reported that body weight, plasma glucose, free fatty acid and insulin levels were significantly increased in db/db mice compared to controls (Table 11). Moreover, they found reduced contractile function in the db/db mouse compared to heterozygous control. [75, 106]

Table 11. Baseline metabolic characteristics of control heterozygous (db/+) and obese (db/db) male mice at 10-12 weeks of age

	10-12 weeks	
	db/ +	**db/db**
Body weight (g)	27.9±0.5	43.6±1.2 *
Plasma glucose (mmol/L) #	12.7±0.5	46.2±2.3 *
Plasma insulin (μIU/ml)	34±9	165±40 *
Plasma FFA (mmol/L)	1.4±0.1	2.1±0.2 *

Data adapted from Aasum et al. (2003). [75] *Values are expressed as mean ± S.E.M. for 4-16 animals. *$p<0.05$ compared with age-matched db/+ mice. # Postprandial levels were determined.*

For this thesis, we did not set out to re-measure these parameters in mice aged 10-12 weeks. However, when we compared 10-12 week old db/db vs. db/+ mice, gross macroscopic differences were readily apparent i.e. body mass and internal fat content were markedly increased for the obese db/db mice compared to matched controls (Figs. 13 and 14).

Figure 13. Photograph of the heterozygous control (db/+) (on the left) and homozygous mutant (db/db) (on the right) at age 10-12 weeks.

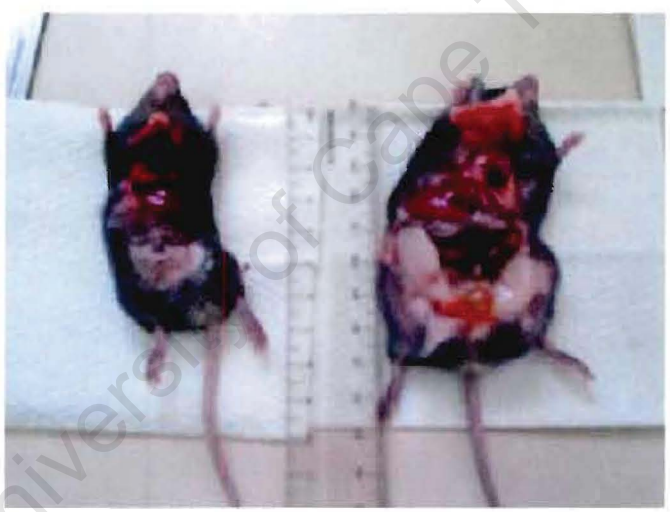

Figure 14. Internal fat content of the control mouse (db/+) (on the left) and matched homozygous mutant (db/db) (on the right) at age 10-12 weeks.

7.1.2. Baseline metabolic characterization (18-20 weeks)

At 18-20 weeks of age, we found that body weight was markedly increased in obese mice compared to matched controls (Table 12). Consonant with metabolic data for the earlier time point (10-12 weeks), we observed that plasma glucose levels were also significantly increased in the db/db mice versus controls. However, the degree of elevation was less when compared to the increase observed at the 10-12 weeks time

point (Note: plasma glucose levels at 10-12 weeks were measured by Dr. Ellen Aasum's laboratory and we used a glucose-meter [ACCU-CHECK® Active Meter, Roche] for the 18-20 week point).

Table 12. Baseline metabolic characterization of heterozygous (db/+) and diabetic (db/db) mice at 10-12 and 18-20 weeks of age

	10-12 weeks		18-20 weeks	
	db/+	db/db	db/+	db/db
Body weight (g)	28.3±0.7	47.0±0.8 *	28.0±0.7	47.2±1.7 §
Plasma glucose (mmol/L)	11.2±0.4	32.2±1.6 *	15.3±1.5	23.4±3.2 *
Insulin (µg/L)	1.2 ± 0.2	4.8 ± 0.8 *	N.D	N.D
FFA (mmol/L)	0.5 ± 0.04	1.03 ± 0.1 *	N.D	N.D

Data at 10-12 weeks was published in How et al. (2006). [106] *Values are expressed as mean ± S.E.M. for 6-19 animals.*

N.D = Not determined.

** $p<0.05$ compared with age-matched heterozygous db/+ mice.*

§ $p<0.001$ compared with age-matched heterozygous db/+ mice.

7.1.3. Mitochondrial respiration

After establishing baseline parameters, we next measured respiration in isolated mitochondria from db/+ and db/db hearts at the 10-12 week and 18-20 week time points. Here, state 2 respiration was similar between db/+ and db/db at both time points (Table 13).

Table 13. Respiratory parameters for mitochondria isolated from control (db/+) and obese (db/db) mouse hearts at 10-12 weeks and 18-20 weeks of age

	10-12 weeks		18-20 weeks	
	db/+	db/db	db/+	db/db
State 2 respiration (nmol/min/mg protein)	35.3±3.5	39.0±2.1	29.4±1.6	32.6±1.9
State 3 respiration (nmol/min/mg protein)	103.9±19.1	161.6±10.6 #	144.9±9.6	165.8±9.8
State 4 respiration (nmol/min/mg protein)	18.2±4.8	16.8±2.5	33.5±2.0 *	30.7±2.4 **
ADP/O ratio	2.2±0.1	2.4±0.1	2.5±0.08	2.6±0.1
Phosphorylation rate (nmol/min/mg protein)	307.6±19.1	392.3±36.1	363.4±28.3	435.9±32.3

Cardiac mitochondria were isolated as described in the Materials and Methods section of this thesis. Respiration rates were determined at 25°C with malate and carnitine-L-palmitoyl (MCP) as substrates. Values are expressed as mean ± S.E.M. for 5-13 animals.

 # $p<0.05$ compared with db/+ at 10-12 weeks.

** $p<0.01$ compared with db/+ at 10-12 weeks.*

*** $p<0.01$ compared with db/db at 10-12 weeks.*

At the 10-12 week point, state 3 respiration was significantly increased in db/db compared to control mice (161.6±10.6 vs. 103.9±19.1 nmol/min/mg protein) (Fig. 15). However, at 18-20 weeks of age, this increase was abolished and there was no significant difference in state 3 respiration between the db/+ and db/db heart mitochondria (Fig. 15).

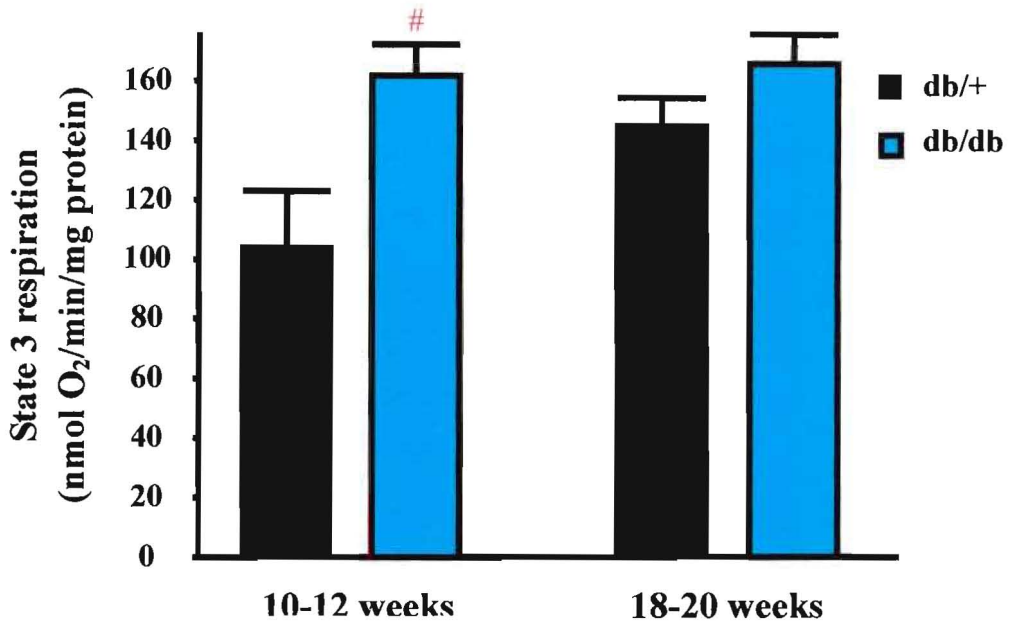

Figure 15. State 3 respiration rates for control (db/+) and obese (db/db) heart mitochondria at 10-12 weeks and 18-20 weeks of age. *MCP was used as substrate. Respiration rates are expressed as nmol of oxygen/minute/mg protein.*

 # $p<0.05$ compared with db/+ at 10-12 weeks.

State 4 respiration was elevated at the 18-20 week time point versus the 10-12 week time point for the db/+ control mitochondria (33.5±2.0 vs. 18.2±4.8 nmol/min/mg protein) ($p<0.01$) (Fig. 16). Likewise, state 4 respiration was increased at the 18-20 versus 10-12 week time points for the db/db mouse (30.7±2.4 vs. 16.8±2.5 nmol/min/mg protein).

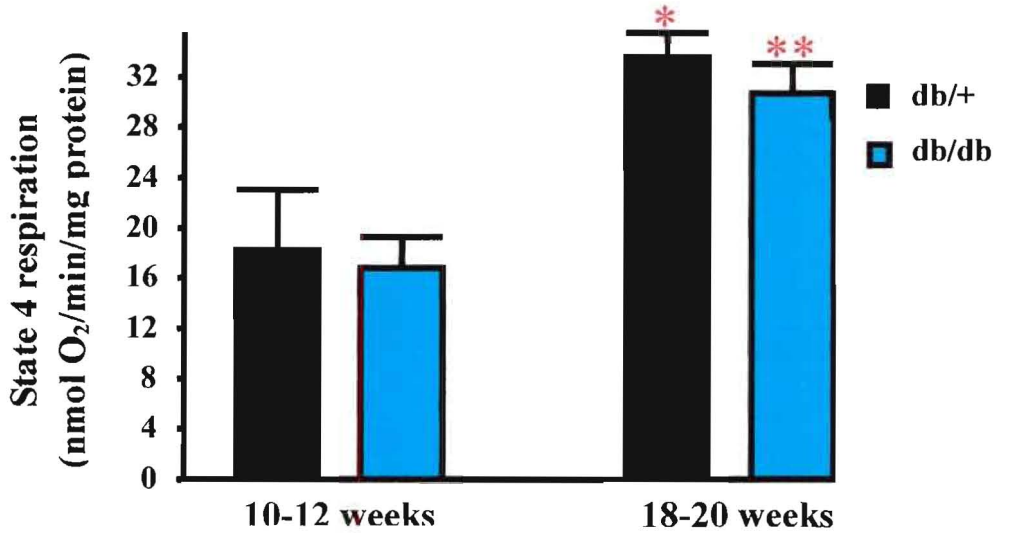

Figure 16. State 4 respiration for control (db/+) and obese (db/db) heart mitochondria at 10-12 weeks and 18-20 weeks of age. *MCP was used as substrate. State 4 respiration represents mitochondrial oxygen consumption after completion of ADP phosphorylation. Respiration rates are expressed as nmol of oxygen/minute/mg protein.*

** $p<0.01$ compared with db/+ at 10-12 weeks.*

*** $p<0.01$ compared with db/db at 10-12 weeks.*

The ADP/O ratio, an index of the mitochondrial efficiency (ratio between nmol of ADP phosphorylated and oxygen consumed during state 3 respiration) did not differ at any of the time points (Fig. 17).

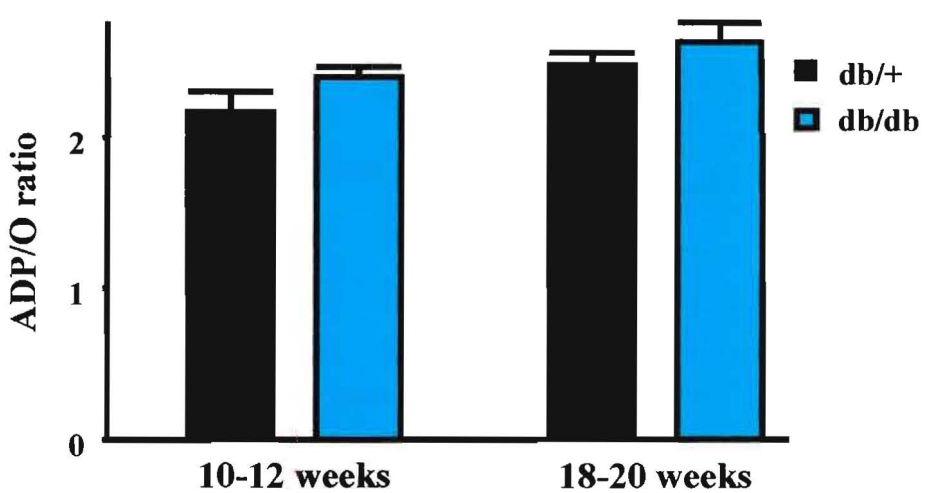

Figure 17. ADP/O ratio for control (db/+) and obese (db/db) heart mitochondria at 10-12 weeks and 18-20 weeks of age. *MCP was used as substrate.*

The ADP phosphorylation rate was unchanged between the db/+ and db/db at both time points (Fig. 18).

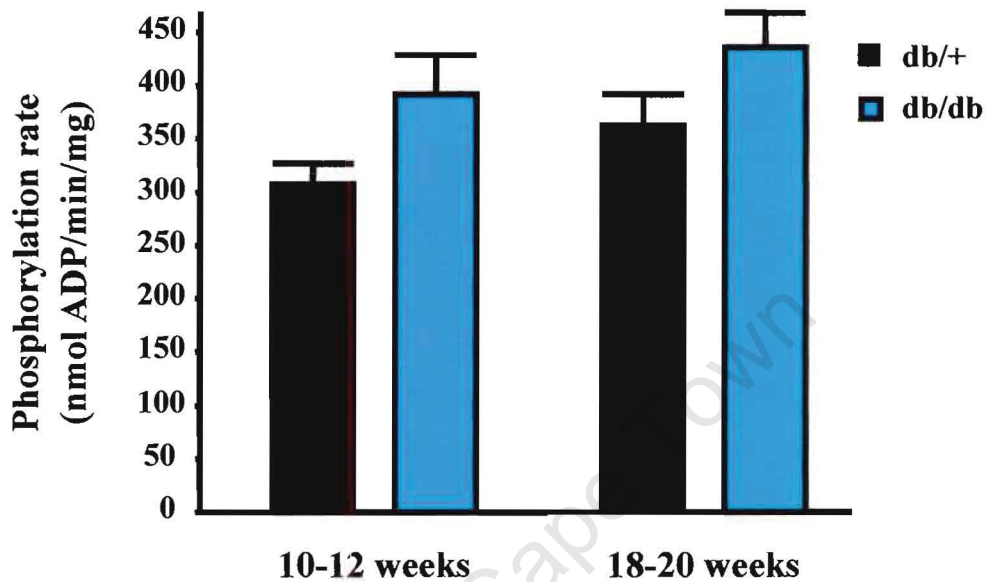

Figure 18. ADP phosphorylation rate in isolated heterozygous control (db/+) and obese (db/db) heart mitochondria at 10-12 weeks and 18-20 weeks of age. *MCP was used as substrate. Phosphorylation rate is expressed as nmol of ADP/minute/mg protein.*

7.1.4. Histology

To assess whether any structural alterations occurred in the obese mouse heart, we performed H&E staining analysis. However, no significant alterations were found in the db/db mouse heart at any of the time points examined (Fig. 19).

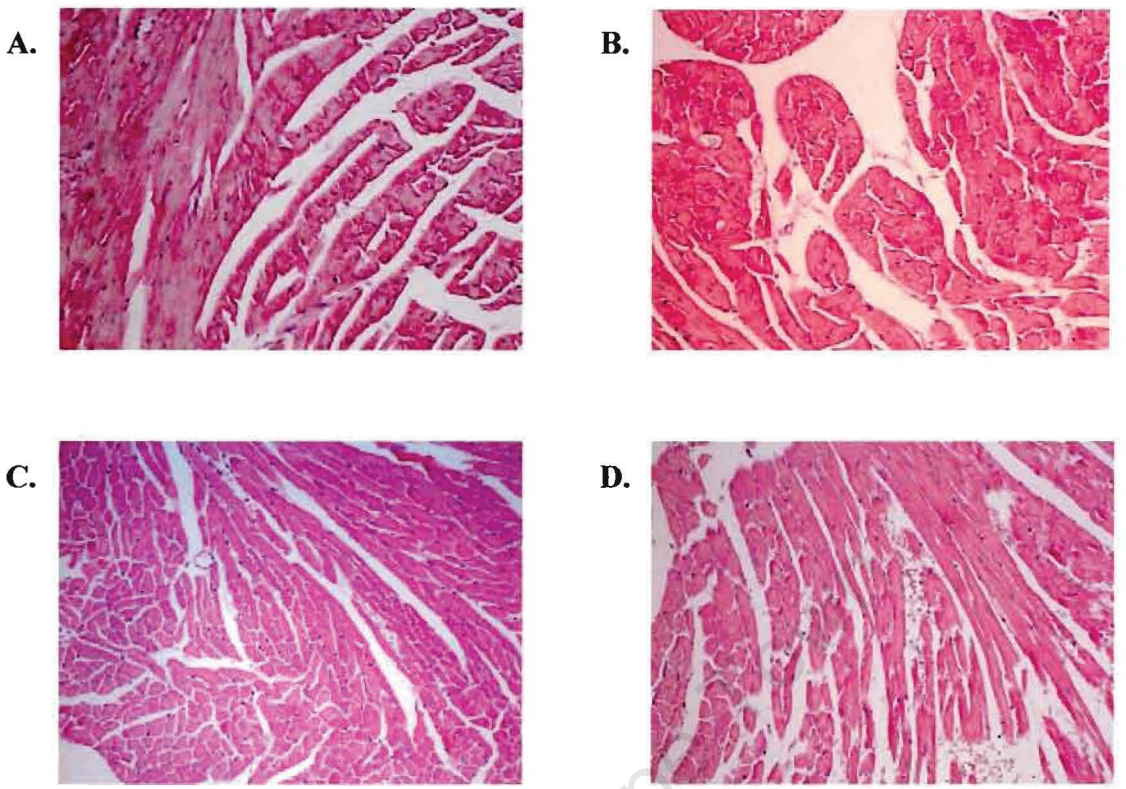

Figure 19. Hematoxylin and eosin (H&E) stained heart tissues. *Magnification 200X. A) Control (db/+) and B) obese (db/db) mice at the 10-12 weeks of age; C) Control (db/+) and D) obese (db/db) mice at 18-20 weeks of age (n=6).*

We next wanted to determine if there was any intracellular lipid accumulation within the obese heart muscle and subsequently stained slides with O_5O_4, used as a stain for lipid droplets. [107] Here, we found no histological evidence for significant lipid deposition in db/db mice vs. matched controls at the 10-12 week or the 18-20 week time points (Fig. 20).

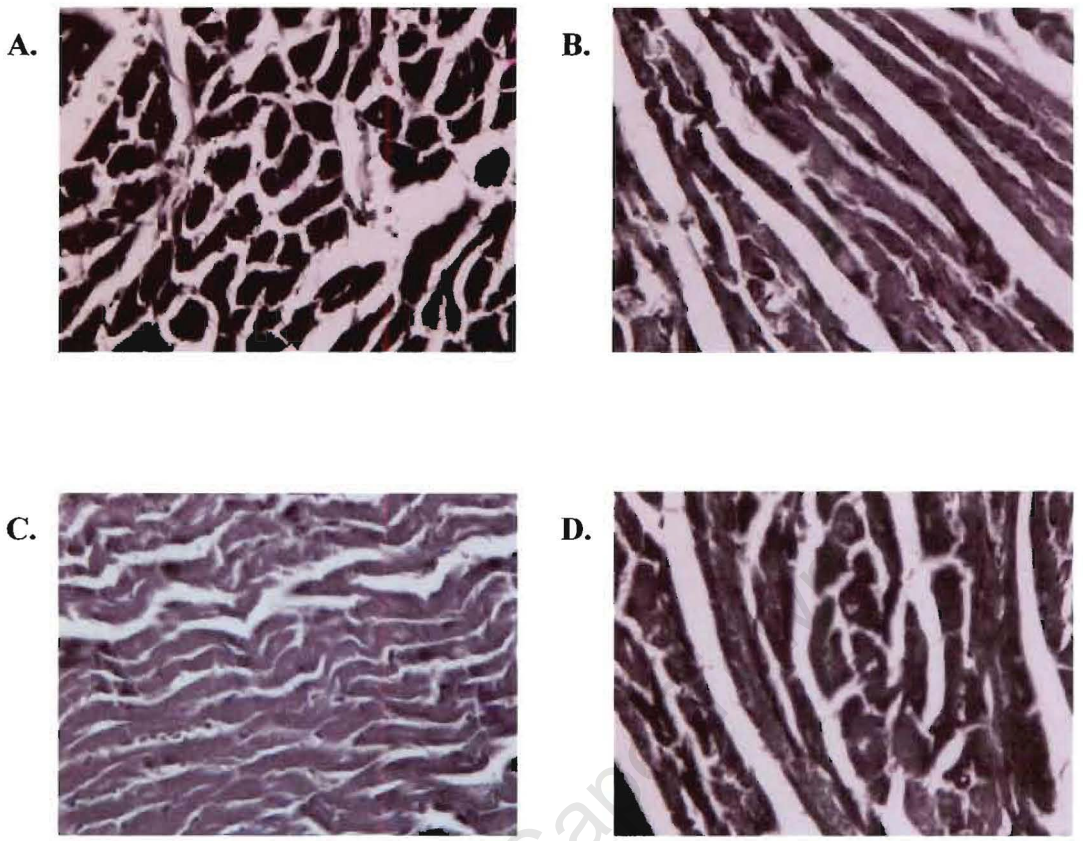

Figure 20. Osmium tetroxide (O_5O_4) stained heart tissues. *Magnifications 200X. A) Control (db/+) and B) obese (db/db) mice at the 10-12 weeks of age; C) Control (db/+) and D) obese (db/db) mice at 18-20 weeks of age (n=6).*

7.2. Gender-dependent changes in mitochondrial respiratory function

7.2.1. Baseline metabolic characterization

To investigate our hypothesis that females possess innate cardioprotective programs, we focused on the 18-20 week time point. Here, gender did not have a significant effect on body weight and plasma glucose levels (Table 14). Interestingly, heart weight and heart: body weight ratio were significantly decreased in both male and female db/db compared to matched controls.

Table 14. Baseline characterization of male and female heterozygous (db/+) and diabetic (db/db) mice at the age of 18-20 weeks

	Body weight (g)	Heart weight (mg)	Heart: body weight ratio, (X 1000)	Blood glucose (mmol/L)	Fasting blood glucose (mmol/L)
Male					
db/+	28.0±0.7	110.2±3.2	4.0±0.1	10.5±0.8	5.5±0.4
db/db	47.15±1.7 **	98.9±1.5	2.1±0.1 **	26.4±1.5 **	26.8±0.9 **
Female					
db/+	20.8±0.5	75.7±1.6	3.6±0.1	7.3±0.5	4.2±0.2
db/db	44.7±1.2 **	98.1±2.5 **	2.2±0.1 **	22.0±2.3 **	25.9±1.2 **

Values are expressed as mean ± S.E.M. for10-24 animals.

*** p<0.001 compared with age-matched heterozygous db/+ mice.*

7.2.2. Mitochondrial respiration

We next compared cardiac mitochondrial respiratory function between male and female db/+ and db/db mice at the 18-20 week time point (Table 15).

Table 15. Cardiac mitochondrial respiratory function for male and female control (db/+) and obese (db/db) mice

	Male		Female	
	db/+	db/db	db/+	db/db
State 2 respiration (nmol/min/mg protein)	29.4±1.6	32.6±1.9	36.6±1.7 *	35.0±2.0
State 3 respiration (nmol/min/mg protein)	145.0±9.6	165.8±9.8	175.6±7.1	177.8±12.9
State 4 respiration (nmol/min/mg protein)	33.5±2.0	30.7±2.4	38.8±1.3	36.8±1.6
ADP/O	2.5±0.1	2.6±0.1	2.2±0.04	2.3±0.1 **
Phosphorylation rate (nmol/min/mg protein)	363.4±28.3	436.0±32.3	381.0±20.4	411.6±40.0

Cardiac mitochondria were isolated as described in the Materials and Methods section of this thesis.

Respiration rates were determined using MCP as substrates.

Values are expressed as mean ± S.E.M. for 7-9 animals in each group.

** $p<0.05$ compared with male heterozygous db/+ mice.*

*** $p<0.05$ compared with male obese db/db mice.*

State 2 respiration was similar between db/+ and db/db for male mice. However, state 2 respiration was increased for female db/+ compared to male db/+ heart mitochondria (36.6 ± 1.7 vs. 29.4 ± 1.6 nmol/min/mg protein) ($p<0.05$) (Fig. 21).

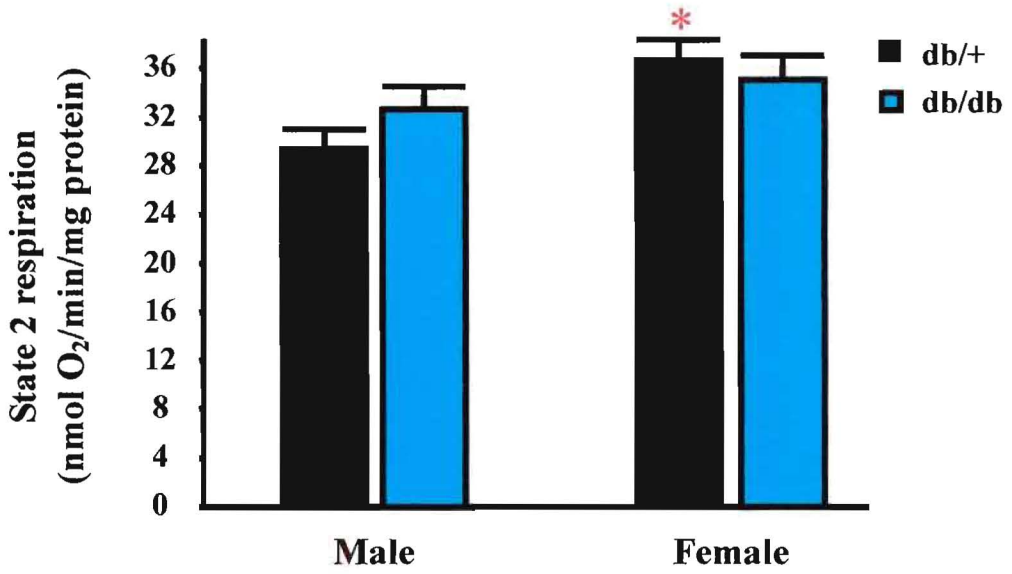

Figure 21. State 2 mitochondrial respiration: gender-dependent changes for control (db/+) and obese (db/db) heart mitochondria. *MCP was used as substrate. Respiration rates are expressed as nmol of oxygen/minute/mg protein.*

** $p<0.05$ compared with male heterozygous db/+ mice.*

State 3 respiration was similar between male and female db/+ and db/db mice (Fig. 22).

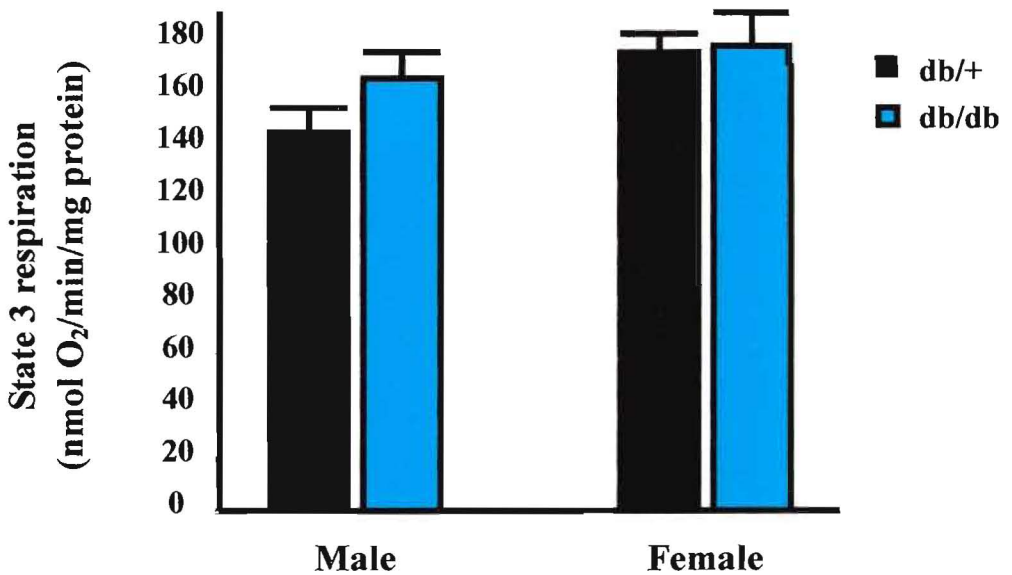

Figure 22. State 3 mitochondrial respiration: gender-dependent changes for control (db/+) and obese (db/db) heart mitochondria. *MCP was used as substrate. Respiration rates are expressed as nmol of oxygen/minute/mg protein.*

Furthermore, state 4 respiration was similar between male and female db/+ and db/db heart mitochondria (Fig. 23).

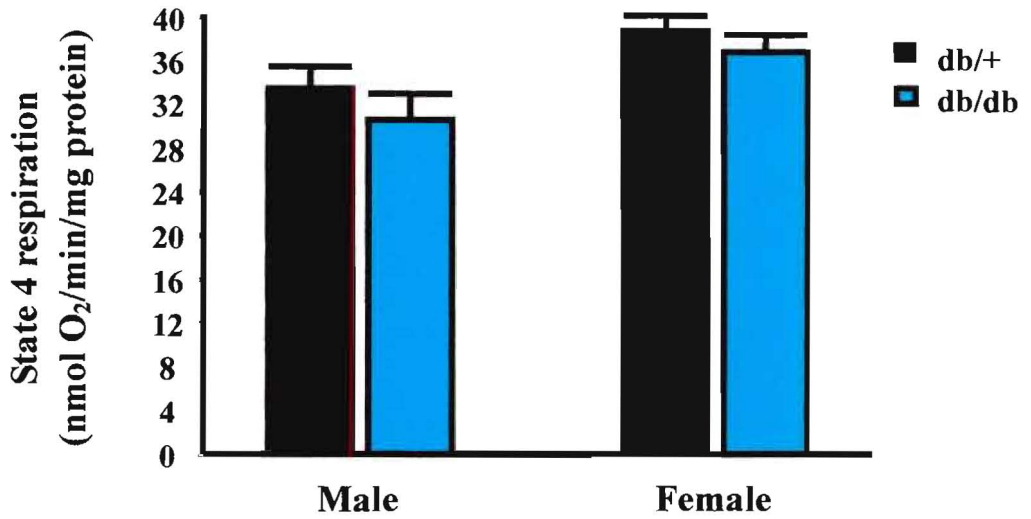

Figure 23. State 4 mitochondrial respiration: gender-dependent changes for control (db/+) and obese (db/db) heart mitochondria. *MCP was used as substrate Respiration rates are expressed as nmol of oxygen/minute/mg protein.*

The ADP/O ratio was moderately but significantly reduced in the db/db female versus db/db male 2.6±0.1 vs. 2.3±0.1 (Fig. 24).

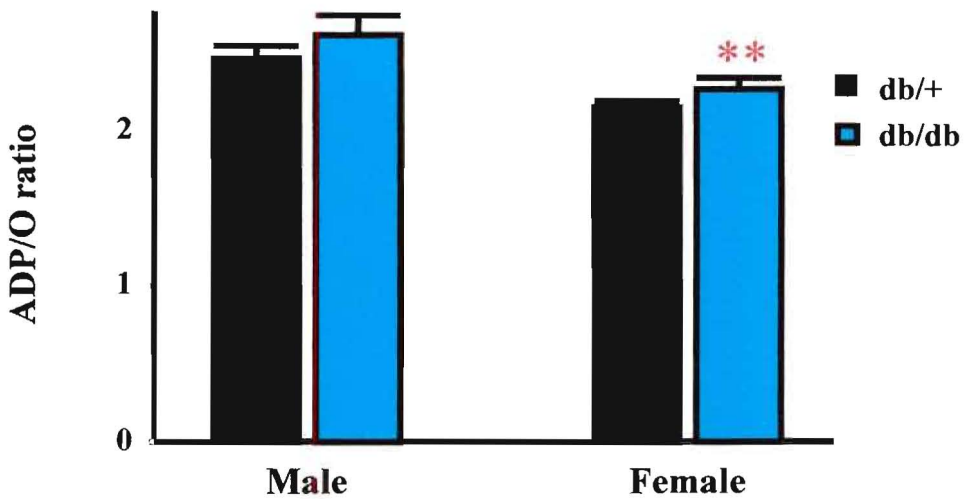

Figure 24. ADP/O ratio: gender-dependent changes for control (db/+) and obese (db/db) heart mitochondria. *MCP was used as substrate*

*** p<0.05 compared with male obese db/db mice.*

ADP phosphorylation rate was unchanged between male and female db/+ and db/db mitochondria (Fig. 25).

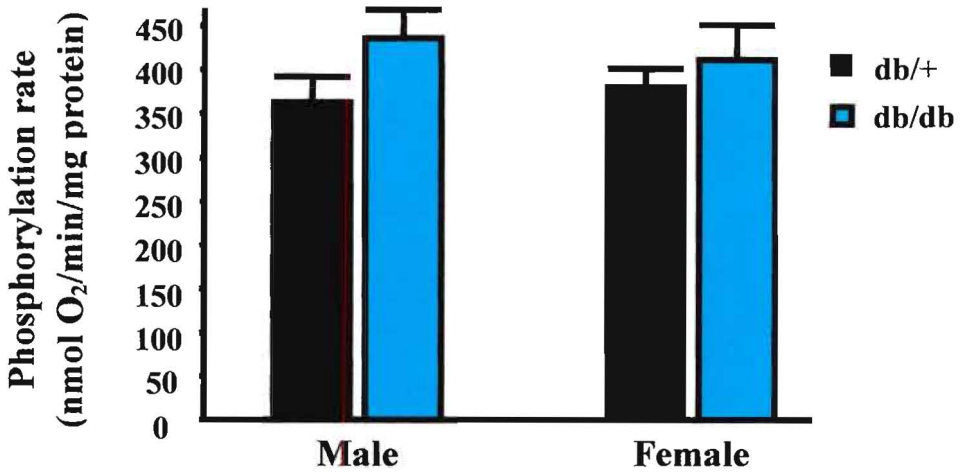

Figure 25. ADP phosphorylation rate: gender-dependent changes for control (db/+) and obese (db/db) heart mitochondria. *MCP was used as substrate. Phosphorylation rates are expressed as nmol of ADP/minute/mg protein.*

Interestingly, state 3 mitochondrial respiration recovery in response to anoxia was increased in female compared to male control hearts (23.6±1.6 vs. 16.4±2.6) ($p<0.05$) (Fig. 26). However, this improved recovery was lost in the obese (db/db) female.

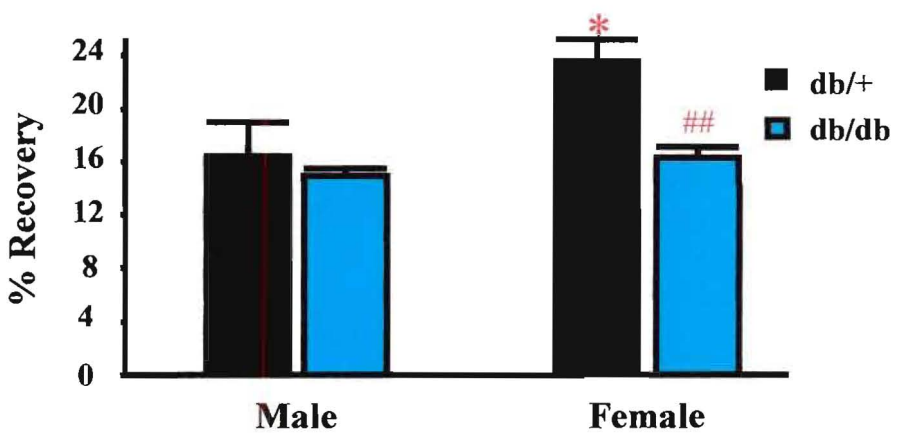

Figure 26. Percentage of state 3 respiration recovery in isolated heterozygous control (db/+) vs. obese (db/db) heart mitochondria. *MCP was used as substrate. Percentage recovery of state 3 respiration was determined by measuring the oxygen uptake for 5 minutes after 20 minutes of anoxia.*

* *$p<0.05$ compared with male heterozygous db/+ mice.*

$p<0.05$ compared with female heterozygous db/+ mice.

To determine whether such improved recovery related to an increased bioenergetic capacity, we next measured total mitochondrial ATP levels. Here, the total cardiac mitochondrial ATP concentration was significantly increased in female compared to male control mice (39.0±2.7 vs. 26.2±2.6 μmol/mg protein) (Fig. 27). In agreement with our respiration data, this effect was abolished in the obese female mouse.

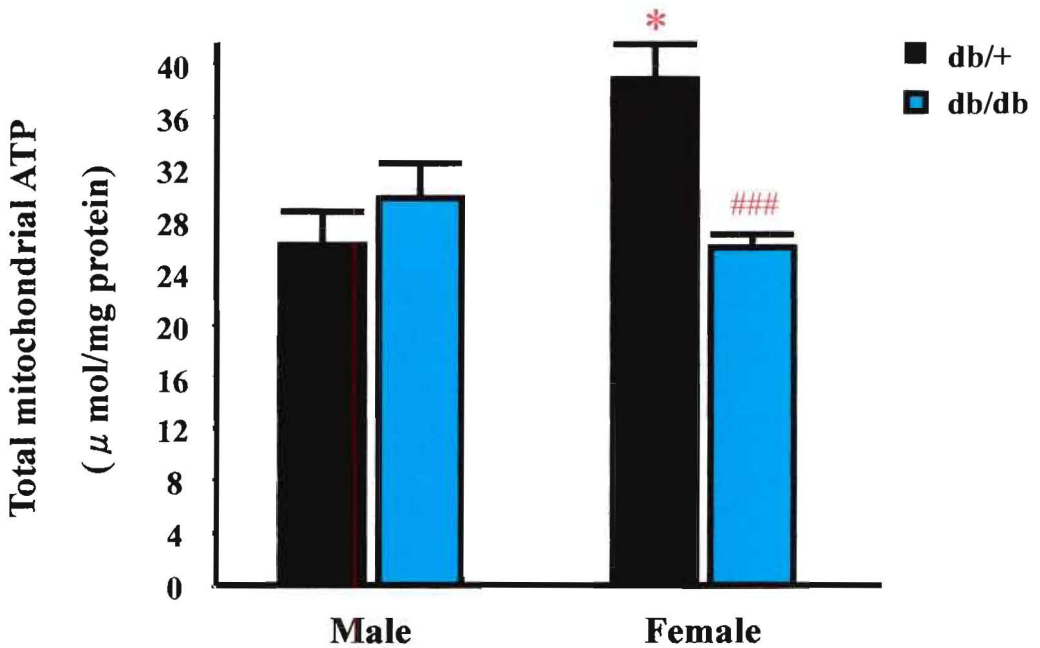

Figure 27. Gender-dependent changes of total mitochondrial ATP in heterozygous control (db/+) and obese (db/db) heart mitochondria. *Total mitochondrial ATP concentration was assayed using a luciferin-luciferase luminometry luminescence method modified from Fryer et al. (2000)* [102] *Concentration of the total mitochondrial ATP is expressed as μmol/mg protein.*

** $p<0.05$ compared with male heterozygous db/+ mice.*

$p<0.001$ compared with female heterozygous db/+ mice.

7.2.3. Histology

To examine whether any morphological differences existed between male and female mouse hearts, we performed hematoxylin and eosin (H&E) and osmium tetroxide staining analysis. Here, we found that male and female db/+ and db/db were not histologically different (Figs. 28 and 29).

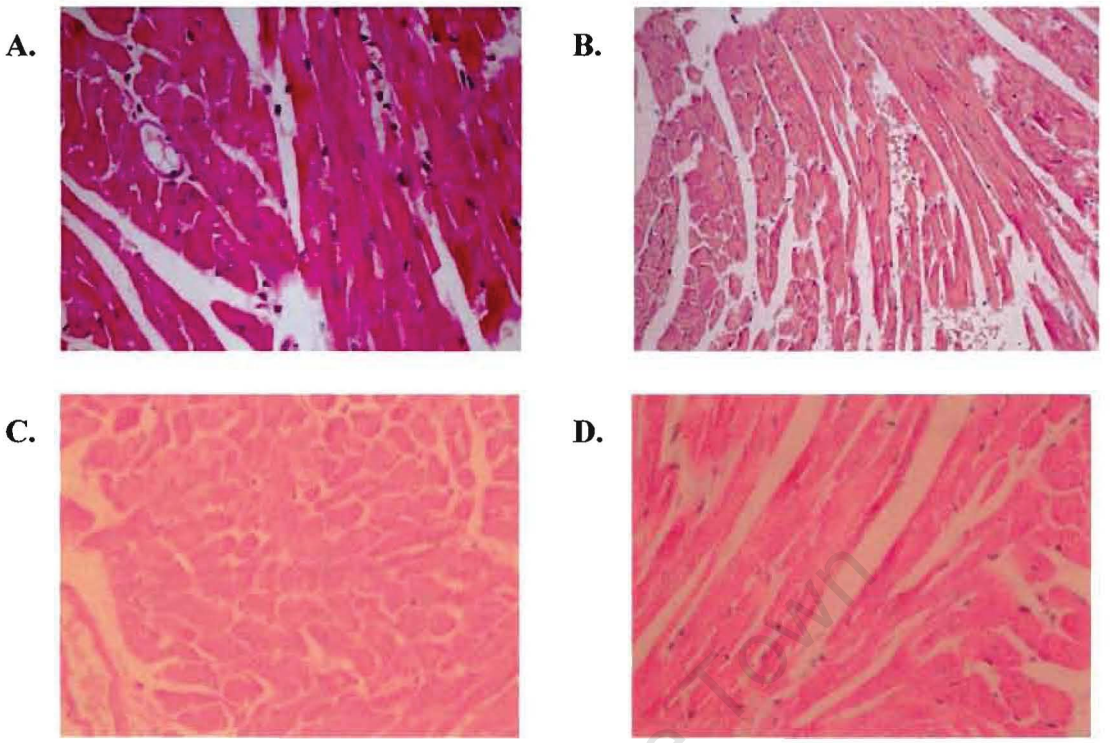

Figure 28. Hematoxylin and eosin (H&E) stained heart tissues. *Magnification 200X. A) Male control (db/+), B) obese (db/db) mice, C) Female control (db/+) and D) obese (db/db) mice at 18-20 weeks of age (n=6).*

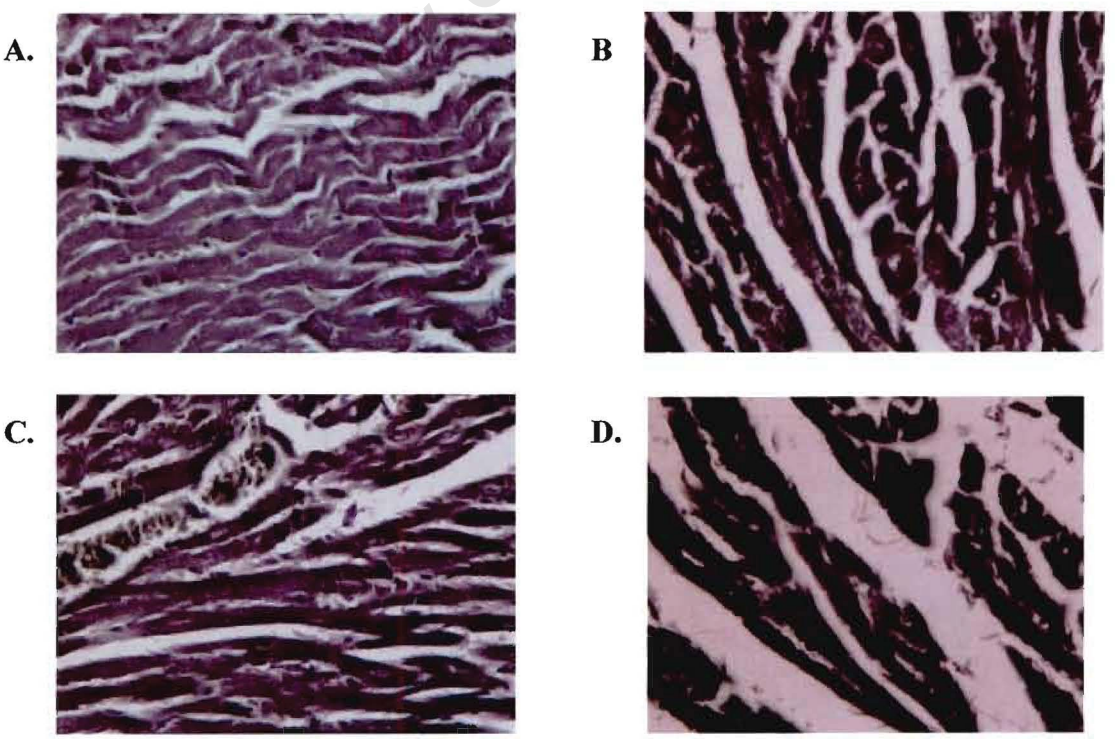

Figure 29. Osmium tetroxide (O_SO_4) stained heart tissues. *Magnification 200X. A) Male control (db/+), B) obese (db/db) mice, C) Female control (db/+) and D) obese (db/db) mice at 18-20 weeks of age (n=6).*

7.2.4. Electron microscopy

To gain further insight into the role of the mitochondrion in the diabetic heart, we performed EM at the 10-12 and 18-20 week time points. Since no significant morphological (i.e. H&E staining) and lipid abnormalities (i.e. O_5O_4 staining) were found in db/+ compared to db/db mouse hearts at 10-12 and 18-20 weeks, we next focused on whether any mitochondrial ultrastructural changes occurred in a gender-dependent manner. Unfortunately, due to limited availability of db/db mice at 10-12 weeks of age, only db/+ hearts from this age group were examined.

At 10-12 weeks, control db/+ heart mitochondria were highly organized, the condensed cristae suggesting functional mitochondria with high metabolic efficiency. However, no visible abnormalities were detected between male and female mouse heart mitochondria (Fig. 30).

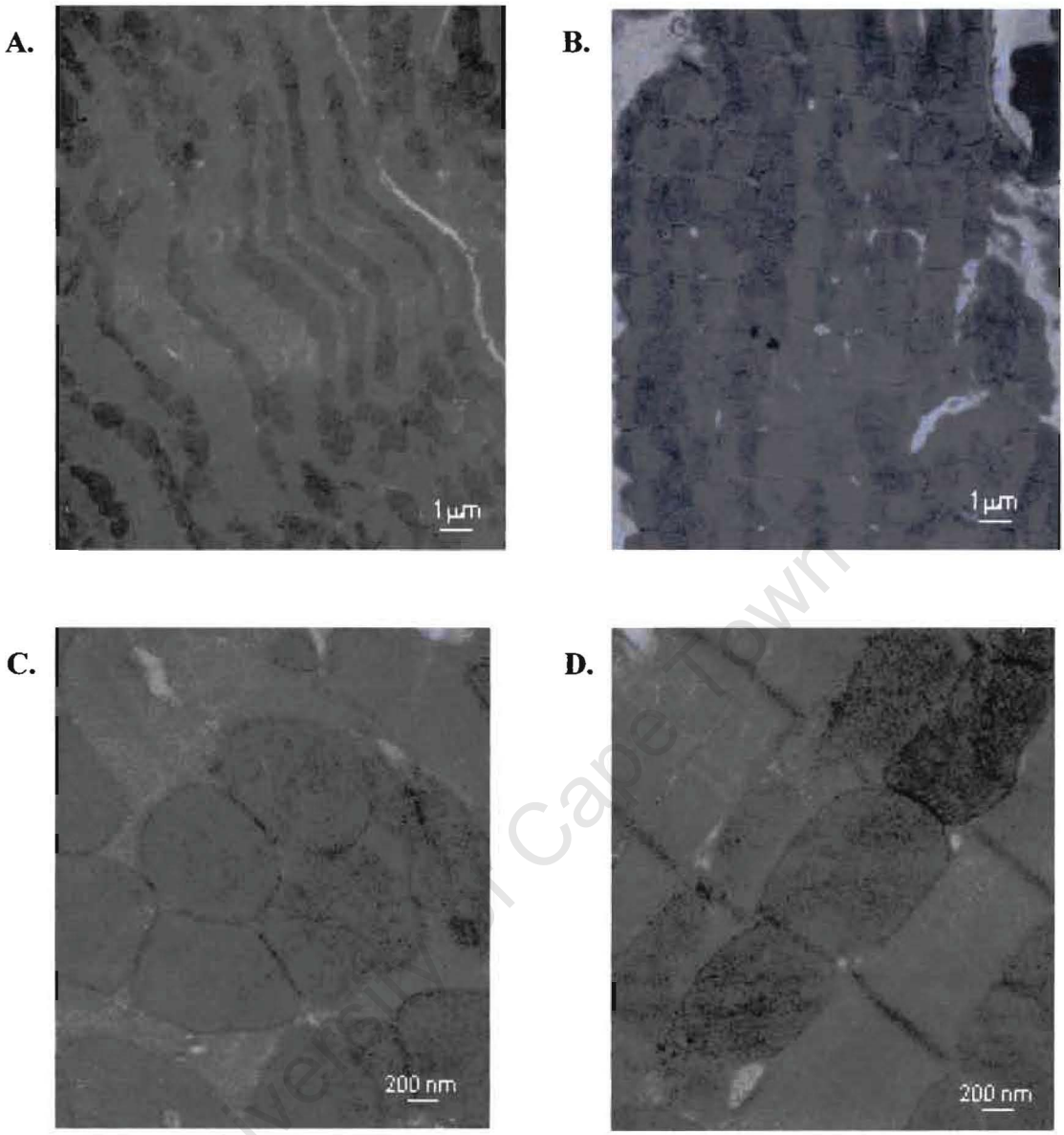

Figure 30. Electron Microscopy (EM) for male and female control (db/+) hearts at 10-12 weeks age. *Low magnification (5000X): A) male and B) female (db/+) mice; High magnification (25,000X): C) male and D) female (db/+) mice at 10-12 weeks of age (n=3).*

Although male db/+ mitochondria at 18-20 weeks displayed an organized mitochondrial profile, it did not display the same degree of condensed cristae like the earlier time point (Figs. 31 A and C). This suggests that the severity of the mitochondrial distortion is age dependent.

Intriguingly, male obese db/db hearts displayed further mitochondrial ultrastructural

damage i.e. distorted cristae organization, lipid deposition and vacuole accumulation were observed (Figs. 31 B and D).

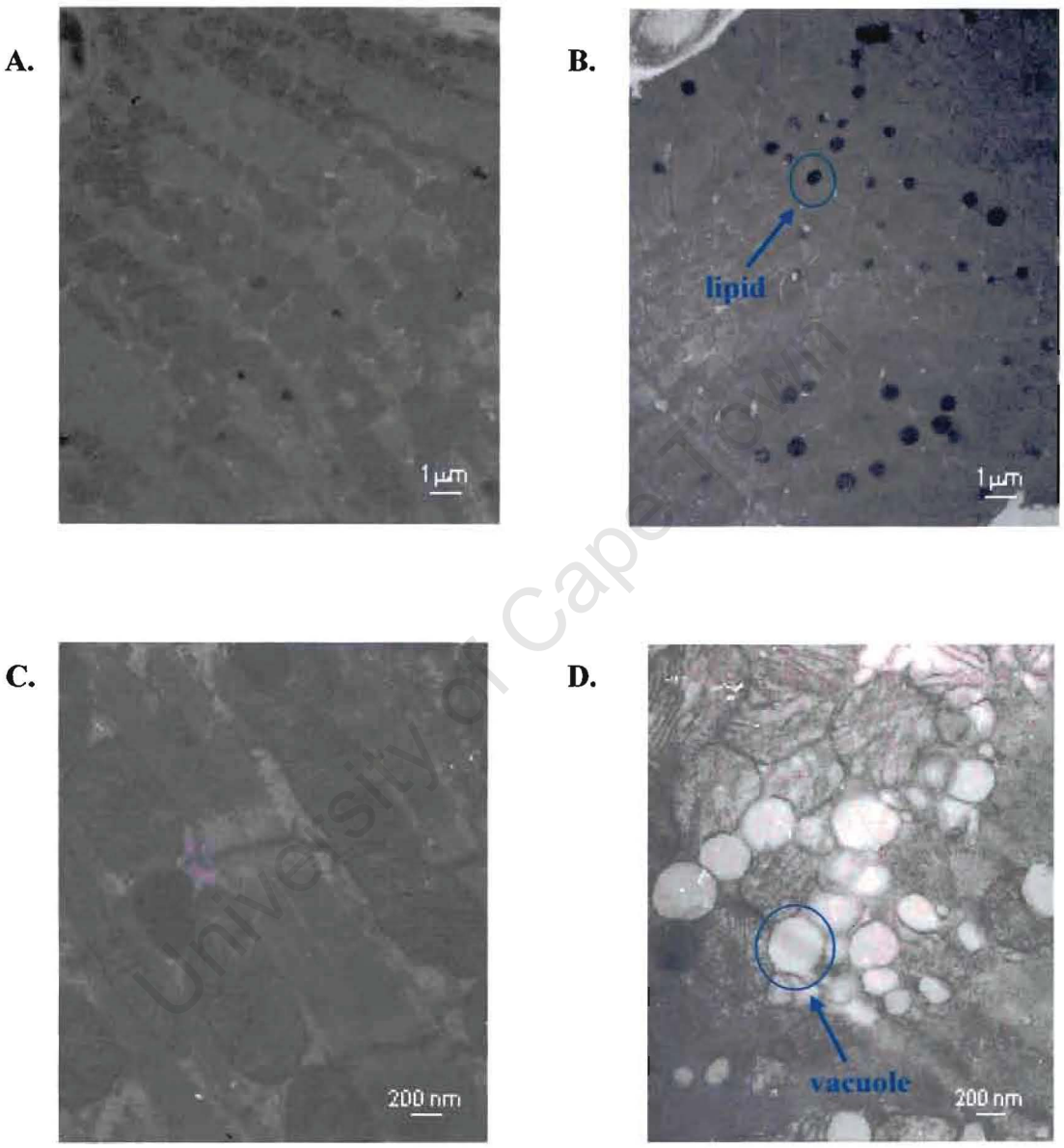

Figure 31. Electron Microscopy (EM) for male control (db/+) and obese (db/db) hearts at 18-20 weeks age. *Low magnification (5000X): A) male control (db/+), B) obese (db/db) mice; High magnification (25,000X): C) male control (db/+) and D) obese (db/db) mice at 18-20 weeks of age (n=3).*

For the females, db/+ mitochondria were well organized and the number of mitochondria was highly expressed compared to the age-matched male controls (Figs.

32 A and C). Unlike the controls, lipid droplets were stained in the female db/db. However, the degree of matrix distortion in females appeared to be reduced compared to age-matched male db/db (Figs. 32 B and D). This suggests a higher degree of mitochondrial ultrastructural changes in male versus female db/db mouse hearts. However, like obese male, female db/db hearts also displayed increased lipid deposition.

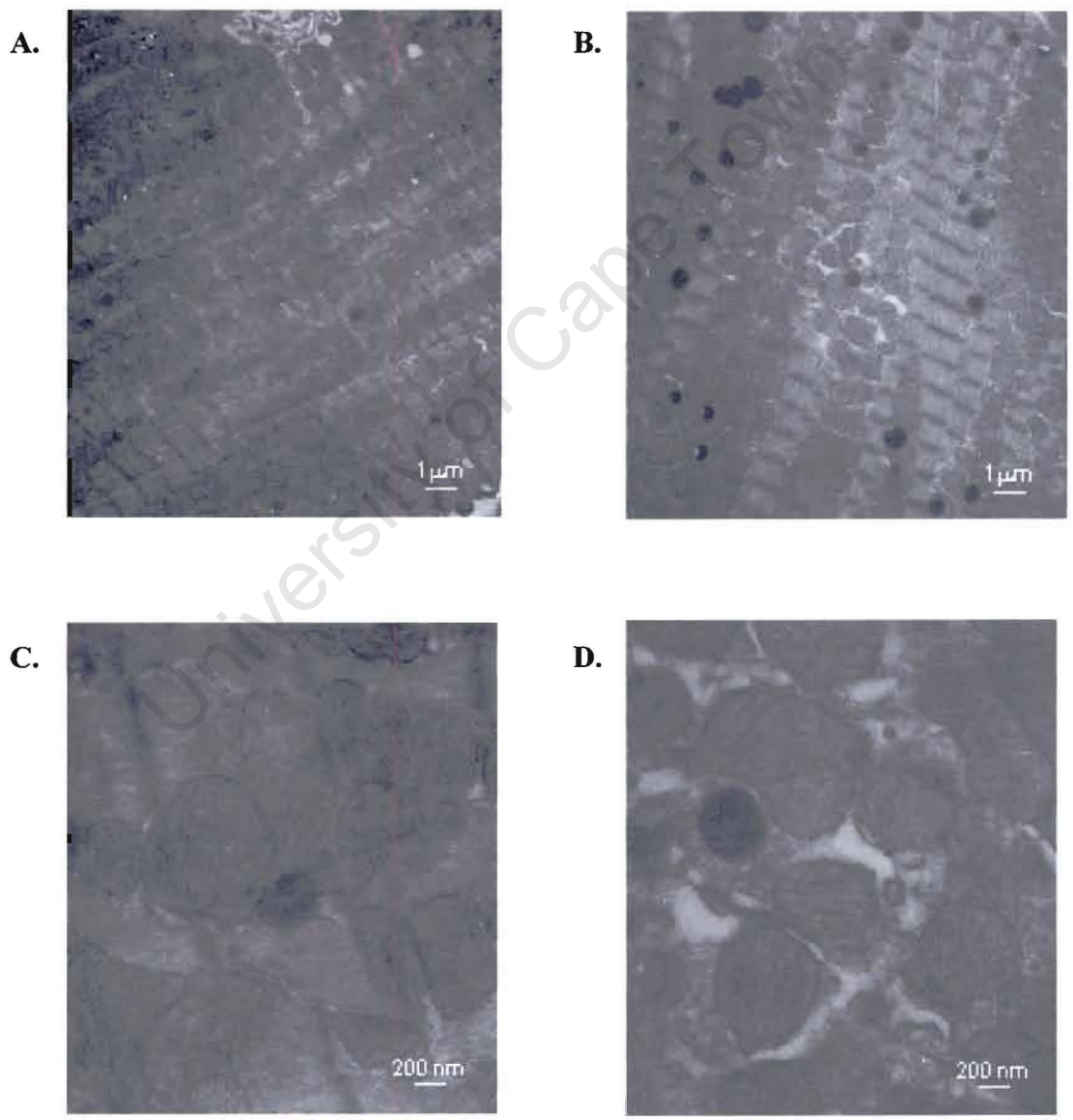

Figure 32. Electron Microscopy (EM) in female control (db/+) and obese (db/db) heart at 18-20 weeks of age. *Low magnification (5000X): A) female control (db/+), B) obese (db/db) mice; High magnification (25,000X): C) female control (db/+) and D) obese (db/db) mice at 18-20 weeks of age (n=).*

Recently, we initiated a long-term study of the db/db mouse to further investigate our hypothesis. For the pilot study we investigated mitochondrial respiratory function and histological/ morphological changes in db/db mice aged 55-56 weeks.

8. Pilot Study: Age- and Gender-Dependent Changes in a Type II Diabetic Mouse Model

8.1. Baseline metabolic characterization (55-56 weeks)

Body weight was significantly increased in obese animals, although gender did not have any effect (Table 16). Initially, postprandial plasma glucose levels were measured, but it was surprisingly low. Thereafter, we measured fasting plasma glucose levels to better reflect the changes in glucose levels in these animals. Interestingly, postprandial and fasting blood glucose levels were not significantly different in 55-56 week-old male and female db/db mice compared to age-matched controls. However, these values were much lower compared to earlier time points investigated i.e. 10-12 and 18-20 weeks. In addition, trace levels of ketone bodies in urine were observed using gluco/ ketone urine test strips.

Table 16. Baseline characterization of male and female heterozygous (db/+) and diabetic (db/db) mice at the age of 55-56 weeks

		Body weight (g)	Blood glucose (mmol/L)	Fasting blood glucose (mmol/L)
Male	**db/+**	26.8±0.3	7.5±0.4	6.6±0.3
	db/db	51.8±1.0 §	7.2±0.7	6.1±0.5
Female	**db/+**	21.9±0.2	6.8±0.3	6.2±0.2
	db/db	55.7±2.7 §	8.4±2.0	7.8±0.9

Values are expressed as mean ± S.E.M. (n=3-6). § *$p<0.001$ compared with age-matched heterozygous db/+ mice.*

8.2. Mitochondrial respiration

We subsequently determined cardiac mitochondrial respiratory function at the 55-56 week time point (Table 17).

Table 17. Cardiac mitochondrial respiratory function for male and female control (db/+) and obese (db/db) mice

	Male		Female	
	db/+	db/db	db/+	db/db
State 2 respiration (nmol/min/mg protein)	10.5±1.0	25.1±1.3 §	11.8±1.6	23.6±1.1 §
State 3 respiration (nmol/min/mg protein)	61.7±7.9	117.7±13.3 $^{\#}$	60.6±8.2	150.5±7.5 §
State 4 respiration (nmol/min/mg protein)	7.5±1.0	26.3±1.3 §	10.1±1.5	20.9±1.6 §
ADP/O	3.1±0.01	2.3±0.2 §	2.5±0.1	2.6±0.1
Phosphorylation rate (nmol/min/mg protein)	194.5±25.7	276.6±44.6	164.77±26.6	390.7±10.2 § **

Cardiac mitochondria were isolated as described in the Materials and Methods section of this thesis. Respiration rates were determined using MCP as substrates. Values are expressed as mean ± S.E.M. for 5-8 animals in each group.

** *$p<0.05$ compared with male obese db/db mice.*

$^{\#}$ *$p<0.01$ compared with age-matched heterozygous db/+ mice.*

§ *$p<0.001$ compared with age-matched heterozygous db/+ mice*

At the 55-56 week point, state 2 respiration was significantly increased in male db/db (25.1±1.3 vs. 10.5±1.0 nmol/min/mg protein) and female db/db (23.6±1.1 vs. 11.8±1.6 nmol/min/mg protein) ($p<0.001$) compared to control mice (Fig. 33).

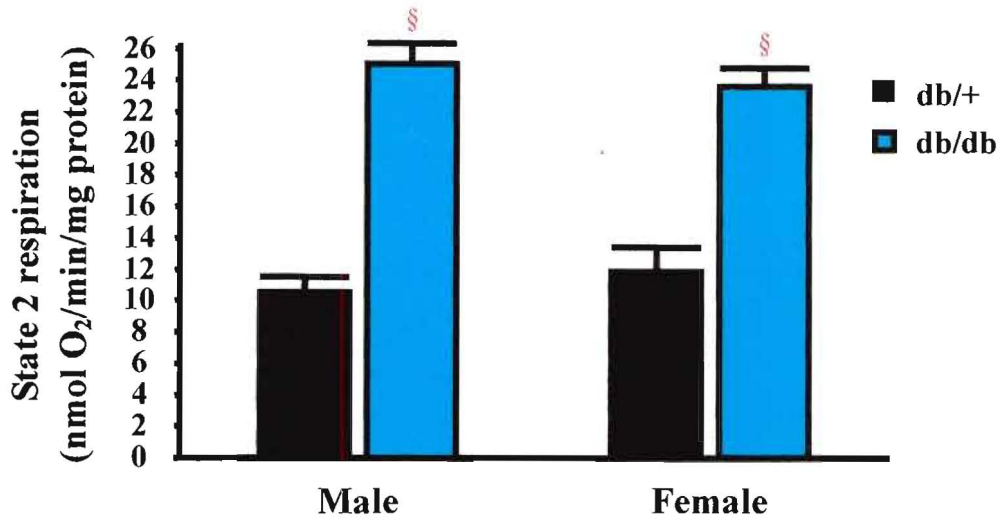

Figure 33. State 2 mitochondrial respiration for control (db/+) and obese (db/db) heart mitochondria. *MCP was used as substrate. Respiration rates are expressed as nmol of oxygen/minute/mg protein.*

§ *p<0.001 compared with age-matched heterozygous db/+ mice*

State 3 respiration was elevated in db/db compared to control mice in male (117.7±13.3 vs. 61.7±7.9 nmol/min/mg protein) ($p<0.01$) and in female mitochondria (150.5±7.5 vs. 60.6±8.2 nmol/min/mg protein) ($p<0.001$) (Fig. 34).

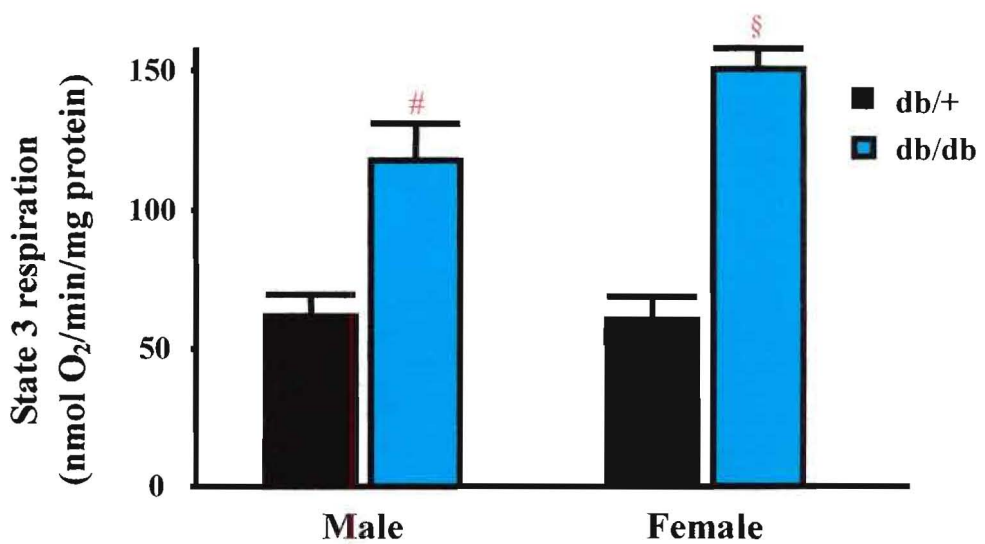

Figure 34. State 3 mitochondrial respiration for control (db/+) and obese (db/db) heart mitochondria. *MCP was used as substrate. Respiration rates are expressed as nmol of oxygen/minute/mg protein.*

§ *p<0.001 compared with age-matched heterozygous db/+ mice.*

= *p<0.01 compared with age-matched heterozygous db/+ mice.*

State 4 respiration was increased for male db/db (26.3±1.3 vs. 7.5±1.0 nmol/min/mg protein) (P<0.001) and for female db/db (20.9±1.6 vs. 10.1±1.5 nmol/min/mg protein) (P<0.001) compared to age-matched controls (Fig. 35).

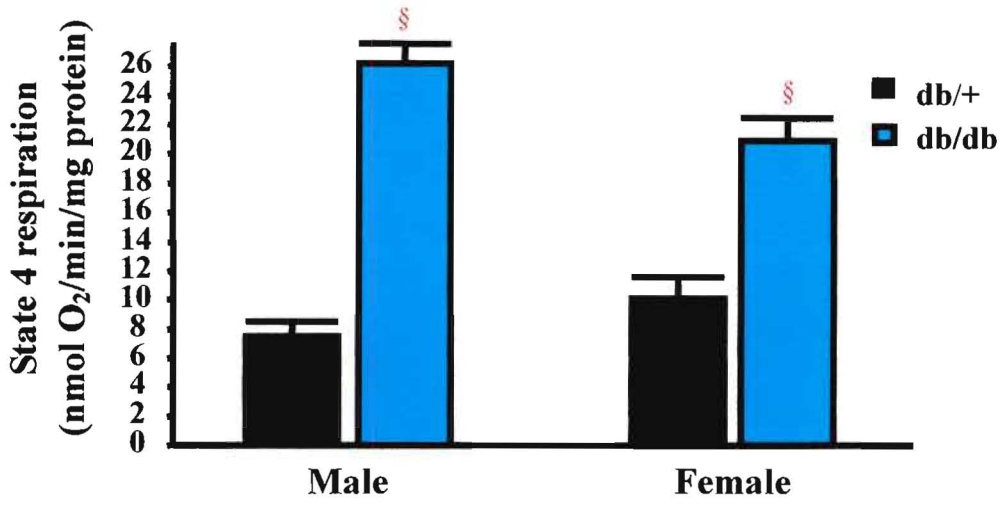

Figure 35. State 4 mitochondrial respiration for control (db/+) and obese (db/db) heart mitochondria. *MCP was used as substrate. Respiration rates are expressed as nmol of oxygen/minute/mg protein.*

§ *p<0.001 compared with age-matched heterozygous db/+ mice*

The ADP/O ratio was significantly reduced in db/db male compared to age-matched controls (2.3±0.2 vs. 3.1±0.01). However, ADP/O ratio was similar between female db/+ and db/db (Fig. 36).

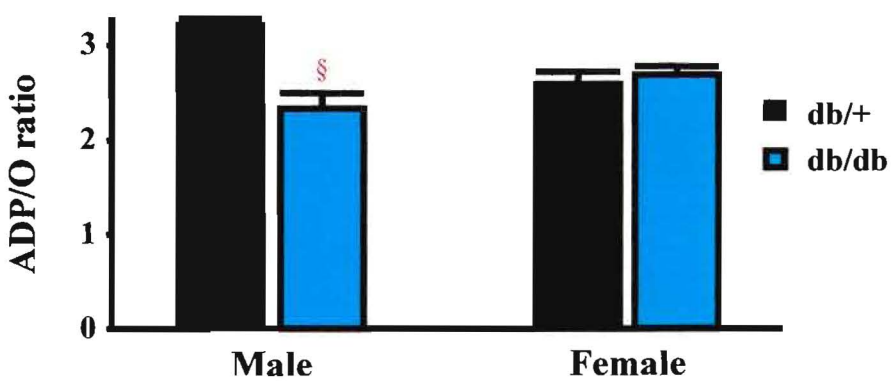

Figure 36. ADP/O ratio mitochondrial respiration for control (db/+) and obese (db/db) heart mitochondria. *MCP was used as substrate. Respiration rates are expressed as nmol of oxygen/minute/mg protein.*

§ *p<0.001 compared with age-matched heterozygous db/+ mice*

ADP phosphorylation rate was unchanged in male. However, female db/db mitochondria displayed increased ADP phosphorylation rate compared to age-matched db/+ control (390.7±10.2 vs. 164.77±26.6 nmol/min/mg protein) ($p<0.001$). In addition, ADP phosphorylation rate in female db/db was significantly higher compared to male db/db (390.7±10.2 vs. 276.6±44.6 nmol/min/mg protein) ($p< 0.05$) (Fig. 37).

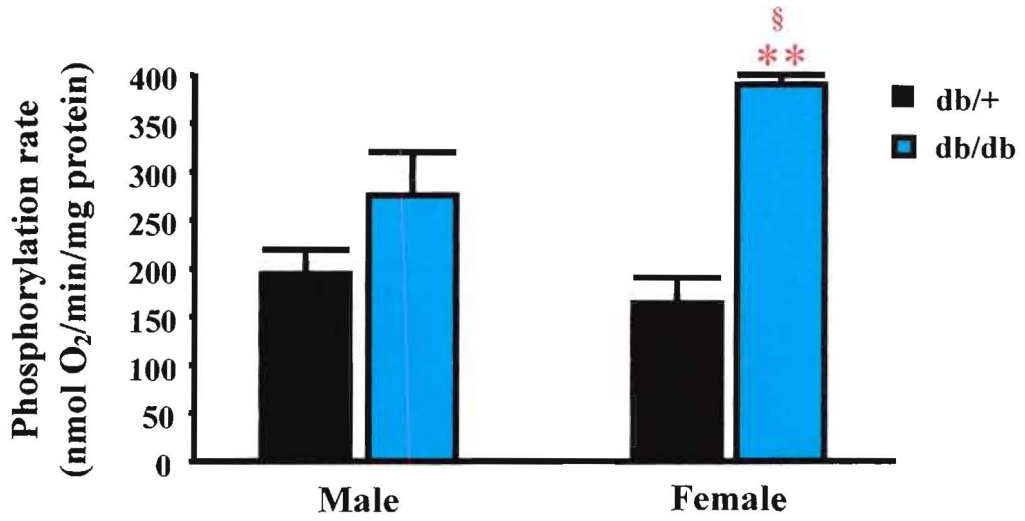

Figure 37. ADP phosphorylation rate in isolated control (db/+) and obese (db/db) heart mitochondria. *MCP was used as substrate. Respiration rates are expressed as nmol of oxygen/minute/mg protein.*

§ *$p<0.001$ compared with age-matched heterozygous db/+ mice.*

** *$p<0.05$ compared with male obese db/db mice.*

In response to 20 minutes anoxia and 5 minutes of reoxygenation, state 3 mitochondrial respiration recovery was increased in male db/db compared to controls ($p<0.05$) (Fig. 38). However, no differences were observed between female db/+ and db/db mitochondria.

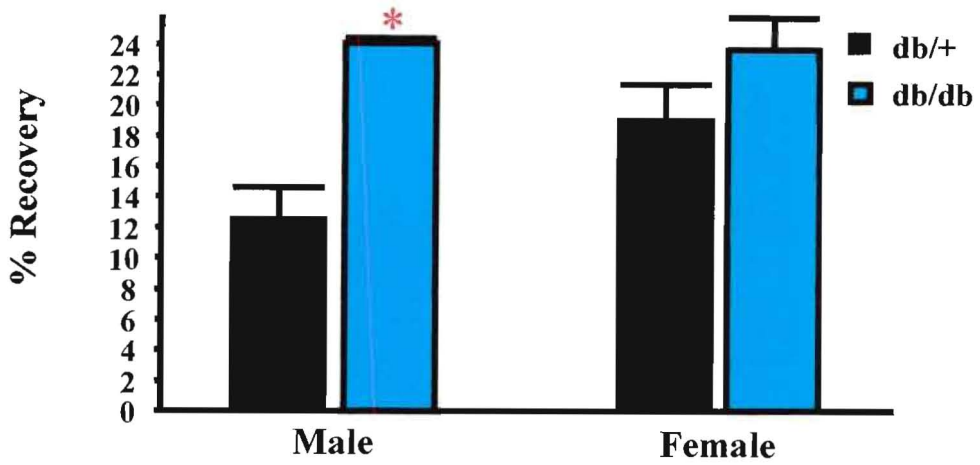

Figure 38. Percentage of state 3 respiration recovery in isolated heterozygous control (db/+) vs. obese (db/db) heart mitochondria. *MCP was used as substrate. Percentage recovery of state 3 respiration was determined by measuring the oxygen uptake for 5 minutes after 20 minutes of anoxia.*

** $p<0.05$ compared with male heterozygous db/+ mice.*

8.3. Histology

Since systemic glucose levels in the obese db/db were sequentially reduced compared to the earlier time points, we next examined morphological changes (H&E staining) in heart, liver and pancreas in order to gain more in insight into this phenomenon.

Here, morphological changes were similar in male and female db/+ and db/db mice. No morphological changes were observed in db/+ and db/db mouse hearts. However, in the liver, non-alcoholic steatohepatitis (NASH) was evident as shown by increased TG accumulation and inflammation. Enlarged islet was observed in the db/db pancreatic β-cells (Figs. 39 and 40).

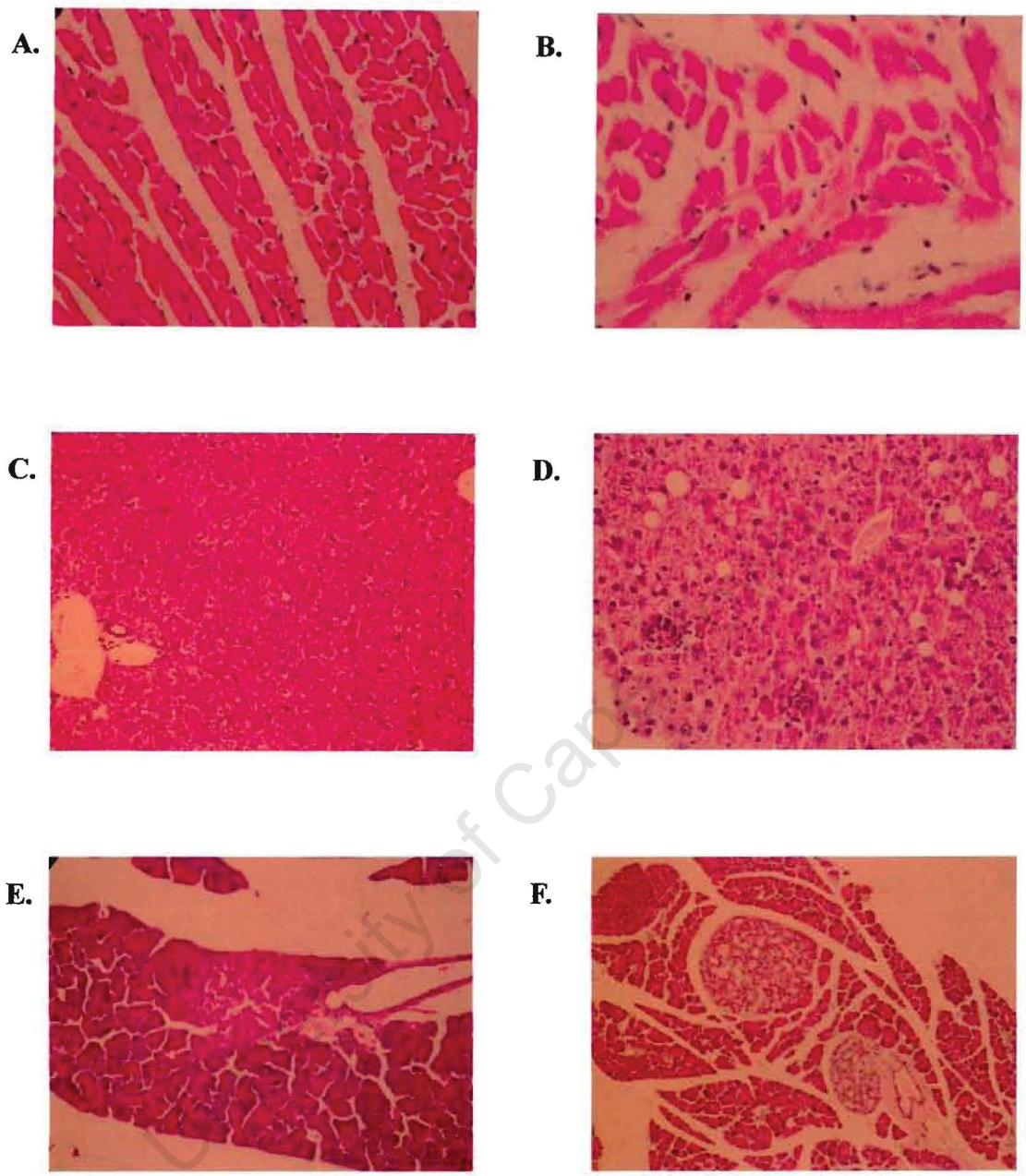

Figure 39. Hematoxylin and eosin (H&E) stained for male heart, liver and pancreatic tissues at 55-56 weeks age. *Magnification 200X. For heart tissue A) control (db/+), B) obese (db/db); liver C) control (db/+), D) obese (db/db); pancreas E) control (db/+) and F) obese (db/db) mice at 55-56 weeks of age (n=3).*

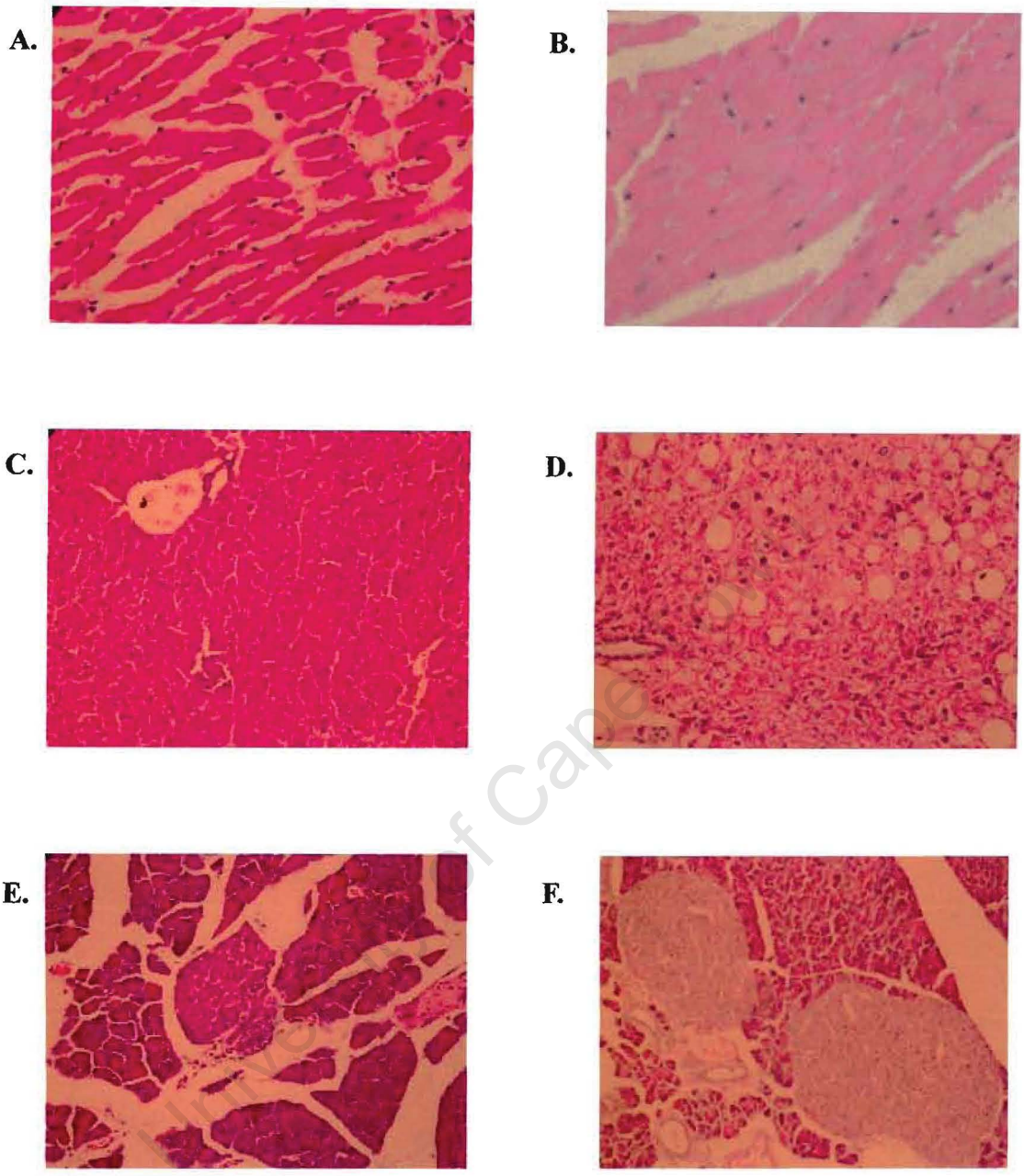

Figure 40. Hematoxylin and eosin (H&E) stained for female heart, liver and pancreatic tissues at 55-56 weeks age. *Magnification 200X. For heart tissue A) control (db/+), B) obese (db/db); liver C) control (db/+), D) obese (db/db); pancreas E) control (db/+) and F) obese (db/db) mice at 55-56 weeks of age (n=3).*

IV: DISCUSSION

9. Discussion

Obesity is a major contributor to the global burden of disease. [3] Moreover, it is closely associated with the development of type II diabetes. [12, 13] Recent studies have demonstrated that obese and/ or type II diabetic subjects have markedly increased circulating FFAs. [19, 61] It has been proposed that increased FFA supply plays a major role in the development of insulin resistance. [58] For example, elevated FFA levels have been associated with metabolic abnormalities such as a reduction in PDH activity, glucose transport, glycogen synthesis and ATP production. [61, 82] These data reflect impairment of carbohydrate metabolism and mitochondrial oxidative phosphorylation. As a result, the diabetic heart switches its substrate preference to high FA utilization. Moreover, ketone bodies also become a more prominent fuel substrate in this instance. [19] Thus, it has been proposed that metabolic remodeling by the diabetic heart may lead to mitochondrial and contractile dysfunction.

In light of this, we tested the hypothesis that obesity-induced insulin resistance/ type II diabetes, excessive FFA supply decreases mitochondrial bioenergetic capacity of the heart. Moreover, we hypothesized that females possess innate cardioprotective programs that result in enhanced mitochondrial bioenergetic capacity compared to males. We explored our hypothesis employing two rodent models i.e. a) a rat model of diet-induced obesity and b) a transgenic mouse model of obesity-induced type II diabetes.

Rat Model of Diet-Induced Obesity

We found that body weights were significantly increased in rats fed the cafeteria diet. Moreover, heart: body weight ratio was increased, suggesting the development of

cardiac hypertrophy. This is consistent with previous work on diabetic Goto-Kakizaki (GK) rats. [31] Fasting plasma insulin, HbA1c, NEFA and TG levels were elevated in obese rats. HDL cholesterol levels were also reduced. However, plasma glucose levels were not significantly increased. Moreover, a glucose tolerance test performed by our collaborator Dr. Eugene du Toit, found no differences between obese and control rats. Together these data suggest that the rat model we employed may be considered as a model of obesity and insulin resistance.

We next assessed cardiac mitochondrial respiratory function in obese and control rats. Here, obesity did not have any effect on baseline state 3 mitochondrial respiration rates. Moreover, mitochondrial efficiency (ADP/O) was maintained in obese rats. However, ADP phosphorylation rate was reduced in obese rats. These data therefore suggest reduced bioenergetic capacity in the obese rats. Mitochondria from obese rats displayed reduced state 4 respiration when glutamate was employed as oxidative substrate. This may indicate improved mitochondrial coupling in the presence of glycolytic substrates. Also, state 2 (endogenous) respiration and ADP phosphorylation rate were attenuated in obese rats when malate and carnitine-L-palmitoyl was used as fuel substrates. This suggests impaired FA metabolic capacity despite sustained state 3 respiratory rates at baseline. To gain further insight into possible mitochondrial respiratory defects, we exposed isolated heart mitochondria to an acute anoxic insult followed by reoxygenation. Interestingly, we found that recovery of state 3 respiration was significantly impaired in heart mitochondria from obese rats.

In parallel, our collaborator (Dr. du Toit) found that contractile function in these obese rats was significantly reduced before subjecting hearts to ischemia-reperfusion.

Together these data show that bioenergetic capacity may be impaired in obese rats at baseline. Furthermore, in response to oxidative stress, there is an association between impaired mitochondrial respiratory function and contractile function in obese, insulin-resistant rats. At present, we are investigating the underlying mechanisms responsible for this. There are several possibilities that may explain these findings. However, we are of the opinion that elevated FFA supply to the diabetic heart may be a critical component leading to attenuated respiratory capacity and contractile function. We propose that in this instance, components of the mitochondrial respiratory chain are downregulated. For example, Mootha *et al.* [108] and Patti *et al.* (2003) [109] reported coordinate downregulation of several nuclear-encoded mitochondrial genes in response to high fat exposure. Moreover, Boudina *et al.* (2005) [82] found reduced protein levels of mitochondrial respiratory chain complexes in a mouse model of type II diabetes.

Mouse Model of Obesity-Induced Type II Diabetes

We initially set out to determine temporal changes in male mitochondrial respiratory function in the db/db mouse strain. Here, we found that state 3 mitochondrial respiration was significantly increased in the obese mouse at 10-12 weeks. However, there were no differences between state 2 and state 4 mitochondrial respiration rates. Furthermore, ADP/O and ADP phosphorylation rates were similar for obese versus control heart mitochondria. These data suggest that at 10-12 weeks age, thought to be at the metabolic syndrome stage, the respiration rate is increased but that this does not significantly impact on the efficiency and the rate of mitochondrial ATP production. Increased state 3 mitochondrial respiration rate is consistent with enhanced rates of *ex vivo* FA oxidation reported for db/db hearts at this age. [106] However, decreased cardiac efficiency (work/ oxygen consumption) was reported for

obese hearts at age 10-12 weeks. Since we found that the ADP/O ratio was unchanged, we propose that uncoupling of respiration may not be a factor in this instance. However, since we did not measure oligomyocin-induced proton leak we cannot totally exclude increased uncoupling associated with the higher oxygen consumption. To gain further insight we also attempted to measure cardiac UCP protein levels, but had great difficulty in optimizing the Western blotting technique for UCP2 and UCP3 detection. We employed different commercially available antibodies for UCP2 and UCP3, but the degree of non-specificity were routinely found to be too high to make any meaningful conclusions.

At 18-20 weeks age, there was no difference in state 3 respiration between controls and obese mice. These data show that the db/+ mice had increased state 3 respiration in an age-dependent manner to match levels found in the obese mouse. However, state 3 respiration rates in obese mice were not further increased compared to the younger mice (10-12 weeks). This suggests that the oxidative capacity of the 18-20 week old obese mouse may be reduced. In agreement, others reported reduced state 3 oxidative rates in diabetic mice. [110] Here, it was suggested that reduced mitochondrial content and lower NAD^+ and NADH levels were responsible for the lower state 3 respiration rate. Consistent with the 10-12 week point, no differences were found for ADP/O, ADP phosphorylation rate and state 2/ 4 respiration rates. However, state 4 respiration for both control and obese mitochondria were significantly increased at the 18-20 week point compared to the 10-12 week point. This may reflect an overall, age-dependent increase in uncoupled respiration.

Aasum *et al.* (2003) [75] recently showed that 16-18 week old db/db hearts exhibited contractile dysfunction and reduced post-ischemic recovery of function. To further

assess mitochondrial respiratory capacity in the db/db hearts, we exposed isolated mitochondria to an anoxic insult followed by reoxygenation and determined state 3 respiration rates. However, recovery of state 3 respiration was not different between control and obese mitochondria. We subsequently investigated whether there were any ultrastructural changes between control and obese hearts at the 18-20 week point. Here, we found no major differences between these hearts. Moreover, histological analysis showed no significant increase in lipid deposition in obese hearts.

We next performed EM analysis of heart tissues to examine whether the ultrastructure of obese mouse mitochondria was intact. Here, obese hearts displayed mitochondrial ultrastructural damage i.e. distorted cristae organization, lipid deposition and vacuole accumulation. Similar observations were found in db/db ovarian tissues [111] and in skeletal muscle of type II diabetic patients. [112] We propose that changes in mitochondrial ultrastructure may be responsible for obese mice not being able to further increase respiratory capacity to deal with increased FFA supply. We therefore speculate that increased FA uptake may exceed FA oxidation capacity thereby resulting in intracellular lipid accumulation in 18-20 week-old diabetic hearts. Our data are consistent with previous studies investigating mitochondrial ultrastructure in the diabetic heart. For example, Hsaio *et al.* (1987) [113] found lipid accumulation and glycogen granules around diabetic mitochondria. In agreement, Shen *et al.* (2004) [114] reported severe damage to mitochondria of type I diabetic mice. Moreover, Morinho *et al.* (2005) [115] found reduced mitochondrial content in skeletal muscle of type II diabetic patients, suggesting that this would lead to impaired FA oxidation and therefore intracellular lipid accumulation. Increased intracellular lipid accumulation is thought to result in apoptosis via a ceramide-induced signaling pathway or lead to reduced expression of mitochondrial respiratory chain

components. In support, Kanazawa *et al.* (2002) [116] found reduced expression of cytochrome b and ATP synthase subunits in diabetic rat hearts. Moreover, previous workers reported reduced expression of nuclear-encoded mitochondrial genes in response to high fat exposure. [108, 109] Therefore, a reduction in mitochondrial respiratory chain components together with damaged mitochondria may contribute to the diabetic heart's inability to increase respiratory capacity. In addition, other non-metabolic mechanisms including alterations in calcium handling could also contribute to the change in cardiac function in diabetes.

Gender-dependent Changes in Mitochondrial Respiratory Function

Heart failure appears to be less common and less severe especially in young females. [23, 117] Human and animal studies show that young females display more favorable cardiac adaptation in several experimental and clinical conditions. [117] However, the precise mechanisms underlying this protection are unclear.

Our results indicate no significant differences in mitochondrial respiration for female control and obese mitochondria (18-20 weeks of age). When comparing male with female respiratory function, we found that state 2 respiration was significantly higher in female controls. We also found that female controls displayed less mitochondrial ultrastructural damage compared to males. Together these data suggest that females possess a protective phenotype at baseline. To further investigate male and female differences, we subjected these mitochondria to an oxidative stress i.e. anoxia-reoxygenation. Here, we found that female controls showed improved state 3 mitochondrial respiration recovery compared to male controls. In agreement, mitochondrial ATP levels were significantly increased in female compared to male controls. Together our respiration data suggest that females have increased

bioenergetic capacity at baseline that protects against external stresses.

The precise mechanisms underlying this protective phenotype in females are unclear. However, previous studies indicate that this may be due to several factors e.g. estrogens, [118] higher intrinsic HDL cholesterol content, [91] activation of anti-apoptotic mechanisms [117] and augmented antioxidant ability [93, 119] in young females compared to male and postmenopausal females. [120] For example, estrogen has been found to increase "good cholesterol" i.e. HDL [92], lower VLDL/ TG ratio and lower "bad cholesterol" i.e. LDL by increasing its clearance. [91] Furthermore, females possess higher HDL levels compared to males, with levels remaining steady throughout their lives. [91]

Others have suggested that altered MAP kinase pathways may play a role in gender-related cardioprotection. For example, Wang *et al.* (2006) [118] demonstrated increased ERK activation in females suggesting that such activation of MAP kinase pathways may mediate gender-related protection. Moreover, they also proposed that activated ERK may mediate the antioxidant effects of estrogens. Here, ERK activation activated the transcriptional regulator NF-$_K$B, which in turn induced superoxide dismutase (SOD) and glutathione peroxidase (GP_x) gene expression. [118] Lower free radical production observed in female mice may therefore reflect increased SOD and GP_x expression. Furthermore, estrogens also increase the expression and activity of Akt/ PKB [120] thereby providing a further rationale for increased resistance of females to myocardial apoptosis [117] In addition, others have shown that female rat hearts showed improved recovery in response to ischemia-reperfusion. [121] Here, the authors found increased activation of Akt and PKCε cardioprotective pathways in female rats. In light of these data, we propose

that increased antioxidant capacity and hence reduced ROS production may result in improved recovery in mitochondrial respiratory function in female mice in response to oxidative stress.

Interestingly, we found that the augmented bioenergetic capacity observed in female controls at baseline was abolished with obesity. Here, obese female mice displayed similar rates of recovery as males in response to anoxia-reoxygenation. Moreover, mitochondrial ATP levels were also significantly reduced in obese females. We are currently investigating whether signaling pathways (e.g. Akt and PKCε) and/ or expression of mitochondrial respiratory chain components are reduced in obese female mice.

Since it is thought that especially younger females are protected from CVD, [120, 122, 123] we initiated a pilot study to investigate older db/db mice (55-56 weeks) to further assess age- and gender-dependent changes in mitochondrial respiration.

Pilot Study: Age- and Gender-Dependent Changes in Type II Diabetic Mouse Model (55-56 weeks)

To the best of my knowledge, this is the first attempt to characterize db/db mice at a much later age (55-56 weeks). Here, state 2, 3 and 4 mitochondrial respiration were significantly reduced in both male and female controls compared to mice aged 18-20 weeks. We propose that this overall reduction in mitochondrial respiratory function is an age-dependent effect i.e. this may be due to increased ROS production due to aging. [124, 125] It has been reported that elevated ROS levels may lead to a number of events, including increased mitochondrial DNA mutations that may contribute to mitochondrial dysfunction. [124, 126]

Surprisingly, we found that 55-56 week old obese mice displayed increased state 2, 3 and 4 mitochondrial respiration versus controls, matching levels observed in the 18-20 week-old mitochondria. This effect was paralleled by the ADP phosphorylation rate. Also, 55-56 week old obese males showed improved recovery in response to anoxia-reoxygenation. These data suggest that the earlier effects of obesity on mitochondrial respiration (i.e. at 10-12 weeks and 18-20 weeks) are compensated for by the older obese mice, especially the obese males. In agreement, no ultrastructural changes were observed for obese heart tissues in mice aged 55-56 weeks. However, significant lipid depositions were found in the liver accompanied by hypertrophy of pancreatic β-cells. Despite the contractile dysfunction reported at the 16-18 week point, [75] we found that obese diabetic mice survived reasonably well up to the 55-56 week point. We therefore speculate that age-dependent compensatory mechanisms are induced to ensure maintenance of cardiac contractility in these animals. It is likely that protective mechanisms activated by obese males may be independent of changes in mitochondrial bioenergetic capacity.

As indicated earlier, this was a first attempt to use older animals (55-56 weeks). Due to a limited animal availability, it is difficult to speculate why the glucose levels returned to normal. However, lipid deposition may be oversaturated in the liver thereby affecting its normal function i.e. leading to a reduction in hepatic gluconeogenesis and reduced plasma glucose levels. Furthermore, I propose that β-cell enlargement forms part of a compensatory process (early on during diabetic phenotype) to increase the release of insulin in order to deal with the high level of glucose in diabetes. This process is probably irreversible, hence a situation may arise during late diabetes where β –cells are enlarged while plasma glucose levels are low. However, further studies need to be performed to examine this hypothesis.

Conclusion

We have determined cardiac mitochondrial respiratory function in rodent models of obesity and obesity-induced type II diabetes. Our data show that mitochondrial respiratory capacity is impaired in obese rats when stressed. We speculate that this may be due to reduced expression of mitochondrial respiratory chain complexes in the diabetic heart. For the mouse model of type II diabetes we found increased respiratory capacity at 10-12 weeks, with no evidence of oxygen wastage or reduction of respiratory capacity. However, 18-20 week-old obese mice were unable to further increase respiratory capacity. We also found increased mitochondrial ultrastructural damage and intracellular lipid accumulation in these diabetic hearts. We speculated that lipid accumulation occurs as a result of a mismatch between increased FA uptake and decreased FA oxidative capacity. However, FA uptake and FA oxidation need to be measured to confirm this. Mitochondrial respiratory function in the two models was different and it could be due to species-specific differences since the genetic make up of the two models was different. Hence, this may have lead to variation in mitochondrial function. Also, obesity in the two models was induced either genetically or by diet manipulation. This plays an important role regarding the impact on mitochondrial respiratory function.

We also found interesting gender-dependent changes i.e. younger female mice showed enhanced protection when mitochondria were stressed by anoxia-reoxygenation. These data were paralleled by increased mitochondrial ATP levels, suggesting that young female mice possess increased mitochondrial bioenergetic capacity at baseline. Moreover, our EM data suggest that the ultrastructure of male mitochondria is more disorganized when compared to females at baseline. Interestingly, we found that the protective phenotype observed in female

mice at baseline is abolished with obesity.

At the later age (55-56 weeks), mitochondrial respiratory function and bioenergetic capacity is reduced in both male and female mice at baseline. We suggest that this is an age-dependent phenomenon and speculate that it may be caused by a number of factors, including increased ROS production. Surprisingly, we found that older, obese males and females induced compensatory mechanisms to deal with the chronic diabetic mileu. Here, mitochondrial respiratory function was increased, reaching levels observed in younger mice (18-20 weeks). Together, this study highlights the significance of sustained biogenetic capacity to ensure an organism's survival. However, with obesity and obesity-induced type II diabetes mitochondrial energetic homeostasis is perturbed, and we speculate that this may eventually impact on the heart's contractile function. Our data suggest that therapeutic interventions aimed at enhancing mitochondrial energy homeostasis may improve the diabetic heart's function and therefore help to alleviate the increasing burden of disease of obesity-induced type II diabetes.

10. Limitations

The homozygous mutants of the db/db (BKS.Cg-m+/+Lepr^{db}/J) strain are sterile. [94] Propagation of this strain therefore mainly depends on the availability of heterozygous (db/+) mice. According to Mendelian law, there should be 1: 2: 1 ratio of obtaining homozygous obese animals. However, the breeding period was longer than what we expected and only a few offspring were produced, especially the obese db/db. There's abnormality in the sexual organ of the female db/db which leads to sterility of the homozygous mutant. However, the heterozygous female is phenotypically normal and generally used in breeding. It is possible that the heterozygous female has lower estrogen levels than normal thus resulting in few offspring produced. The lack of animal numbers therefore represented a major challenge to complete the current study. As a result, mice used for the 10-12 and the 55-56 week studies were bred in-house at the Animal Unit of the University of Cape Town's Faculty of Health Sciences. For the 18-20 week study, we purchased mice directly from The Jackson Laboratory (Bar Harbor, Maine).

High-quality mitochondrial yield is dependent on the process of mitochondrial isolation since any delays would affect the respiratory function. Arrested hearts with the last pumping of oxygen may affect the oxygen content in the cells and the consumption by the mitochondria. Thus, mitochondrial yield/ g heart weight and some of the basal characterization for e.g. heart dry weight was not measured. In addition, during the process of mitochondrial isolation, even a gentle homogenization may result in mitochondrial damage (including the rupture of the mitochondrial membrane). Thus, such ruptured mitochondria might be misinterpreted and incorrectly correlated to the degree of diabetes and associated apoptosis. This in

turn may lead to an incorrect association of mitochondrial damage to the degree of diabetes. In light of this, EM was performed only on cross sections of heart tissue and not on isolated mitochondria.

The heterozygous mice (db/+) used in this project are described to be phenotypically normal [94] and is widely used as a control to compare with its obese counterpart. In light of the breeding difficulties we faced, we therefore used db/+ as controls. However, it would be more appropriate to include the donor strains (C57BLKS and DBA/J) as positive controls.

We did not succeed to measure UCP2 and UCP3 gene and protein levels in this study. I had numerous attempts at Western blotting but did not manage to optimize the protocol. Recently, we have learnt from others in the field that new antibodies have been developed for UCP2 and UCP3. We are planning to purchase these antibodies in order to complete our analysis.

11. Future Studies

We are currently performing a gene expression study (on collected heart tissues) to determine expression levels of several FA and glucose metabolic genes. Also, we are planning to measure gene expression levels of mitochondrial respiratory chain components. We will subsequently perform Western blotting to confirm that protein levels match the gene data generated.

For the gene study, we intend to measure Akt and PKCε phosphorylation states (Western blotting) to assess whether these pathways are activated in females at baseline and attenuated with obesity. We plan to measure ROS production for all the time points by measuring catalase and SOD activities (indirect measurement).

Furthermore, cardiac function will be performed at the 55-56 week-old point (in collaboration with Dr. Ellen Aasum, Norway).

V: PUBLICATIONS

12. Publications and Abstracts

How O-J, Aasum E, Severson DL, Chan WYA, Essop MF. Increased myocardial oxygen consumption reduces cardiac efficiency in diabetic mice. *Diabetes* 2006;55:466-473.

Chan WYA, Essop MF, How O-J, Aasum E, Larsen TS. Reduced cardiac efficiency – A component of diabetic cardiomycopathy? 33rd Congress of the Physiology Society of South Africa (PSSA). Cape Town, South Africa (2005).

VI: REFERENCES

13. References

1. Novak M, Ahlgren C, Hammarstrom A. A life-course approach in explaining social inequity in obesity among young adult men and women. *Int J Obes (Lond)* 2006;30:191-200.

2. World Health Organization. Obesity and overweight: World Health Organization, 2004.

3. World Health Organization. World Health Report 2002. *World Health Organization* 2002.

4. Puoane T, Steyn K, Bradshaw D, Laubscher R, Fourie J, Lambert V, Mbananga N. Obesity in South Africa: the South African demographic and health survey. *Obes Res* 2002;10:1038-48.

5. Weiss R, Caprio S. The metabolic consequences of childhood obesity. *Best Pract Res Clin Endocrinol Metab* 2005;19:405-19.

6. Centers for Disease Control and Prevention (CDC). Overweight and obesity: defining overweight and obesity. [Online] available at: URL: http://www.cdc.gov/nccdphp/dnpa/obesity/defining.htm

7. US National Heart Lung and Blood Institute (NHLBI). Guildelines on overweight and obesity: electronic textbook. [Online] available at: URL: http://www.nhlbi.nih.gov/guidelines/obesity/e_txtbk/txgd/4142.htm, 2005.

8. Chan JM, Rimm EB, Colditz GA, Stampfer MJ, Willett WC. Obesity, fat distribution, and weight gain as risk factors for clinical diabetes in men. *Diabetes Care* 1994;17:961-9.

9. Dowling HJ, Pi-Sunyer FX. Race-dependent health risks of upper body obesity. *Diabetes* 1993;42:537-43.

10. Hancox RJ, Poulton R. Watching television is associated with childhood obesity: but is it clinically important? *Int J Obes (Lond)* 2006;30:171-5.

11. Eberwine D. Globesity: The crisis of growing proportions Perspectives in Health Magazine: The Magazine of the Pan American Health Organization, 2002.

12. Janus ED. Metabolic syndrome and its relevance to Asia. *International Congress Series* 2004;1262:535-537.

13. Eckel RH, Grundy SM, Zimmet PZ. The metabolic syndrome. *Lancet* 2005;365:1415-28.

14. Alberti KG, Zimmet P, Shaw J. The metabolic syndrome--a new worldwide definition. *Lancet* 2005;366:1059-62.

15. Miranda PJ, DeFronzo RA, Califf RM, Guyton JR. Metabolic syndrome: definition, pathophysiology, and mechanisms. *Am Heart J* 2005;149:33-45.

16. World Health Organization. [Online] available at: URL: http://www.who.int/diabetes/facts/world_figures/en/index1.html.

17. Reaven GM. Banting lecture 1988. Role of insulin resistance in human disease. *Diabetes* 1988;37:1595-607.

18. Weiss R, Dziura J, Burgert TS, Tamborlane WV, Taksali SE, Yeckel CW, Allen K, Lopes M, Savoye M, Morrison J, Sherwin RS, Caprio S. Obesity and the metabolic syndrome in children and adolescents. *N Engl J Med* 2004;350:2362-74.

19. Stanley WC. Rationale for a metabolic approach in diabetic coronary patients. *Coron Artery Dis* 2005;16 Suppl 1:S11-5.

20. Hanson RL, Imperatore G, Bennett PH, Knowler WC. Components of the "metabolic syndrome" and incidence of type 2 diabetes. *Diabetes* 2002;51:3120-7.

21. Hu G, Qiao Q, Tuomilehto J, Balkau B, Borch-Johnsen K, Pyorala K. Prevalence of the metabolic syndrome and its relation to all-cause and cardiovascular mortality in nondiabetic European men and women. *Arch Intern Med* 2004;164:1066-76.

22. American Heart Association. Cardiovascular disease statistics: American Heart Association, 2005.

23. De Backer G, Ambrosioni E, Borch-Johnsen K, Brotons C, Cifkova R, Dallongeville J, Ebrahim S, Faergeman O, Graham I, Mancia G, Manger Cats V, Orth-Gomer K, Perk J, Pyorala K, Rodicio JL, Sans S, Sansoy V, Sechtem U, Silber S, Thomsen T, Wood D. European guidelines on cardiovascular disease prevention in clinical practice. Third Joint Task Force of European and Other Societies on Cardiovascular Disease Prevention in Clinical Practice. *Eur Heart J* 2003;24:1601-10.

24. Fodor JG, Tzerovska R, Dorner T, Rieder A. Do we diagnose and treat coronary heart disease differently in men and women? *Wien Med Wochenschr* 2004;154:423-5.

25. Opie LH. Heart physiology: from cell to circultaion. Fourth edition. Philadelphia: Lippincott Williams and Wilkins, 2004:ch 11.

26. Young ME, McNulty P, Taegtmeyer H. Adaptation and maladaptation of the heart in diabetes: Part II: potential mechanisms. *Circulation* 2002;105:1861-70.

27. Carley AN, Severson DL. Fatty acid metabolism is enhanced in type 2 diabetic hearts. *Biochim Biophys Acta* 2005;1734:112-26.

28. Pessin JE, Bell GI. Mammalian facilitative glucose transporter family: structure and molecular regulation. *Annu Rev Physiol* 1992;54:911-30.

29. Stryer L. Biochemistry: fourth edition. New York: W.H. Freeman and Company, 1999:463-507.

30. Mader SS. Biology. 5th Edition. Dubyque: Wm. C. Brown Publishers, 1996:777-778.

31. Desrois M, Sidell RJ, Gauguier D, King LM, Radda GK, Clarke K. Initial steps of insulin signaling and glucose transport are defective in the type 2 diabetic rat heart. *Cardiovasc Res* 2004;61:288-96.

32. Shulman GI. Cellular mechanisms of insulin resistance. *J Clin Invest* 2000;106:171-6.

33. Makinde AO, Kantor PF, Lopaschuk GD. Maturation of fatty acid and carbohydrate metabolism in the newborn heart. *Mol Cell Biochem* 1998;188:49-56.

34. Pogatsa G. Metabolic energy metabolism in diabetes: therapeutic implications. *Coron Artery Dis* 2001;12 Suppl 1:S29-33.

35. Brownlee M. Biochemistry and molecular cell biology of diabetic complications. *Nature* 2001;414:813-20.

36. Lowell BB, Shulman GI. Mitochondrial dysfunction and type 2 diabetes. *Science* 2005;307:384-7.

37. Russell R. Insulin stimulates translocation of both GLUT4 and GLUT1 in the heart. *Circulation* 1996;94:1-308.

38. Randle PJ, Garland PB, Hales CN, Newsholme EA. The glucose fatty-acid cycle. Its role in insulin sensitivity and the metabolic disturbances of diabetes mellitus. *Lancet* 1963;1:785-9.

39. Hakansson ML, Meister B. Transcription factor STAT3 in leptin target neurons of the rat hypothalamus. *Neuroendocrinology* 1998;68:420-7.

40. Bahrenberg G, Behrmann I, Barthel A, Hekerman P, Heinrich PC, Joost HG, Becker W. Identification of the critical sequence elements in the cytoplasmic domain of leptin receptor isoforms required for Janus kinase/signal transducer and activator of transcription activation by receptor heterodimers. *Mol Endocrinol* 2002;16:859-72.

41. Niswender KD, Schwartz MW. Insulin and leptin revisited: adiposity signals with overlapping physiological and intracellular signaling capabilities. *Front Neuroendocrinol* 2003;24:1-10.

42. Porte D, Jr., Baskin DG, Schwartz MW. Leptin and insulin action in the central nervous system. *Nutr Rev* 2002;60:S20-9; discussion S68-84, 85-7.

43. Barouch LA, Berkowitz DE, Harrison RW, O'Donnell CP, Hare JM. Disruption of leptin signaling contributes to cardiac hypertrophy independently of body weight in mice. *Circulation* 2003;108:754-9.

44. Friedman JM. Leptin, leptin receptors, and the control of body weight. *Nutr Rev* 1998;56:s38-46; discussion s54-75.

45. Atkinson LL, Fischer MA, Lopaschuk GD. Leptin activates cardiac fatty acid oxidation independent of changes in the AMP-activated protein kinase-acetyl-CoA carboxylase-malonyl-CoA axis. *J Biol Chem* 2002;277:29424-30.

46. Maffei M, Halaas J, Ravussin E, Pratley RE, Lee GH, Zhang Y, Fei H, Kim S, Lallone R, Ranganathan S, et al. Leptin levels in human and rodent: measurement of plasma leptin and ob RNA in obese and weight-reduced subjects. *Nat Med* 1995;1:1155-61.

47. Heymsfield SB, Greenberg AS, Fujioka K, Dixon RM, Kushner R, Hunt T, Lubina JA, Patane J, Self B, Hunt P, McCamish M. Recombinant leptin for weight loss in obese and lean adults: a randomized, controlled, dose-escalation trial. *Jama* 1999;282:1568-75.

48. Cases JA, Gabriely I, Ma XH, Yang XM, Michaeli T, Fleischer N, Rossetti L, Barzilai N. Physiological increase in plasma leptin markedly inhibits insulin secretion in vivo. *Diabetes* 2001;50:348-52.

49. Kostis JB, Sanders M. The association of heart failure with insulin resistance and the development of type 2 diabetes. *Am J Hypertens* 2005;18:731-7.

50. Himsworth H. Diabetes mellitus: A differentiation into insulin-sensitive and insulin-insensitive types. *Lancet* 1936;1:127-130.

51. Eckel RH. Lipoprotein lipase. A multifunctional enzyme relevant to common metabolic diseases. *N Engl J Med* 1989;320:1060-8.

52. Jensen MD, Caruso M, Heiling V, Miles JM. Insulin regulation of lipolysis in nondiabetic and IDDM subjects. *Diabetes* 1989;38:1595-601.

53. Swislocki AL, Chen YD, Golay A, Chang MO, Reaven GM. Insulin suppression of plasma-free fatty acid concentration in normal individuals and patients with type 2 (non-insulin-dependent) diabetes. *Diabetologia* 1987;30:622-6.

54. Lewis GF, Steiner G. Acute effects of insulin in the control of VLDL production in humans. Implications for the insulin-resistant state. *Diabetes Care* 1996;19:390-3.

55. Lee Y, Hirose H, Ohneda M, Johnson JH, McGarry JD, Unger RH. Beta-cell lipotoxicity in the pathogenesis of non-insulin-dependent diabetes mellitus of obese rats: impairment in adipocyte-beta-cell relationships. *Proc Natl Acad Sci U S A* 1994;91:10878-82.

56. Rhodes CJ. Type 2 diabetes-a matter of beta-cell life and death? *Science* 2005;307:380-4.

57. Stanley WC, Hall JL, Smith KR, Cartee GD, Hacker TA, Wisneski JA. Myocardial glucose transporters and glycolytic metabolism during ischemia in hyperglycemic diabetic swine. *Metabolism* 1994;43:61-9.

58. Dresner A, Laurent D, Marcucci M, Griffin ME, Dufour S, Cline GW, Slezak LA, Andersen DK, Hundal RS, Rothman DL, Petersen KF, Shulman GI. Effects of free fatty acids on glucose transport and IRS-1-associated phosphatidylinositol 3-kinase activity. *J Clin Invest* 1999;103:253-9.

59. Yu C, Chen Y, Cline GW, Zhang D, Zong H, Wang Y, Bergeron R, Kim JK, Cushman SW, Cooney GJ, Atcheson B, White MF, Kraegen EW, Shulman GI. Mechanism by which fatty acids inhibit insulin activation of insulin receptor substrate-1 (IRS-1)-associated phosphatidylinositol 3-kinase activity in muscle. *J Biol Chem* 2002;277:50230-6.

60. Boden G. Free fatty acids, insulin resistance, and type 2 diabetes mellitus. *Proc Assoc Am Physicians* 1999;111:241-8.

61. Brehm A, Krssak M, Schmid AI, Nowotny P, Waldhausl W, Roden M. Increased lipid availability impairs insulin-stimulated ATP synthesis in human skeletal muscle. *Diabetes* 2006;55:136-40.

62. Kraegen EW, Cooney GJ, Ye JM, Thompson AL, Furler SM. The role of lipids in the pathogenesis of muscle insulin resistance and beta cell failure in type II diabetes and obesity. *Exp Clin Endocrinol Diabetes* 2001;109 Suppl 2:S189-201.

63. Goldstein BJ. Insulin resistance as the core defect in type 2 diabetes mellitus. *Am J Cardiol* 2002;90:3G-10G.

64. Paolisso G, Gambardella A, Galzerano D, D'Amore A, Rubino P, Verza M, Teasuro P, Varricchio M, D'Onofrio F. Total-body and myocardial substrate oxidation in congestive heart failure. *Metabolism* 1994;43:174-9.

65. Golay A, Chen YD, Reaven GM. Effect of differences in glucose tolerance on insulin's ability to regulate carbohydrate and free fatty acid metabolism in obese individuals. *J Clin Endocrinol Metab* 1986;62:1081-8.

66. Hollenbeck C, Reaven GM. Variations in insulin-stimulated glucose uptake in healthy individuals with normal glucose tolerance. *J Clin Endocrinol Metab* 1987;64:1169-73.

67. Lewis GF, Uffelman KD, Szeto LW, Weller B, Steiner G. Interaction between free fatty acids and insulin in the acute control of very low density lipoprotein production in humans. *J Clin Invest* 1995;95:158-66.

68. Brandt JM, Djouadi F, Kelly DP. Fatty acids activate transcription of the muscle carnitine palmitoyltransferase I gene in cardiac myocytes via the peroxisome proliferator-activated receptor alpha. *J Biol Chem* 1998;273:23786-92.

69. Young ME, Patil S, Ying J, Depre C, Ahuja HS, Shipley GL, Stepkowski SM, Davies PJ, Taegtmeyer H. Uncoupling protein 3 transcription is regulated by peroxisome proliferator-activated receptor (alpha) in the adult rodent heart. *Faseb J* 2001;15:833-45.

70. Zhou YT, Grayburn P, Karim A, Shimabukuro M, Higa M, Baetens D, Orci L, Unger RH. Lipotoxic heart disease in obese rats: implications for human obesity. *Proc Natl Acad Sci U S A* 2000;97:1784-9.

71. Garg A. Lipodystrophies. *Am J Med* 2000;108:143-52.

72. Hickson-Bick DL, Buja ML, McMillin JB. Palmitate-mediated alterations in the fatty acid metabolism of rat neonatal cardiac myocytes. *J Mol Cell Cardiol* 2000;32:511-9.

73. Unger RH, Orci L. Diseases of liporegulation: new perspective on obesity and related disorders. *Faseb J* 2001;15:312-21.

74. Schupp M, Kintscher U, Fielitz J, Thomas J, Pregla R, Hetzer R, Unger T, Regitz-Zagrosek V. Cardiac PPARalpha expression in patients with dilated cardiomyopathy. *Eur J Heart Fail* 2005.

75. Aasum E, Hafstad AD, Severson DL, Larsen TS. Age-dependent changes in metabolism, contractile function, and ischemic sensitivity in hearts from db/db mice. *Diabetes* 2003;52:434-41.

76. Severson DL. Diabetic cardiomyopathy: recent evidence from mouse models of type 1 and type 2 diabetes. *Can J Physiol Pharmacol* 2004;82:813-23.

77. Sparks LM, Xie H, Koza RA, Mynatt R, Hulver MW, Bray GA, Smith SR. A high-fat diet coordinately downregulates genes required for mitochondrial oxidative phosphorylation in skeletal muscle. *Diabetes* 2005;54:1926-33.

78. Echtay KS, Roussel D, St-Pierre J, Jekabsons MB, Cadenas S, Stuart JA, Harper JA, Roebuck SJ, Morrison A, Pickering S, Clapham JC, Brand MD. Superoxide activates mitochondrial uncoupling proteins. *Nature* 2002;415:96-9.

79. Lashin O, Romani A. Mitochondria respiration and susceptibility to ischemia-reperfusion injury in diabetic hearts. *Arch Biochem Biophys* 2003;420:298-304.

80. Samec S, Seydoux J, Dulloo AG. Role of UCP homologues in skeletal muscles and brown adipose tissue: mediators of thermogenesis or regulators of lipids as fuel substrate? *Faseb J* 1998;12:715-24.

81. Dulloo AG, Samec S, Seydoux J. Uncoupling protein 3 and fatty acid metabolism. *Biochem Soc Trans* 2001;29:785-91.

82. Boudina S, Sena S, O'Neill BT, Tathireddy P, Young ME, Abel ED. Reduced mitochondrial oxidative capacity and increased mitochondrial uncoupling impair myocardial energetics in obesity. *Circulation* 2005;112:2686-95.

83. Porter RK. Mitochondrial proton leak: a role for uncoupling proteins 2 and 3? *Biochim Biophys Acta* 2001;1504:120-7.

84. Weigle DS, Selfridge LE, Schwartz MW, Seeley RJ, Cummings DE, Havel PJ, Kuijper JL, BeltrandelRio H. Elevated free fatty acids induce uncoupling protein 3 expression in muscle: a potential explanation for the effect of fasting. *Diabetes* 1998;47:298-302.

85. Giacobino JP. Uncoupling protein 3 biological activity. *Biochem Soc Trans* 2001;29:774-7.

86. Samec S, Seydoux J, Dulloo AG. Post-starvation gene expression of skeletal muscle uncoupling protein 2 and uncoupling protein 3 in response to dietary fat levels and fatty acid composition: a link with insulin resistance. *Diabetes* 1999;48:436-41.

87. Teshima Y, Akao M, Jones SP, Marban E. Uncoupling protein-2 overexpression inhibits mitochondrial death pathway in cardiomyocytes. *Circ Res* 2003;93:192-200.

88. Essop MF, Razeghi P, McLeod C, Young ME, Taegtmeyer H, Sack MN. Hypoxia-induced decrease of UCP3 gene expression in rat heart parallels metabolic gene switching but fails to affect mitochondrial respiratory coupling. *Biochem Biophys Res Commun* 2004;314:561-4.

89. Mazumder PK, O'Neill BT, Roberts MW, Buchanan J, Yun UJ, Cooksey RC, Boudina S, Abel ED. Impaired cardiac efficiency and increased fatty acid oxidation in insulin-resistant ob/ob mouse hearts. *Diabetes* 2004;53:2366-74.

90. Borras C, Sastre J, Garcia-Sala D, Lloret A, Pallardo FV, Vina J. Mitochondria from females exhibit higher antioxidant gene expression and lower oxidative damage than males. *Free Radic Biol Med* 2003;34:546-52.

91. Knopp RH, Zhu X, Bonet B. Effects of estrogens on lipoprotein metabolism and cardiovascular disease in women. *Atherosclerosis* 1994;110 Suppl:S83-91.

92. Genest J, Frohlich J, Fodor G, McPherson R. Recommendations for the management of dyslipidemia and the prevention of cardiovascular disease: summary of the 2003 update. *Cmaj* 2003;169:921-4.

93. Vina J, Borras C, Gambini J, Sastre J, Pallardo FV. Why females live longer than males? Importance of the upregulation of longevity-associated genes by oestrogenic compounds. *FEBS Lett* 2005;579:2541-5.

94. Coleman DL. Obese and diabetes: two mutant genes causing diabetes-obesity syndromes in mice. *Diabetologia* 1978;14:141-8.

95. Aasum E, Belke DD, Severson DL, Riemersma RA, Cooper M, Andreassen M, Larsen TS. Cardiac function and metabolism in Type 2 diabetic mice after treatment with BM 17.0744, a novel PPAR-alpha activator. *Am J Physiol Heart Circ Physiol* 2002;283:H949-57.

96. The Jackson Laboratory. JAX Mice Data Sheet. [Online] available at: URL: http://jaxmice.jax.org.

97. Sordahl LA, Besch HR, Jr., Allen JC, Crow C, Lindenmayer GE, Schwartz A. Enzymatic aspects of the cardiac muscle cell: mitochondria, sarcoplasmic reticulum and nonovalent cation active transport system. *Methods Achiev Exp Pathol* 1971;5:287-346.

98. Lowry OH, Rosebrough NJ, Farr AL, Randall RJ. Protein measurement with the Folin phenol reagent. *J Biol Chem* 1951;193:265-75.

99. Stavinoha MA, Rayspellicy JW, Hart-Sailors ML, Mersmann HJ, Bray MS, Young ME. Diurnal variations in the responsiveness of cardiac and skeletal muscle to fatty acids. *Am J Physiol Endocrinol Metab* 2004;287:E878-87.

100. Laboratory Corporation of America Holdings. [Online] available at: URL: http://www.labcorp.com/datasets/labcorp/html/chapter/mono/sc028500.htm, 2005.

101. Trinder P. Determination of blood glucose using an oxidase-peroxidase system with a non-carcinogenic chromogen. *J Clin Pathol* 1969;22:158-61.

102. Fryer RM, Eells JT, Hsu AK, Henry MM, Gross GJ. Ischemic preconditioning in rats: role of mitochondrial K(ATP) channel in preservation of mitochondrial function. *Am J Physiol Heart Circ Physiol* 2000;278:H305-12.

103. Glauert A. Fixation, dehydration and embedding of biological specimens: Pracical methods in Electron Microscopy. Amsterdam and New York: North-Holland and American Elsevier publishing company, 1975:44-45, 111-113.

104. Bancroft J, Stevens A. Theory and practics of histological techniques. London: Churchill Livingstone and Edinburgh, 1990:109.

105. Giancoli D. Physics: Principles with applications. Fifth Edition. New Jersey: Prentice Hall International, 1998:838.

106. How OJ, Aasum E, Severson DL, Chan WY, Essop MF, Larsen TS. Increased myocardial oxygen consumption reduces cardiac efficiency in diabetic mice. *Diabetes* 2006;55:466-73.

107. Hayat M. Stains and cytochemical methods. New York: Plenum Press, 1993:260-265, 273-275.

108. Mootha VK, Lindgren CM, Eriksson KF, Subramanian A, Sihag S, Lehar J, Puigserver P, Carlsson E, Ridderstrale M, Laurila E, Houstis N, Daly MJ, Patterson N, Mesirov JP, Golub TR, Tamayo P, Spiegelman B, Lander ES, Hirschhorn JN, Altshuler D, Groop LC. PGC-1alpha-responsive genes involved in oxidative phosphorylation are coordinately downregulated in human diabetes. *Nat Genet* 2003;34:267-73.

109. Patti ME, Butte AJ, Crunkhorn S, Cusi K, Berria R, Kashyap S, Miyazaki Y, Kohane I, Costello M, Saccone R, Landaker EJ, Goldfine AB, Mun E, DeFronzo R, Finlayson J, Kahn CR, Mandarino LJ. Coordinated reduction of genes of oxidative metabolism in humans with insulin resistance and diabetes: Potential role of PGC1 and NRF1. *Proc Natl Acad Sci U S A* 2003;100:8466-71.

110. Kuo TH, Moore KH, Giacomelli F, Wiener J. Defective oxidative metabolism of heart mitochondria from genetically diabetic mice. *Diabetes* 1983;32:781-7.

111. Garris DR. Ovarian hypercytolipidemia induced by obese (ob/ob) and diabetes (db/db) mutations: basis of female reproductive tract involution II. *Tissue Cell* 2004;36:157-69.

112. Kelley DE, He J, Menshikova EV, Ritov VB. Dysfunction of mitochondria in human skeletal muscle in type 2 diabetes. *Diabetes* 2002;51:2944-50.

113. Hsiao YC, Suzuki K, Abe H, Toyota T. Ultrastructural alterations in cardiac muscle of diabetic BB Wistar rats. *Virchows Arch A Pathol Anat Histopathol* 1987;411:45-52.

114. Shen X, Zheng S, Thongboonkerd V, Xu M, Pierce WM, Jr., Klein JB, Epstein PN. Cardiac mitochondrial damage and biogenesis in a chronic model of type 1 diabetes. *Am J Physiol Endocrinol Metab* 2004;287:E896-905.

115. Morino K, Petersen KF, Dufour S, Befroy D, Frattini J, Shatzkes N, Neschen S, White MF, Bilz S, Sono S, Pypaert M, Shulman GI. Reduced mitochondrial density and increased IRS-1 serine phosphorylation in muscle of insulin-resistant offspring of type 2 diabetic parents. *J Clin Invest* 2005;115:3587-93.

116. Kanazawa A, Nishio Y, Kashiwagi A, Inagaki H, Kikkawa R, Horiike K. Reduced activity of mtTFA decreases the transcription in mitochondria isolated from diabetic rat heart. *Am J Physiol Endocrinol Metab* 2002;282:E778-85.

117. Biondi-Zoccai GG, Baldi A, Biasucci LM, Abbate A. Female gender, myocardial remodeling and cardiac failure: are women protected from increased myocardiocyte apoptosis? *Ital Heart J* 2004;5:498-504.

118. Wang M, Crisostomo P, Wairiuko G, Meldrum D. Estrogen receptor alpha mediates acute mycocardial protection in female. *Am J Physiol Heart Circ Physiol* 2006;ahead of print.

119. Ruiz OA, Ugalde RA. Partial characterization and photolabeling of a Rhizobium meliloti polysaccharide methyltransferase with S-adenosylmethionine. *Int Microbiol* 1998;1:225-30.

120. Camper-Kirby D, Welch S, Walker A, Shiraishi I, Setchell KD, Schaefer E, Kajstura J, Anversa P, Sussman MA. Myocardial Akt activation and gender: increased nuclear activity in females versus males. *Circ Res* 2001;88:1020-7.

121. Bae S, Zhang L. Gender differences in cardioprotection against ischemia/reperfusion injury in adult rat hearts: focus on Akt and protein kinase C signaling. *J Pharmacol Exp Ther* 2005;315:1125-35.

122. Franklin SS. Definition and epidemiology of hypertensive cardiovascular disease in women: the size of the problem. *J Hypertens Suppl* 2002;20:S3-5.

123. Desrois M, Sidell RJ, Gauguier D, Davey CL, Radda GK, Clarke K. Gender differences in hypertrophy, insulin resistance and ischemic injury in the aging type 2 diabetic rat heart. *J Mol Cell Cardiol* 2004;37:547-55.

124. Beckman KB, Ames BN. The free radical theory of aging matures. *Physiol Rev* 1998;78:547-81.

125. Maechler P, Wollheim CB. Mitochondrial function in normal and diabetic beta-cells. *Nature* 2001;414:807-12.

126. Coordt MC, Ruhe RC, McDonald RB. Aging and insulin secretion. *Proc Soc Exp Biol Med* 1995;209:213-22.

VII: APPENDIX

14. Appendix

1. Cafeteria Diet for Diet-Induced Rat Model

1320 g Animal chow
1 L Water
4 cans Full cream condensed milk
280 g Sugar
Animal chow was soaked in water for 2 hours. Mixed all ingredients and kept at 4 °C.

2. Mitochondrial Isolation for Diet-Induced Rat Model

Potassium-EDTA (KE) isolation buffer [pH 7.4]
0.18 M KCl
10 mM EDTA

Incubation buffer [pH7.4]
10 mM Tris-HCl
250 mM sucrose
8.5 mM KH_2PO_4

3. Mitochondrial Isolation for Obesity-Induced Type II diabetic Mouse Model

Potassium-EDTA (KE) isolation buffer [pH 7.4]
0.18 M KCl
10 mM EDTA

Incubation buffer [pH7.4]
25 mM Tris-HCl
250 mM sucrose
8.5 mM KH_2PO_4

4. Lowry Protein Assay

Solution A (CTC reagent) – equal volume of each of the following:
1) 20%w/v Na_2CO_3; 0.2% w/v $CuSO_4.5H_2O$ and 0.4%w/v K_2 tartrate
2) 10% SDS
3) 0.1M NaOH
Solution B
1:6 dilutions of Folin-Ciocalteu's phenol reagent (Merck, Germany)

6. Prepare the grid:

Place the ultra thin cut tissue onto the copper grid

7. Staining:

Stain with heavy metals-Uranyl acetate and Lead nitrate